Water-soluble organic compounds in air particulate matter analyzed by HPLC-DAD-MS and HPLC-MS/MS: abundance, sources and transformation of carboxylic acids, nitrophenols and nitrated proteins

Dissertation zur Erlangung des Grades

„Doktor der Naturwissenschaften“

am Fachbereich Chemie, Pharmazie und Geowissenschaften

der Johannes Gutenberg-Universität Mainz

vorgelegt von

M.Sc. Yingyi Zhang

geboren in Guangzhou (Guangdong), VR China

Mainz, 2010

Zwei Dinge erfüllen das Gemüt mit immer neuer und zunehmender Bewunderung und Ehrfurcht, je öfter und anhaltender sich das Nachdenken damit beschäftigt: Der bestirnte Himmel über mir, und das moralische Gesetz in mir.

- Immanuel Kant

In „Kritik der praktischen Vernunft“

Abstract

Water-soluble organic compounds (WSOCs) are major components of atmospheric aerosols, accounting for ~50% or more of the organic fraction of particulate matter. They can influence the optical properties and hygroscopicity of aerosol particles and their effects on climate. Moreover, they can contribute to the toxicity and allergenicity of air particulate matter.

In this study, high performance liquid chromatography coupled with optical diode array detection and mass spectrometry (HPLC-DAD-MS and HPLC-MS/MS) has been applied to measure WSOCs with a wide range of molecular masses and structures that are characteristic for different aerosol types, sources, and processes. Carboxylic acids and nitrophenols with low molecular mass were investigated as tracers for fossil fuel combustion and the formation and aging of secondary organic aerosols (SOA) from biogenic precursors. Protein macromolecules were investigated with regard to the influence of air pollution and nitration on the allergenicity of primary biological particles like pollen and fungal spores.

Filter samples of fine and coarse aerosol particles collected over a period of one year in central Europe (Mainz, Germany) were analyzed for WSOCs, including the α- and β-pinene oxidation products (pinic acid, pinonic acid and 3-methyl-1,2,3-butanetricarboxylic acid (3-MBTCA)) as well as a variety of dicarboxylic acids and nitrophenols. Seasonal variations and other characteristic features are discussed with regard to aerosol sources and sinks in comparison to data from other studies and regions. The ratios of adipic acid and phthalic acid to azelaic acid indicate that the investigated aerosol samples were mainly influenced by biogenic sources. A strong Arrhenius-type correlation was found between the 3-MBTCA concentration and inverse temperature ($R^2 = 0.79$, $E_a = 126\pm10$ kJ mol^{-1}, temperature range: 275–300 K). Model calculations suggest that the temperature dependence observed for 3-MBTCA can be explained by enhanced photochemical production due to an increase of OH radical concentration with increasing temperature, whereas the influence of gas-particle partitioning appears to play a minor role. The results suggest that the OH-initiated oxidation of pinonic acid is the rate-limiting step in the formation of 3-MBTCA, and that 3-MBTCA may be a suitable tracer for the chemical aging of biogenic SOA by OH radicals. An Arrhenius-type temperature dependence was also observed for the concentration of pinic acid ($R^2 = 0.60$, $E_a = 84\pm9$ kJ mol^{-1}); it can be tentatively explained by the temperature dependence of biogenic pinene emission as the rate-limiting step of pinic acid formation.

For the investigation of protein nitration, nitrated protein standards were synthesized by liquid-phase reaction of bovine serum albumin (BSA) and ovalbumin (OVA) with tetranitromethane (TNM). Protein nitration occurs primarily on residues of the aromatic amino acid tyrosine, and UV-Vis photometry was used to determine the protein nitration degree (ND), which is defined as the average number of nitrotyrosine residues divided by the total number of tyrosine residues in a protein molecule. BSA and OVA exhibited different relations between ND and TNM/tyrosine ratios in the reaction mixture, which is likely due to the different solubilities and molecular structures of the two proteins.

The nitration of BSA and OVA upon exposure to gas mixtures of nitrogen dioxide (NO_2) and (O_3) was investigated with a newly developed analytical method using HPLC-DAD. This simple and robust method enables the determination of ND without hydrolysis or digestion of the investigated protein macromolecules, and thus efficient investigation of the reaction kinetics of protein nitration. For detailed product studies, however, nitrated BSA and OVA were enzymatically digested. The obtained oligopeptides were analyzed using advanced HPLC-MS/MS techniques and database search functions, and high sequence coverage was achieved. The nitration degrees of individual nitrotyrosine residues (ND_Y) were well correlated with the overall protein ND, and different ratios of ND_Y to ND provided insight into the regioselectivity of the reaction. The nitration patterns observed in BSA and OVA nitrated with TNM indicate that the vicinity of negatively charge amino acids promotes the nitration of tyrosine residues. The nitration patterns observed in BSA nitrated by NO_2 and O_3 differed from those obtained with TNM, which indicates that the regioselectivity of protein nitration depends on the nitrating agent. However, tyrosine residues located in loop structures were preferentially nitrated regardless of the nitrating agent.

The methods and results of this study provide a basis for further detailed investigations of the reaction kinetics, products and mechanisms of protein nitration. They shall help to elucidate the relations between traffic-related air pollutants like nitrogen oxides and O_3 and the allergenicity of air particulate matter.

Zusammenfassung

Wasserlösliche organische Verbindungen (WSOCs) sind Hauptbestandteile atmosphärischer Aerosole, die bis zu ~ 50% und mehr der organischen Aerosolfraktion ausmachen. Sie können die optischen Eigenschaften sowie die Hygroskopizität von Aerosolpartikeln und damit deren Auswirkungen auf das Klima beeinflussen. Darüber hinaus können sie zur Toxizität und Allergenität atmosphärischer Aerosole beitragen.In dieser Studie wurde Hochleistungsflüssigchromatographie gekoppelt mit optischen Diodenarraydetektion und Massenspektrometrie (HPLC-DAD-MS und HPLC-MS/MS) angewandt, um WSOCs zu analysieren, die für verschiedene Aerosolquellen und -prozesse charakteristisch sind. Niedermolekulare Carbonsäuren und Nitrophenole wurden als Indikatoren für die Verbrennung fossiler Brennstoffe und die Entstehung sowie Alterung sekundärer organischer Aerosole (SOA) aus biogenen Vorläufern untersucht. Protein-Makromoleküle wurden mit Blick auf den Einfluss von Luftverschmutzung und Nitrierungsreaktionen auf die Allergenität primärer biologischer Aerosolpartikel – wie Pollen und Pilzsporen – untersucht.

Filterproben von Grob- und Feinstaubwurden über ein Jahr hinweg gesammelt und auf folgende WSOCs untersucht: die Pinen-Oxidationsprodukte Pinsäure, Pinonsäure und 3-Methyl-1,2,3-Butantricarbonsäure (3-MBTCA) sowie eine Vielzahl anderer Dicarbonsäuren und Nitrophenole. Saisonale Schwankungen und andere charakteristische Merkmale werden mit Blick auf Aerosolquellen und -senken im Vergleich zu Daten anderen Studien und Regionen diskutiert. Die Verhätlnisse von Adipinsäure und Phthalsäure zu Azelainsäure deuten darauf hin, dass die untersuchten Aerosolproben hauptsächlich durch biogene Quellen beeinflusst werden. Eine ausgeprägte Arrhenius-artige Korrelation wurde zwischen der 3-MBTCA--Konzentration und der inversen Temperatur beobachtet (R^2 = 0.79, E_a = 126±10 kJ mol^{-1}, Temperaturbereich 275–300 K). Modellrechnungen zeigen, dass die Temperaturabhängigkeit auf eine Steigerung der photochemischen Produktionsraten von 3-MBTCA durch erhöhte OH-Radikal-Konzentrationen bei erhöhten Temperaturen zurückgeführt werden kann. Im Vergleich zur chemischen Reaktionskinetik scheint der Einfluss von Gas-Partikel-Partitionierungseffekten nur eine untergeordnete Rolle zu spielen. Die Ergebnisse zeigen, dass die OH-initiierte Oxidation von Pinosäure der geschwindigkeitsbestimmende Schritt der Bildung von 3-MBTCA ist. 3-MBTCA erscheint somit als Indikator für die chemische Alterung von biogener sekundärer organischer Aerosole (SOA) durch OH-Radikale geeignet. Eine Arrhenius-artige Temperaturabhängigkeit wurde auch für Pinäure beobachtet und kann durch die Temperaturabhängigkeit der biogenen Pinen-Emissionen als geschwindigkeitsbestimmender Schritt der Pinsäure-Bildung erklärt werden (R^2 = 0.60, E_a = 84±9 kJ mol^{-1}).

Für die Untersuchung von Proteinnitrierungreaktionen wurde nitrierte Proteinstandards durch Flüssigphasenreaktion von Rinderserumalbumin (BSA) und Ovalbumin (OVA) mit Tetranitromethan (TNM) synthetisiert.Proteinnitrierung erfolgt vorrangig an den Resten der aromatischen Aminosäure Tyrosin auf, und mittels UV-Vis-Photometrie wurde der Proteinnnitrierungsgrad (ND) bestimmt. Dieser ist definiert als Verhältnis der mittleren Anzahl von Nitrotyrosinresten zur Tyrosinrest-Gesamtzahl in den Proteinmolekülen. BSA und OVA zeigten verschiedene Relationen zwischen ND und TNM/Tyrosin-Verhältnis im Reaktionsgemisch, was vermutlich auf Unterschiede in den Löslichkeiten und den molekularen Strukturen der beiden Proteine zurück zu führen ist.

Die Nitrierung von BSA und OVA durch Exposition mit einem Gasgemisch aus Stickstoffdioxid (NO_2) und Ozon (O_3) wurde mit einer neu entwickelten HPLC-DAD--Analysemethode untersucht. Diese einfache und robuste Methode erlaubt die Bestimmung des ND ohne Hydrolyse oder Verdau der untersuchten Proteine und ernöglicht somit eine effiziente Untersuchung der Kinetik von Proteinnitrierungs-Reaktionen. Für eine detaillierte Produktstudien wurden die nitrierten Proteine enzymatisch verdaut, und die erhaltenen Oligopeptide wurden mittels HPLC-MS/MS und Datenbankabgleich mit hoher Sequenzübereinstimmung analysiert. Die Nitrierungsgrade individueller Nitrotyrosin-Reste (ND_Y) korrelierten gut mit dem Gesamt-Proteinnitrierungsgrad (ND), und unterschiedliche Verhältnisse von ND_Y zu ND geben Aufschluss über die Regioselektivität der Reaktion. Die Nitrierungmuster von BSA und OVA nach Beahndlung mit TNM deuten darauf hin, dass die Nachbarschaft eines negativ geladenen Aminosäurerestes die Tyrosinnitrierung fördert. Die Behandlung von BSA durch NO_2 und O_3 führte zu anderend Nitrierungemustern als die Behandlung mit TNM, was darauf hindeutet, dass die Regioselektivität der Nitrierung vom Nitrierungsmittel abhängt. Es zeigt sich jedoch, dass Tyrosinreste in Loop-Strukturen bevorzugt und unabhängig vom Reagens nitriert werden.Die Methoden und Ergebnisse dieser Studie bilden eine Grundlage für weitere, detaillierte Untersuchungen der Reaktionskinetik sowie der Produkte und Mechanismen von Proteinnitrierungreaktionen. Sie sollen helfen, die Zusammenhänge zwischen verkehrsbedingten Luftschadstoffen wie Stickoxiden und Ozon und der Allergenität von Luftstaub aufzuklären.

TABLE OF CONTENTS

1. Background and Motivation

An aerosol is defined as a suspension of liquid or solid particles in a gas with particle diameter of 10^{-9}-10^{-4} m. In atmospheric sciences, however, the term aerosol traditionally refers to suspended particles that contain a large proportion of condensed matter other than water (Pöschl, 2005). Atmospheric aerosol particles originate from natural and anthropogenic sources. On the other hand, according the formation process of airborne particles, aerosol particles can be primary particles or secondary particles. Primary particles are directly emitted from a large range of sources including biomass burning, incomplete combustion of fossil fuels, volcanic eruptions and wind-driven or traffic-related suspension of road, soil, and mineral dust, sea salt, and biological materials (plant fragments, microorganisms, pollen, etc.); secondary particles are formed by gas-to-particle conversion in the atmosphere (new particle formation by nucleation and condensation of gaseous precursors) (Pöschl, 2005).

The properties of particulate matter highly depend on its components, which raises the study on the components of the aerosols. However, only a small fraction of particulate matter has been identified on a molecular level. Due to the chemical complexity of aerosol particles, the analysis is often carried out with the division into the following classes: sulphate, nitrate, ammonia, organic, black carbon and other components. The typical composition of continental aerosols is shown in Fig 1-1.

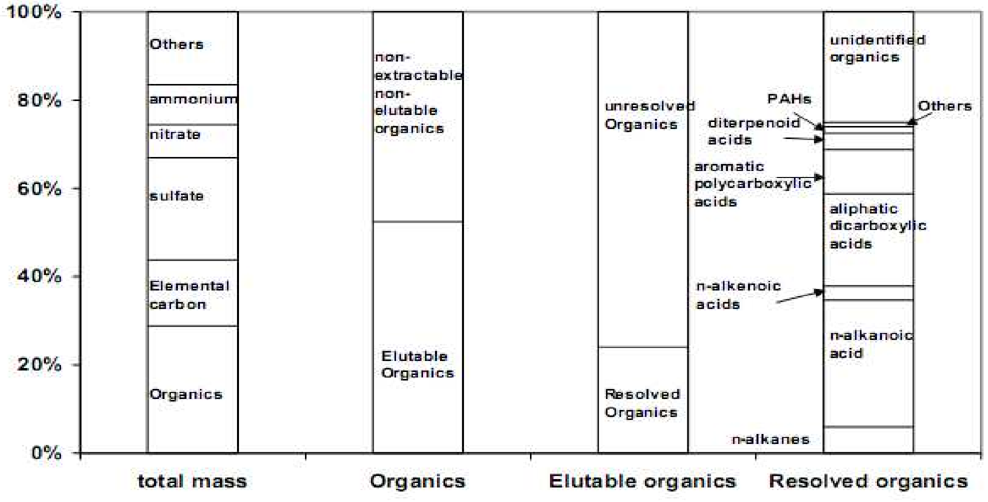

Fig 1-1 Mass balance on the chemical composition of annual mean fine particle concentrations at West Los Angeles in 1982 (Rogge et al., 1993).

Because of the effects of aerosols on the atmosphere, climate, and public health, the research interest of aerosols has been raised. Aerosols not only directly influence the energy balance of the entire globe by scattering and absorbing the incoming solar and terrestrial radiation, which translates into cooling of the atmosphere, but also indirectly cause the cooling of the atmosphere through cloud activation which they are involved, e.g. the formation of clouds and precipitation as cloud condensation and ice nuclei. Aerosol particles also affect the abundance and distribution of atmospheric trace gases by heterogeneous chemical reactions and other multiphase processes (Finlayson-Pitts et al., 2000; Houghton et al., 2001; Lohmann et al., 2005; Seinfeld et al., 1998). Moreover, airborne particles can cause or enhance respiratory, cardiovascular, infectious and allergic diseases during the spreading of biological organisms, reproductive materials, and pathogens (pollen, bacteria, spores, viruses, etc.) (Pöschl, 2005).

1.1 Water-soluble organic compounds in atmospheric aerosols

Organic aerosol mass can contribute 30 % to 70 % to total aerosol mass (Zhang et al., 2007). Most chemical speciation of organic aerosol is performed on an extracted fraction in nonpolar organic solvents such as benzene, ether, hexane, or dichloromethane. The nonpolar organic solvent extractable mass typically accounts for only 50-60 % of the total organic aerosol (Cass, 1998). Besides, a number of studies have also shown that water-soluble organic compounds ($WSOC_S$) constitute a significant fraction of carbon mass. Some studies performed in urban and rural sites have reported that water soluble organic carbon accounts for approximately 20 % to 67 % of the total particulate carbon in the atmosphere (Cadle et al., 1982; Decesari et al., 2000; Mueller et al., 1982; Sempere et al., 1994). They include organic anions, dicarboxylic acids, oxocarboxylic acids, dicarbonyls, carbohydrates, amino acids, aliphatic amines, urea, and some miscellaneous multifunctional compounds containing multiple hydroxyl, carboxyl, and carbonyl groups (e.g. glyceraldehyde, malic acid, citric acid, lactic acid, and tartaric acid) (Saxena et al., 1996). Nevertheless, WSOC composition remains poorly characterized. In this study, main discussions are denoted to analysis and characterization of small molecular weight compounds in the atmosphere including α- and β-pinene (the word pinene in the following text means bothα- and β-pinene) oxidation products, aliphatic and aromatic dicarboxylic acids and nitrophenols and high molecular weight compounds such as native and nitrated proteins.

1.1.1 Terpene oxidation products

Biogenic volatile organic compounds (BVOC) referred to volatile organic aerosol emitted by vegetation. About 800 Tg C yr^{-1} of global emission was estimated (Lathiere et al., 2006). The largest class of emission sources is volatile isoprenoids including isoprene, monoterpenes, and sesquiterpene. Isoprene, the largest class of emitted volatile isoprenoids, is believed to contribute about half of the emission (Guenther et al., 2006). Monoterpenes, the other large class of emitted volatile isoprenoids, contribute about 10-15 % of the emission. The others which contribute to the emission as well are sesquiterpene and oxygenated volatile compounds including alcohols, aldehydes and ketones. The studies on BVOC focus on reactions of monoterpenes and isoprene. Pinic acid and pinonic acid are considered as the oxidation products of α-pinene and β-pinene and received lots of interest before (Christoffersen et al., 1998; Winterhalter et al., 1999), but studies showed other peaks in the OH and NO_x oxidation products of α-pinene and β-pinene. 3-Methyl-1,2,3-butanetricarboxylic acid, is found as a major component of pinene oxidation products in tropical rainforest aerosol from the Amazon basin and in summertime aerosol from Ghent, Belgium (Kubatova et al., 2000) and its structure was identified by Szmigielski et al. (Szmigielski et al., 2007). 3-hydroxyglutaric acid (Claeys et al., 2007), terpenylic acid and its dimmer (Claeys et al., 2009) were identified as the oxidation products of α-pinene and β-pinene as well.

1.1.2 Aliphatic and aromatic dicarboxylic acids and nitrophenols

The total aliphatic dicarboxylic acids account for 0.06-1.1 % of the total aerosol mass (Kawamura et al., 1993). In this group, oxalic acid, malonic acid and succinic acid (C_2 – C_4) are the most abundant species (Kawamura et al., 1993) and mainly found in gas phase. Aliphatic dicarboxylic acids as an important fraction of WSOC were found and studied in urban (Kawamura et al., 2005; Yao et al., 2003), rural (Limbeck et al., 2001), marine (Wang et al., 2006), tropical (Graham et al., 2003) and remote arctic atmosphere (Narukawa et al., 2002). Dicarboxylic acids have primary sources and secondary sources. Direct source includes motor exhaust emission (Kawamura et al., 1987), biomass combustion (Lefer et al., 1994; Legrand et al., 1996; Narukawa et al., 1999), and oceanic emission (Mochida et al., 2003). They were also considered to be secondary organic compounds formed from photo-oxidation of unsaturated fatty aids and cyclic alkenes (Hatakeyama et al., 1987; Kawamura et al., 1996). Pinic acid as a dicarboxylic acid and pinonic acid as an oxocarboxylic acid are considered to be ozonolysis products of pinene (Hatakeyama et al., 1989; Hatakeyama et al., 1991).

Aromatic acids, such as phthalic acid, attract lots of attention because of their abundance in the atmosphere and their toxic properties. Aromatic acids are directly emitted by anthropogenic sources, such as solvent evaporation and automobile exhaust emissions; thus, they are often used as markers of motor emission or combustion. More polar aromatic compounds such as aromatic monocarboxylic acids with additional hydroxyl, alkyl or methoxy groups have also been found in wood smoke (Iinuma et al., 2007; Nolte et al., 2001).

Nitrophenols including 2-nitrophenol and 4-nitrophenol originate from primary anthropogenic sources including combustion processes of motor vehicles (Nojima et al., 1983; Tremp et al., 1993), coal and wood as well as decomposition and hydrolysis reactions of herbicides and insecticides (Shafer et al., 1985). They can also be formed during the secondary processes including the nitration of phenol and the transformation of benzaldehyde under photochemical smog conditions (Grosjean, 1985; Luttke et al., 1997a; Luttke et al., 1997b). Nitrophenols have been found in urban, rural and even remote atmospheric aerosols. They were also found in rainwater and snow samples, which leads to a hypothesis that they plan an active role in cloud formation and precipitation processes (Harrison et al., 2005). Medical studies showed that nitrophenols were toxic to animals, and might be toxic to humans and vegetation (ATSDR – Agency for Toxic Substances and Disease Registry (1995), US).

1.1.3 Proteins

Cellular and protein particles injected into the atmosphere include pollen, spores, fur fibers and other species (Jaenicke, 2005). These materials exit not only in coarse particles such as pollen grains, but also in fine fraction because of fine fragments of pollen, microorganisms or plant debris and mixing of proteins dissolved in rain water with fine soil and road dust particles (Franze et al., 2005; Miguel et al., 1999; Zhang et al., 2003). Protein molecules account for up to 5 % of urban air particles and are the most prominent group of airborne allergens (Pöschl, 2005). They are known to be efficiently nitrated by peroxynitrite ($ONOO^-$). The reaction leads ortho-nitration of the aromatic amino acid tyrosine, 3-nitrotyrosine (Beckman et al., 1992; Graham et al., 1993). 3-Nitrotyrosine in its free or protein-bound form has been detected in association with at least 50 diseases and more than 80 animal models or cell culture systems (Greenacre et al., 2001), e.g. asthma (Kaminsky et al., 1999; Saleh et al., 1998). Medical studies indicate that allergies have been increasing during the last decades (Ring et al., 2001a; Ring et al., 2001b), which could be due to the traffic-related air pollution with high concentration of nitrogen oxides and ozone (Brunekreef, 2001; Brunekreef et al., 2003). Franze et al. (2005) proposed that the promotion of allergies by the traffic-related air pollution could be due to the protein nitration by polluted urban air. In his study, he found the airborne allergens such as Bet v 1 was easily nitrated by the polluted urban air. This hypothesis is supported by the immunological experiments of nitrated proteins with cells, mice and human sera (Gruijthuijsen et al., 2006). This raises the further investigations of protein nitration by air pollutants, including kinetic study and site -specific and -selective information.

1.2 Analytical techniques

1.2.1 Instrumentation: HPLC-MS and HPLC-MS/MS

The instrument used in the analysis is high performance liquid chromatography (HPLC) coupled to mass spectrometer (MS) or tandem mass spectrometer (MS/MS). Normally, an HPLC-MS(/MS) system consists of the following components: an HPLC system, an ion source, a mass analyzer, a detector, a vacuum system, an instrument-control system and a data system. The discussion are focused on the components which are important for the analysis in this study, i.e., the HPLC system, the ion source, and the mass analyzer.

1.2.1.1 HPLC system

The HPLC system consists of a pump, a degasser, a sample injection inlet and a column. An HPLC pump is to pump the mobile phases and sample through the column, and then to the mass spectrometer; a degasser can remove air exiting in the mobile phases leading to high pressure and unstable baseline; a sample injection inlet makes an accurate injection and then an accurate quantification possible. The most important part of an HPLC system is a column, which is for good separations of complex sample and it determines the type of the HPLC. The HPLC columns used in this study are reversed phase chromatography column, and a non-polar stationary phase and polar mobile phases are used in the separation.

1.2.1.2 Ion source

Two kinds of ionization methods are introduced here: electrospray (ESI) and nanoelectrospray (nanoESI). Ion source in HPLC-MS system is the interface between the HPLC system and the vacuum region of mass spectrometer. Nanoelectrospray operates on principles similar to electrospray with a significant reductions of flow rate and needle diameter. Here, the TurboIonSpray source (Applied Biosystems MDS SCIEX QSTAR, Toronto, Canada), which allows the use of flow rates up to 1.0 mL min^{-1}, is used to explain the principle of the ESI source (Figure 1-2).

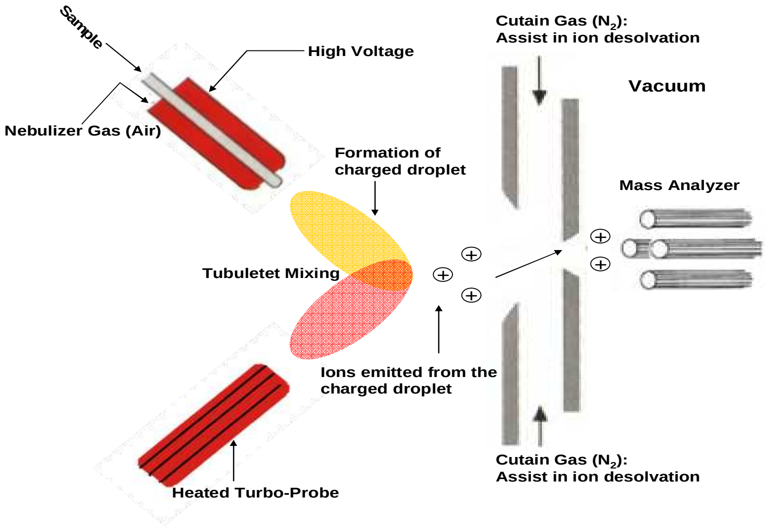

Fig 1-2 The Principle of TurboIonSpray

TurboIonSpray is an Atmospheric Pressure Ion Source in which pre-formed ions in solution are emitted into the gas phase with or without the application of heat. In this way, quasi-molecular ions can be generated from very labile and high molecular weight compounds with no thermal degradation.

When a liquid sample is pumped by an HPLC pump or driven syringe through the IonSpray Inlet, which is maintained at a high voltage, it is sprayed into the ion source creating a mist of highly charged droplets. Once introduced inside the ion source, the droplets evaporate causing the ions to enter the gas phase. At the same time, the TurboProbe directs a jet of heated dry nitrogen at the spray produced by the IonSpray, which helps focus the TurboIonSpray stream and increases the rate of droplet evaporation resulting in an increased ion signal.

1.2.1.3 Mass analyzer

In this study, two kinds of mass spectrometer are used for the analysis: one is singel quadrupole mass spectrometer (6130, Agilent, Waldbronn) and the hybrid mass spectrometer combining tandem quadrupole with the high mass resolution of a time-of-flight detector (Qq-TOF). Figure 1-3 shows the ion path chambers of the hybrid mass spectrometer QSTAR (pannel a, Applied Biosystems MDS SCIEX (Toronto, Canada)) and 6520 mass spectrometer (pannel b, Agilent, Waldbronn). The principle of the two Qq-TOF is similar. Here, the hybrid mass spectrometer QSTAR (pannel a, Applied Biosystems MDS SCIEX (Toronto, Canada)) will be used to explain the priciple.

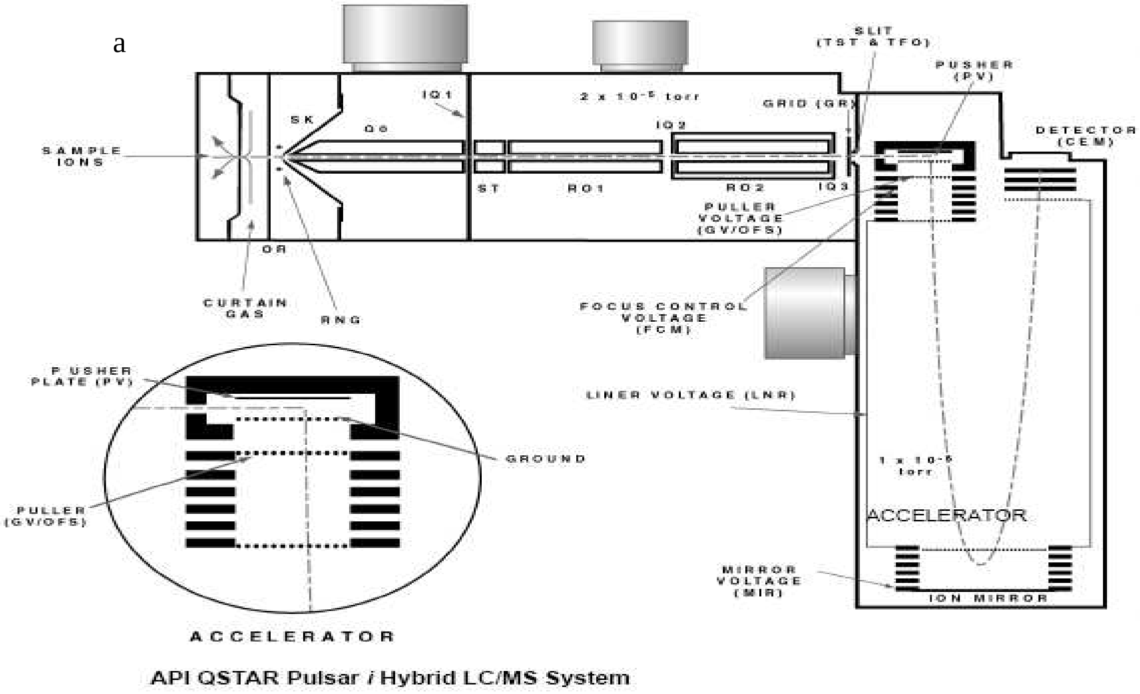

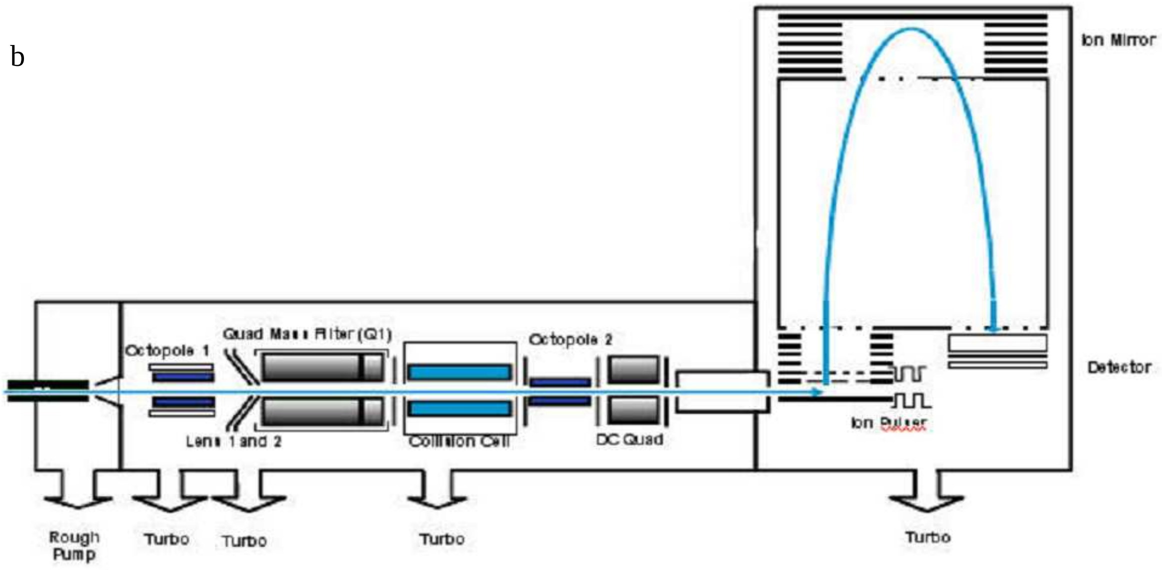

Fig 1-3 Ion Path Chamber of Qq-TOF of Qstar (panel A, applied biostystem, Applied Biosystems MDS SCIEX, Toronto, Canada), and 6520 (Panel B, Agilent, Waldbronn).

The hybrid mass spectrometer can provide tandem mass spectrometry. Fragments of these ions are analyzed in MS/MS experiments in order to obtain information about chemical structure of analytes. The ions of interest are selected in the first quadrupole (Q1). They are fragmented in the collision cell by collision (Q2) with neutral nitrogen molecules. The resulting fragment ions are analyzed in the TOF mass analyzer. This method is also called collision-induced dissociation (CID).

The TOF chamber inside the QSTAR hybrid system is located in an orthogonal direction relative to the set of three quadrupoles. This provides ion acceleration in a direction, which is perpendicular to the quadrupole ion beam, to correct the initial kinetic energy differences of ions with the same m/z values. There is a reflectron at the end of the drift zone, which refocuses the kinetic energy of ions with same m/z values. The reflectron consists of a series of metallic electrodes with different applied voltages, which generate a series of repulsing electric fields. This enables the detector to record all ions with the same m/z values at the same time, thus enhances the resolution.

1.2.2 Analysis of WSOC by HPLC-MS and HPLC-MS/MS

Many techniques and instruments have been developed to analyze WSOC in aerosols. Gas chromatography (GC) and GC coupled to mass spectrometer (GC-MS), HPLC-MS and HPLC-MS/MS, ion chromatography (IC) and other analytical techniques have been applied after the extraction procedure. About 85 % of WSOC are not sufficiently volatile or stable to be analyzed by GC, and LC is considered to be a suitable separation technique. Using HPLC, polar compounds could be separated and analyzed without derivatization. MS and MS/MS, which can provide information of WSOC such as the molecular weight and functional groups, have been applied as the detector. With the use of WSOC standards, quantitative analysis of them is possible. Several interfaces have been developed, which direct the flow from HPLC to MS and turn the target compounds into ions. In this study, ESI and nanoESI were used for the analysis of WSOC in the atmosphere such as carboxylic acids, nitrophenols as well as proteins and nitrated proteins.

Many techniques have been applied to analyze the carboxylic acid group in the atmosphere. To analyze a homologous series of dicarboxylic acids in the atmosphere, GC-MS, which requires derivatization of carboxylic acids (Kawamura et al., 1987), and IC equipped with electric conductivity detector (ECD) (Koch et al., 2000) have been reported before. HPLC-MS, which avoids derivatization of extracted samples, allows the qualitative and quantitative analysis of the dicarboxylic group in low concentration range. Rompp et al. (2006) has used this technique to analyze both dicarboxylic acids and oxocarboxylic acids in the atmosphere. Capillary electrophoresis (CE) has also been reported as an analyzing technique of this class of compounds in aerosol samples and vehicle emissions (Dabek-Zlotorzynska et al., 2001).

For the analysis of nitrophenols, GC-MS or GC with ECD or with nitrogen phosphorous detector (NPD) have been reported (Herterich, 1991; Leuenberger et al., 1985; Luttke et al., 1997b). High performance liquid chromatography coupled with a diode array detector (HPLC-DAD) was also used for nitrophenol detection (Belloli et al., 1999). In this study, HPLC-MS is used to quantify 2-nitrophenol and 4-nitrophenol, simultaneously with dicarboxylic acid and other compounds.

Many methods have been reported to analyze 3-nitrotyrosine either in its free form or in its protein binding form. The separation methods include two-dimensional polyacrylamide gel electrophoresis (2D-GE), solution isoelectric focusing (IEF) followed by polyacrylamide gel electrophoresis in the presence of sodium dodecylsulfate (SDS-PAGE), immunoprecipitation (IP), HPLC and so on. Mass spectrometric analysis has been widely applied for the identification of nitrotyrosine-containing proteins and peptides with the introduction of “soft” ionization techniques suitable for proteins and peptides. The so-called “soft” ionization techniques are ESI introduced by Whitehouse et al. (1985) and matrix-assisted laser desorption/ionization (MALDI) by Karas and Hillenkamp (Karas and Hillenkamp, 1988). MALDI with laser light at 337 nm with MS is widely used for protein and peptide analysis. However, nitrotyrosine-containing proteins and peptides are sensitive to the light of this wavelength and undergo decomposition. Reduction to aminotyrosine can circumvent this problem (Sarver et al., 2001). ESI has the advantage that it can generate ions from the effluent of an HPLC column, thus, provide the possibility of HPLC separation and further confirmation of nitrated protein or peptides by light absorbance at 360±5 nm under acidic conditions prior to MS (Crow and Ischiropoulos, 1996; Jiao et al., 2001; Souza et al., 1999; vanderVliet et al., 1996; Wong and Van Der Vliet, 2002). To better understand the nitration mechanism, the site-specific information is important, which needs to localize the nitrated amino acid in protein sequence. The reduction of nitrotyrosine to aminotyrosine may result in too little fragment information (Ghesquiere et al., 2006). Therefore, HPLC-MS/MS is a suitable technique to identify and localize tyrosine nitration. Moreover, quantification of nitrated peptides could be accomplished by the native reference peptide method, that is, to quantify modified peptides in a protein digest by selecting another reference peptide from the protein of interest as the internal standard (Willard et al., 2003).

1.3 Objectives

The aim of this study is to analyze and characterize the WSOC using HPLC-DAD-MS or HPLC-MS/MS. The thesis includes two parts: to analyze and characterize the low molecular weight WSOC in the atmosphere such as pinene oxidation products pinic acid, pinonic acid, 3-methyl-1,2,3-butanetricarboxylic acid (3-MBTCA), aliphatic and aromatic carboxylic acids and nitrophenols; to analyze and characterize the native and nitrated proteins.

One part in this thesis is to analyze and characterize the small molecular weight water-soluble organic in the atmosphere. Filter samples were collected over a period of one year from June, 2006 to May, 2007. Water-soluble organic compounds such as carboxylic acids and nitrophenols were extracted and analyzed. HPLC-MS allows the analysis of the pinene oxidation products pinic acid, pinonic acid and 3-MBTCA as well as a variety of dicarboxylic acids and nitrophenols at one run without any derivatization. In the study, seasonal variations and possible source of the compounds were discussed. Arrhenius-type temperature dependences of 3-MBTCA and pinic acid concentrations were observed. Model study has been complied to explain the observed temperature dependences.

The other part in this thesis is dedicated to the analysis of proteins and nitrated proteins. Standard proteins bovine serum albumin (BSA) and ovalbumin (OVA) were nitrated by tetronitromethane to obtain the nitrated BSA and OVA standards. An HPLC-DAD-MS method was developed to determine the nitration degrees (ND) of the nitrated proteins and proved to be suitable for the kinetic study of protein nitration. To get more details on protein nitration, e.g. the site-specific information, a tryptic digestion method followed by an HPLC-chip-MS/MS analysis was applied. The ND of individual nitrotyrosine (ND_Y) was determined and strong linear correlations between ND and ND_Y were found. Different slopes of the linear correlations suggest protein nitration is site-selective. Possible factors causing the site selectivity were discussed.

1.4 References

Beckman, J. S., H. Ischiropoulos, L. Zhu, M. Vanderwoerd, C. Smith, J. Chen, J. Harrison, J. C. Martin and M. Tsai (1992). " Kinetics of superoxide dismutase- and iron-catalyzed nitration of phenolics by peroxynitrite." Archives of Biochemistry and Biophysics **298**(2): 438-445.

Belloli, R., B. Barletta, E. Bolzacchini, S. Meinardi, M. Orlandi and B. Rindone (1999). "Determination of toxic nitrophenols in the atmosphere by high-performance liquid chromatography." Journal of Chromatography A **846**(1-2): 277-281.

Brunekreef, B. (2001). "NO_2: the gas, that won't go away." Clinical and Experimental Allergy **31**(8): 1170-1172.

Brunekreef, B. and J. Sunyer (2003). "Asthma, rhinitis and air pollution: is traffic to blame?" European Respiratory Journal **21**(6): 913-915.

Cadle, S. H., P. J. Groblicki and P. A. Mulawa (1982). " Factors affecting the sampling and analysis of atmospheric carbonaceous particulate matter." Abstracts of Papers of the American Chemical Society **183**(Mar): 60-Envr.

Cass, G. R. (1998). "Organic molecular tracers for particulate air pollution sources." Trac-Trends in Analytical Chemistry **17**(6): 356-366.

Christoffersen, T. S., J. Hjorth, O. Horie, N. R. Jensen, D. Kotzias, L. L. Molander, P. Neeb, L. Ruppert, R. Winterhalter, A. Virkkula, K. Wirtz and B. R. Larsen (1998). "Cis-pinic acid, a possible precursor for organic aerosol formation from ozonolysis of alpha-pinene." Atmospheric Environment **32**(10): 1657-1661.

Claeys, M., Y. Iinuma, R. Szmigielski, J. D. Surratt, F. Blockhuys, C. Van Alsenoy, O. Boge, B. Sierau, Y. Gomez-Gonzalez, R. Vermeylen, P. Van der Veken, M. Shahgholi, A. W. H. Chan, H. Herrmann, J. H. Seinfeld and W. Maenhaut (2009). "Terpenylic acid and related compounds from the oxidation of alpha-pinene: implications for new particle formation and growth above forests." Environmental Science & Technology **43**(18): 6976-6982.

Claeys, M., R. Szmigielski, I. Kourtchev, P. Van der Veken, R. Vermeylen, W. Maenhaut, M. Jaoui, T. E. Kleindienst, M. Lewandowski, J. H. Offenberg and E. O. Edney (2007). "Hydroxydicarboxylic acids: markers for secondary organic aerosol from the photooxidation of alpha-pinene." Environmental Science & Technology **41**(5): 1628-1634.

Crow, J. P. and H. Ischiropoulos (1996). "Detection and quantitation of nitrotyrosine residues in proteins: In vivo marker of peroxynitrite." Nitric Oxide, Pt B **269**: 185-194.

Dabek-Zlotorzynska, E., M. Piechowski, M. McGrath and E. P. C. Lai (2001). "Determination of low-molecular-mass carboxylic acids in atmospheric aerosol and vehicle emission samples by capillary electrophoresis." Journal of Chromatography A **910**(2): 331-345.

Decesari, S., M. C. Facchini, S. Fuzzi and E. Tagliavini (2000). "Characterization of water-soluble organic compounds in atmospheric aerosol: a new approach." Journal of Geophysical Research-Atmospheres **105**(D1): 1481-1489.

Finlayson-Pitts, B. J. and J. N. Pitts (2000). "Chemistry of the Upper and Lower Atmosphere." San Diego, Academic Press.

Franze, T., M. G. Weller, R. Niessner and U. Pöschl (2005). "Protein Nitration by Polluted Air." Environ. Sci. Technol. **39**(6): 1673-1678.

Ghesquiere, B., M. Goethals, J. Van Damme, A. Staes, E. Timmerman, J. Vandekerckhove and K. Gevaert (2006). "Improved tandem mass spectrometric characterization of 3-nitrotyrosine sites in peptides." Rapid Communications in Mass Spectrometry **20**(19): 2885-2893.

Graham, A., N. Hogg, B. Kalyanaraman, V. Oleary, V. Darleyusmar and S. Moncada (1993). "Peroxynitrite modification of low-density-lipoprotein leads to recognition by the macrophage scavenger receptor." Febs Letters **330**(2): 181-185.

Graham, B., P. Guyon, W. Maenhaut, P. E. Taylor, M. Ebert, S. Matthias-Maser, O. L. Mayol-Bracero, R. H. M. Godoi, P. Artaxo, F. X. Meixner, M. A. L. Moura, C. Rocha, R. Van Grieken, M. M. Glovsky, R. C. Flagan and M. O. Andreae (2003). "Composition and diurnal variability of the natural Amazonian aerosol." Journal of Geophysical Research-Atmospheres **108**(D24): 4765, doi:10.1029/2003JD004049.

Greenacre, S. A. B. and H. Ischiropoulos (2001). "Tyrosine nitration: localisation, quantification, consequences for protein function and signal transduction." Free Radical Research **34**(6): 541-581.

Grosjean, D. (1985). "Reactions of o-cresol and nitrocresol with NO_X in sunlight and with ozone nitrogen-dioxide mixtures in the dark." Environmental Science & Technology **19**(10): 968-974.

Gruijthuijsen, Y. K., I. Grieshuber, A. Stoecklinger, U. Tischler, T. Fehrenbach, M. G. Weller, L. Vogel, S. Vieths, U. Pöschl and A. Duschl (2006). "Nitration enhances the allergenic potential of proteins." International Archives of Allergy and Immunology **141**: 265-275.

Guenther, A., T. Karl, P. Harley, C. Wiedinmyer, P. I. Palmer and C. Geron (2006). "Estimates of global terrestrial isoprene emissions using MEGAN (Model of Emissions of Gases and Aerosols from Nature)." Atmospheric Chemistry and Physics **6**: 3181-3210.

Harrison, M. A. J., S. Barra, D. Borghesi, D. Vione, C. Arsene and R. L. Olariu (2005). "Nitrated phenols in the atmosphere: a review." Atmospheric Environment **39**(2): 231-248.

Hatakeyama, S., K. Izumi, T. Fukuyama and H. Akimoto (1989). "Reactions of ozone with alpha-pinene and beta-pinene in air - yields of gaseous and particulate products." Journal of Geophysical Research-Atmospheres **94**(D10): 13013-13024.

Hatakeyama, S., K. Izumi, T. Fukuyama, H. Akimoto and N. Washida (1991). "Reactions of OH with alpha-pinene and beta-pinene in air - estimate of global CO production from the atmospheric oxidation of terpenes." Journal of Geophysical Research-Atmospheres **96**(D1): 947-958.

Hatakeyama, S., M. Ohno, J. H. Weng, H. Takagi and H. Akimoto (1987). "Mechanism for the formation of gaseous and particulate products from ozone-cycloalkene reactions in air." Environmental Science & Technology **21**(1): 52-57.

Herterich, R. (1991). "Gas-chromatographic determination of nitrophenols in atmospheric liquid water and airborne-particulates." Journal of Chromatography **549**(1-2): 313-324.

Houghton, J. T., Y. Ding, D. J. Griggs, M. Noguer, P. J. van der Linden, X. Dai, K. Maskell and C. A. Johnson (2001). Climate change 2001: the scientific basis. Contributions of working group I to the third assessment report of the intergovernmental panel on climate change. Cambridge, Cambridge University Press.

Iinuma, Y., E. Bruggemann, T. Gnauk, K. Muller, M. O. Andreae, G. Helas, R. Parmar and H. Herrmann (2007). "Source characterization of biomass burning particles: the combustion of selected European conifers, African hardwood, savanna grass, and German and Indonesian peat." Journal of Geophysical Research-Atmospheres **112**(D8): D08209, doi:10.1029/2006JD007120.

Jaenicke, R. (2005). "Abundance of cellular material and proteins in the atmosphere." Science **308**(5718): 73-73.

Jiao, K. S., S. Mandapati, P. L. Skipper, S. R. Tannenbaum and J. S. Wishnok (2001). "Site-selective nitration of tyrosine in human serum albumin by peroxynitrite." Analytical Biochemistry **293**(1): 43-52.

Kaminsky, D. A., J. Mitchell, N. Carroll, A. James, R. Soultanakis and Y. Janssen (1999). "Nitrotyrosine formation in the airways and lung parenchyma of patients with asthma." Journal of Allergy and Clinical Immunology **104**(4): 747-754.

Karas, M. and F. Hillenkamp (1988). "Laser desorption ionization of proteins with molecular masses exceeding 10000 Daltons." Analytical Chemistry **60**(20): 2299-2301.

Kawamura, K. and K. Ikushima (1993). "Seasonal-changes in the distribution of dicarboxylic-acids in the urban atmosphere." Environmental Science & Technology **27**(10): 2227-2235.

Kawamura, K. and I. R. Kaplan (1987). "Motor exhaust emissions as a primary source for dicarboxylic-acids in Los-Angeles ambient air." Environmental Science & Technology **21**(1): 105-110.

Kawamura, K., H. Kasukabe and L. A. Barrie (1996). "Source and reaction pathways of dicarboxylic acids, ketoacids and dicarbonyls in arctic aerosols: one year of observations." Atmospheric Environment **30**(10-11): 1709-1722.

Kawamura, K. and O. Yasui (2005). "Diurnal changes in the distribution of dicarboxylic acids, ketocarboxylic acids and dicarbonyls in the urban Tokyo atmosphere." Atmospheric Environment **39**(10): 1945-1960.

Koch, S., R. Winterhalter, E. Uherek, A. Kolloff, P. Neeb and G. K. Moortgat (2000). "Formation of new particles in the gas-phase ozonolysis of monoterpenes." Atmospheric Environment **34**(23): 4031-4042.

Kubatova, A., R. Vermeylen, M. Claeys, J. Cafmeyer, W. Maenhaut, G. Roberts and P. Artaxo (2000). "Carbonaceous aerosol characterization in the Amazon basin, Brazil: novel dicarboxylic acids and related compounds." Atmospheric Environment **34**(29-30): 5037-5051.

Lathiere, J., D. A. Hauglustaine, A. D. Friend, N. De Noblet-Ducoudre, N. Viovy and G. A. Folberth (2006). "Impact of climate variability and land use changes on global biogenic volatile organic compound emissions." Atmospheric Chemistry and Physics **6**: 2129-2146.

Lefer, B. L., R. W. Talbot, R. C. Harriss, J. D. Bradshaw, S. T. Sandholm, J. O. Olson, G. W. Sachse, J. Collins, M. A. Shipham, D. R. Blake, K. I. Klemm, O. Klemm, K. Gorzelska and J. Barrick (1994). "Enhancement of Acidic Gases in Biomass Burning Impacted Air Masses over Canada." Journal of Geophysical Research-Atmospheres **99**(D1): 1721-1737.

Legrand, M. and M. DeAngelis (1996). "Light carboxylic acids in Greenland ice: A record of past forest fires and vegetation emissions from the boreal zone." Journal of Geophysical Research-Atmospheres **101**(D2): 4129-4145.

Leuenberger, C., M. P. Ligocki and J. F. Pankow (1985). "Trace Organic-Compounds in Rain .4. Identities, Concentrations, and Scavenging Mechanisms for Phenols in Urban Air and Rain." Environmental Science & Technology **19**(11): 1053-1058.

Limbeck, A., H. Puxbaum, L. Otter and M. C. Scholes (2001). "Semivolatile behavior of dicarboxylic acids and other polar organic species at a rural background site (Nylsvley, RSA)." Atmospheric Environment **35**(10): 1853-1862.

Lohmann, U. and J. Feichter (2005). "Global indirect aerosol effects: a review." Atmospheric Chemistry and Physics **5**: 715-737.

Luttke, J. and K. Levsen (1997a). "Occurrence and formation of nitrated phenols in clouds at two

European sites." Proceedings of Eurotrac Symposium '96 - Transport and Transformation of Pollutants in the Troposphere, Vol 1: 101-107.

Luttke, J., V. Scheer, K. Levsen, G. Wunsch, J. N. Cape, K. J. Hargreaves, R. L. StoretonWest, K. Acker, W. Wieprecht and B. Jones (1997b). "Occurrence and formation of nitrated phenols in and out of cloud." Atmospheric Environment **31**(16): 2637-2648.

Miguel, A. G., G. R. Cass, M. M. Glovsky and J. Weiss (1999). "Allergens in paved road dust and airborne particles." Environmental Science & Technology **33**(23): 4159-4168.

Mochida, M., N. Umemoto, K. Kawamura and M. Uematsu (2003). "Bimodal size distribution of C_2-C_4 dicarboxylic acids in the marine aerosols." Geophysical Research Letters **30**(13): 1672, doi:10.1029/2003GL017451.

Mueller, P. K., K. K. Fung, S. L. Heisler, D. Grosjean and G. M. Hidy (1982). Atmospheric particulate carbon observations in urban and rural areas of the United States. Particulate Carbon—Atmospheric Life Cycle. G. T. W. a. R. L. Klimisch. New York, Plenum Press**:** 343-370.

Narukawa, M., K. Kawamura, S. M. Li and J. W. Bottenheim (2002). "Dicarboxylic acids in the Arctic aerosols and snowpacks collected during ALERT 2000." Atmospheric Environment **36**(15-16): PII S1352-2310(1302)00126-00127.

Narukawa, M., K. Kawamura, N. Takeuchi and T. Nakajima (1999). "Distribution of dicarboxylic acids and carbon isotopic compositions in aerosols from 1997 Indonesian forest fires." Geophysical Research Letters **26**(20): 3101-3104.

Nojima, K., A. Kawaguchi, T. Ohya, S. Kanno and M. Hirobe (1983). "Studies on photochemical-reaction of air-pollutants .10. Identification of nitrophenols in suspended particulates." Chemical & Pharmaceutical Bulletin **31**(3): 1047-1051.

Nolte, C. G., J. J. Schauer, G. R. Cass and B. R. T. Simoneit (2001). "Highly polar organic compounds present in wood smoke and in the ambient atmosphere." Environmental Science & Technology **35**(10): 1912-1919.

Pöschl, U. (2005). "Atmospheric aerosols: Composition, transformation, climate and health effects." Angewandte Chemie-International Edition **44**(46): 7520-7540.

Ring, J., B. Eberlein-Koenig and H. Behrendt (2001a). "Environmental pollution and allergy." Annals of Allergy Asthma & Immunology **87**(6): 2-6.

Ring, J., U. Kramer, T. Schafer and H. Behrendt (2001b). "Why are allergies increasing?" Current Opinion in Immunology **13**(6): 701-708.

Rogge, W. F., M. A. Mazurek, L. M. Hildemann, G. R. Cass and B. R. T. Simoneit (1993). "Quantification of urban organic aerosols at a molecular-level - identification, abundance and seasonal-variation." Atmospheric Environment Part a-General Topics **27**(8): 1309-1330.

Rompp, A., R. Winterhalter and G. K. Moortgat (2006). "Oxodicarboxylic acids in atmospheric aerosol particles." Atmospheric Environment **40**(35): 6846-6862.

Saleh, D., P. Ernst, S. Lim, P. J. Barnes and A. Giaid (1998). "Increased formation of the potent oxidant peroxynitrite in the airways of asthmatic patients is associated with induction of nitric oxide synthase: effect of inhaled glucocorticoid." Faseb Journal **12**(11): 929-937.

Sarver, A., N. K. Scheffler, M. D. Shetlar and B. W. Gibson (2001). "Analysis of peptides and proteins containing nitrotyrosine by matrix-assisted laser desorption/ionization mass spectrometry." Journal of the American Society for Mass Spectrometry **12**(4): 439-448.

Saxena, P. and L. M. Hildemann (1996). "Water-soluble organics in atmospheric particles: A critical review of the literature and application of thermodynamics to identify candidate compounds." Journal of Atmospheric Chemistry **24**(1): 57-109.

Seinfeld, J. H. and S. N. Pandis (1998). Atmospheric chemistry and physics. New York, Wiley.

Sempere, R. and K. Kawamura (1994). "Comparative Distributions of Dicarboxylic-Acids and Related Polar Compounds in Snow Rain and Aerosols from Urban Atmosphere." Atmospheric Environment **28**(3): 449-459.

Shafer, W. E. and J. Schonherr (1985). "Accumulation and transport of phenol, 2-nitrophenol, and 4-nitrophenol in plant cuticles." Ecotoxicology and Environmental Safety **10**(2): 239-252.

Souza, J. M., E. Daikhin, M. Yudkoff, C. S. Raman and H. Ischiropoulos (1999). "Factors determining the selectivity of protein tyrosine nitration." Archives of Biochemistry and Biophysics **371**(2): 169-178.

Szmigielski, R., J. D. Surratt, Y. Gomez-Gonzalez, P. Van der Veken, I. Kourtchev, R. Vermeylen, F. Blockhuys, M. Jaoui, T. E. Kleindienst, M. Lewandowski, J. H. Offenberg, E. O. Edney, J. H. Seinfeld, W. Maenhaut and M. Claeys (2007). "3-methyl-1,2,3-butanetricarboxylic acid: An atmospheric tracer for terpene secondary organic aerosol." Geophysical Research Letters **34**(24).

Tremp, J., P. Mattrel, S. Fingler and W. Giger (1993). "Phenols and nitrophenols as tropospheric pollutants - emissions from automobile exhausts and phase-transfer in the atmosphere." Water Air and Soil Pollution **68**(1-2): 113-123.

vanderVliet, A., J. P. Eiserich, H. Kaur, C. E. Cross and B. Halliwell (1996). "Nitrotyrosine as biomarker for reactive nitrogen species." Nitric Oxide, Pt B **269**: 175-184.

Wang, H. B. and Kawamura, K. (2006). "Stable carbon isotopic composition of low-molecular-weight dicarboxylic acids and ketoacids in remote marine aerosols." Journal of Geophysical Research-Atmospheres **111**(D7): D07304, doi:10.1029/2005JD006466.

Whitehouse, C. M., R. N. Dreyer, M. Yamashita and J. B. Fenn (1985). "Electrospray interface for liquid chromatographs and mass spectrometers." Analytical Chemistry **57**(3): 675-679.

Willard, B. B., C. I. Ruse, J. A. Keightley, M. Bond and M. Kinter (2003). "Site-specific quantitation of protein nitration using liquid chromatography/tandem mass spectrometry." Analytical Chemistry **75**(10): 2370-2376.

Winterhalter, R., P. Neeb, D. Grossmann, A. Kolloff, O. Horie and G. Moortgat (1999). "Products and mechanism of the gas phase reaction of ozone with beta-pinene." Journal of Atmospheric Chemistry **35**(2): 165-197.

Wong, P. S. Y. and A. Van Der Vliet (2002). "Quantitation and localization of tyrosine nitration in proteins." Nitric Oxide, Pt D **359**: 399-410.

Yao, X. H., A. P. S. Lau, M. Fang, C. K. Chan and M. Hu (2003). "Size distributions and formation of ionic species in atmospheric particulate pollutants in Beijing, China: 2 - dicarboxylic acids." Atmospheric Environment **37**(21): 3001-3007.

Zhang, Q. and C. Anastasio (2003). "Free and combined amino compounds in atmospheric fine particles (PM2.5) and fog waters from Northern California." Atmospheric Environment **37**(16): 2247-2258.

Zhang, Q., J. L. Jimenez, M. R. Canagaratna, J. D. Allan, H. Coe, I. Ulbrich, M. R. Alfarra, A. Takami, A. M. Middlebrook, Y. L. Sun, K. Dzepina, E. Dunlea, K. Docherty, P. F. DeCarlo, D. Salcedo, T. Onasch, J. T. Jayne, T. Miyoshi, A. Shimono, S. Hatakeyama, N. Takegawa, Y. Kondo, J. Schneider, F. Drewnick, S. Borrmann, S. Weimer, K. Demerjian, P. Williams, K. Bower, R. Bahreini, L. Cottrell, R. J. Griffin, J. Rautiainen, J. Y. Sun, Y. M. Zhang and D. R. Worsnop (2007). "Ubiquity and dominance of oxygenated species in organic aerosols in anthropogenically-influenced Northern Hemisphere midlatitudes." Geophysical Research Letters **34**(13): L13801, Doi 10.1029/2007gl029979.

2. HPLC-MS analysis of carboxylic acids and nitrophenols

2.1 Introduction

Water-soluble organic compounds (WSOCs) are major components of atmospheric aerosols, accounting for up to ~50% or more of the organic fraction of particulate matter. They can influence the optical properties and hygroscopicity of aerosol particles and their effects on climate. WSOCs originate from primary emissions like fossil fuel combustion and biomass burning as well as from secondary formation in the atmosphere, i.e., photo-oxidation of anthropogenic or biogenic precursors (Pöschl, 2005).

Organic acids are a prominent group of WSOC and were found in urban, rural, marine and polar aerosols in various regions around the world as detailed below (Kawamura and Ikushima, 1993; Kawamura et al., 1996b; Kawamura and Usukura, 1993). This group includes monocarboxylic acids, dicarboxylic acids, oxocarboxylic acids and tricarboxylic acids. The total dicarboxylic acids account for 0.06-1.1 % of the total aerosol mass and oxalic acid, malonic acid and succinic acid (C_2-C_4) are the most abundant species in the dicarboxylic acid group (Kawamura and Ikushima, 1993). Dicarboxylic acids originate from a wide range of sources. Primary sources include motor exhaust (Kawamura and Kaplan, 1987), biomass combustion (Kundu et al., 2010; Lefer et al., 1994; Legrand and DeAngelis, 1996; Narukawa et al., 1999) and oceanic emissions (Mochida et al., 2003b). Secondary formation sources are the photooxidation of unsaturated fatty aids and cyclic alkenes (Hatakeyama et al., 1987; Kawamura et al., 1996a). The photo-oxidation of biogenic hydrocarbons is a major source of secondary organic aerosol (SOA) (Hoffmann et al., 1997), and SOA formation by oxidation of pinene and other terpenes has been studied extensively (Hallquist et al., 2009). Pinic acid as a dicarboxylic acid and pinonic acid as an oxocarboxylic acid are major products of the ozonolysis or OH radical-initiated oxidation of pinene (α- and β- pinene, the word pinene stands for both α- and β- pinene in the following text) (Atkinson and Arey, 2003; Hatakeyama et al., 1989; Hatakeyama et al., 1991; Yu et al., 1999a). Further reaction of the first-generation oxidation products of pinene leads to highly oxidized, acyclic, polar compounds (Jaoui et al., 2005). Among the second-generation products of pinene photooxidation is 3-methyl-1,2,3-butanetricarboxylic acid (3-MBTCA), which is formed by OH-initiated oxidation of cis-pinonic acid (Szmigielski et al., 2007) and was first detected in aerosol samples from Amazonia and Belgium (Kubatova et al., 2002; Kubatova et al., 2000). Another prominent group of WSOC are nitrophenols like 2-nitrophenol and 4-nitrophenol, which have been found in urban and rural aerosol, rainwater and snow samples. They originate from primary sources including motor vehicle exhaust (Nojima et al., 1983; Tremp et al., 1993), coal and wood combustion, as well as decomposition and hydrolysis reactions of herbicides and insecticides (Shafer and Schonherr, 1985). Moreover, they are formed by nitration of phenol and the transformation of benzaldehyde under photochemical smog conditions (Grosjean, 1985; Luttke and Levsen, 1997; Luttke et al., 1997). Road traffic is considered to be the main source of nitrophenols.

Nitrophenols are usually analyzed by gas chromatography coupled with a mass spectrometer (GC-MS), with an electron capture detector (GC-ECD), or with a nitrogen phosphorous detector (GC-NPD) (Herterich, 1991; Leuenberger et al., 1985; Luttke et al., 1997). Belloli et al. (1999) used high performance liquid chromatography coupled with a diode array detector (HPLC-DAD) for nitrophenol detection. Most studies of carboxylic acids used GC-MS after derivatization, i.e., conversion of the acids into methyl- or butylesters (Kawamura and Ikushima, 1993). Rompp et al. (2006) and Warnke et al (2006) applied high performance liquid chromatography coupled with a mass spectrometer (HPLC-MS) for the analysis of organic acids in aerosol samples.

In this study, we apply HPLC-MS for the analysis of nitrophenols as well as carboxylic acids (aliphatic C_5-C_{16} dicarboxylic acids, phthalic, pinic, and pinonic acid, 3-MBTCA) in a large set of fine and coarse aerosol particle samples collected over a period of one year in central Europe (Mainz, Germany, June 2006 to May 2007).

2.2 Methods

2.2.1 Collection of filter samples

Aerosol samples were collected on glass fiber filters (Pall Corporation, Type A/A, 102-mm diameter) over a period of one year in Mainz, Germany (130 m a.s.l., June 2006–May 2007). The sampling station was positioned on a mast at the top of the Max Planck Institute for Chemistry (MPIC, ~5 m above the flat roof of the 3-story building) on the campus of the University of Mainz (49°59′31.36″N and 8°14′15.22″E). The air masses sampled at MPIC represent a mix of urban and rural continental boundary layer air in central Europe (Fröhlich-Nowoisky et al., 2009). A high-volume dichotomous sampler (Solomon et al., 1983) was used to separate and collect coarse and fine aerosol particles on a pair of glass fiber filters. The sampler was operated with a rotary vane pump (Becker VT 4.25) at a total flow rate of approximately 300 L min^{-1}, corresponding to a nominal cut-off diameter of ~3 μm. Coarse particles with aerodynamic diameters larger than the cut-off were collected through a virtual impactor operated in line with the inlet (~27 L min^{-1}), and fine particles with aerodynamic diameters smaller than the cut-off were collected from the main gas flow perpendicular to the inlet (~270 L min^{-1}).

The sampling period was generally ~7 days, corresponding to a sampled air volume of approximately 3000 m^3. A few samples were collected over shorter periods (1 – 5 days, ~400 – 2000 m^3). A list of all investigated air filter samples (57 coarse and 58 fine particle samples) and of the corresponding sampling times and volumes is given in sect. A2 (Table A1 and A2).

For the investigation of seasonal trends, the air samples were grouped into summer (June, July and August, JJA) (coarse: 18; fine: 18), autumn (September October and November, SON) (coarse: 14; fine: 14), winter (December, January and February, DJF) (coarse: 12; fine: 13) and spring (March, April and May, MAM) (coarse: 13; fine: 13). Before use, all glass fiber filters were decontaminated by baking at 500°C over night. Loaded filters were packed in aluminum foil (also prebaked at 500°C), and stored in a freezer at −80°C until WSOC extraction. (Frohlich-Nowoisky et al., 2009).

2.2.2 Sample extraction and analysis (HPLC-MS)

A filter aliquot (typically 1/8 sector) was transferred into a 7 mL glass vial with a PTFE-coated cap and extracted with 2 mL of a water-methanol mixture (methanol volume fraction 10 %, water: chromatography grade, Merck, Darmstadt, Germany; methanol: LC-MS grade, Merck, Darmstadt, Germany). The sample vials were sonicated for 30 minutes in an ice bath. The extract solution was collected using an Eppendorf pipette with polyethylene (PE) tips. Subsequently, the filters were extracted for the second time following the same procedure and the extract solutions were combined and used directly for HPLC-MS analysis (Rompp et al., 2006).

The applied HPLC-MS system consists of a thermostated auto-sampler (Series 200, Perkin Elmer, Norwalk, Connecticut, USA), a degasser and a quaternary pump (1100 Series, Agilent Technologies, Waldbronn, Germany), and a hybrid Qq-TOF mass spectrometer QSTAR (Applied Biosystems MDS SCIEX, Toronto, Canada) with an electrospray ion source (ESI). The ESI source was operated in the negative mode with an ionization voltage of 4 kV at 400 °C. The selected m/z range was 120 to 300 Da. The data processing was performed with the software package Analyst (version QS1.1, Applied Biosystems MDS SCIEX, Toronto, Canada). The room and column temperature were kept at 296 K, and the injection volume was 100 µL. The chromatographic separation of all investigated compounds was performed with a ReproSil-Pur C_{18}-AQ column (250 mm x 2.1 mm I.D., 5 µm particle size) in a stainless steel cartridge (Dr. Maisch GmbH, Ammerbuch, Germany) at a flow rate of 400 µL min^{-1}. For the first 0.5 min of each chromatographic run, the composition of the mobile phase was kept at 100 % water with formic acid (HCOOH volume fraction 0.1 %, Chromasolv, Sigma, Seelze, Germany). Then the acetonitrile (ACN, Chromasolv, Sigma, Seelze, Germany) content was increased to 15 % within 3.5 min, and further to 95 % within 16 min. Finally the mobile phase was reset to initial conditions within 3 min, and the column was equilibrated for 6 min before the next run (Winterhalter et al., 2009). Chromatograms were recorded using the deprotonated molecule ion signals of the analytes ($[M-H]^-$ detected at m/z = M-1). The molecular masses (M) and retention times (RT) of the investigated compounds are listed in Table 2-1.

Table 2- 1 Molecular weight, retention time and detection limits of investigated organic compounds.

Compound	M[a] g mol^{-1}	RT[b] min	LOD[c] nmol L^{-1}	LOQ[d] nmol L^{-1}	ELOD_coarse[e] ng m^{-3}	ELOQ_coarse[f] ng m^{-3}	ELOD_fine[g] ng m^{-3}	ELOQ_fine[h] ng m^{-3}
Glutaric Acid (C_5)	132	7.59	14.36	47.88	0.02	0.08	0.03	0.09
Adipic Acid (C_6)	146	9.01	3.01	10.03	0.01	0.02	0.01	0.02
Pimelic Acid (C_7)	160	10.35	2.69	8.96	0.01	0.02	0.01	0.02
Suberic Acid (C_8)	174	11.59	19.22	64.07	0.04	0.14	0.05	0.16
Azelaic Acid (C_9)	188	12.75	19.10	63.65	0.05	0.15	0.05	0.17
Sebacic Acid (C_{10})	202	13.87	1.83	6.09	0.005	0.02	0.01	0.02
Dodecanedioic Acid (C_{12})	230	15.84	1.68	5.60	0.005	0.02	0.01	0.02
Tridecanedioic Acid (C_{13})	244	17.17	1.74	5.80	0.01	0.02	0.01	0.02
Tetradecanedioic Acid (C_{14})	258	16.77	1.62	5.39	0.01	0.02	0.01	0.02
Hexadecanedioic Acid (C_{16})	286	19.54	1.29	4.30	0.005	0.02	0.01	0.02
Phthalic Acid (Ph)	166	10.72	2.85	9.50	0.01	0.02	0.01	0.02
3-methyl-1,2,3-butanetricarboxylic acid (3-MBTCA)	204	9.45	0.59	1.98	0.002	0.01	0.002	0.01
Pinic Acid	186	11.04	1.90	6.35	0.004	0.01	0.005	0.02
Pinonic Acid	184	13.88	18.06	60.20	0.04	0.14	0.05	0.16
4-Nitrocatechol	155	12.30	20.10	67.00	0.04	0.13	0.04	0.15
2-Nitropnenol	138	14.18	17.28	57.61	0.03	0.10	0.03	0.11
4-Nitrophenol	138	14.86	11.58	38.60	0.02	0.07	0.02	0.08

[a] molecular weight;

[b] retention time;

[c] limit of detection of the HPLC-MS method defined as 3-fold standard deviation of background signal;

[d] limit of quantification of the HPLC-MS method defined as 10-fold standard deviation of background signal;

[e] effective limit of detection of aerosol filter content in coarse particulate matter, corresponding to 7-day sample;

[f] effective limit of quantification of aerosol filter content in coarse particulate matter, corresponding to 7-day sample;

[g] effective limit of detection of aerosol filter content in fine particulate matter, corresponding to 7-day sample;

[h] effective limit of quantification of aerosol filter content in fine particulate matter, corresponding to 7-day sample.

The analytes were identified by comparison of retention time and mass spectra with reference standards (Sigma/Fluka, purity ≥ 98 %; 3-MBTCA from M. Claeys, University of Antwerp) (Winterhalter et al., 2009). As pure cis-pinic acid was not available, we used the mixture of cis- and trans-pinic acid as reference standard and assumed a response factor of 1 between the two isomers for the quantification of cis-pinic acid in aerosol filter samples. Due to limited availability and purity of the 3-MBTCA reference standard, we used a calibration curve obtained with 1,3,5-pentatricarboxylic acid and assumed a response factor of unity for the quantification of 3-MBTCA. Small aliphatic dicarboxylic acids consisting of less than five carbon atoms were eluted in the dead volume of the chromatographic column and were thus not investigated in this study.

For every analyte, a linear calibration function of peak area vs. concentration was established and applied for quantification (correlation coefficient $R^2 > 0.98$, number of data points n =12). As detailed in Table 1, the analytical limits of detection (LOD, 3s method, 0.59-20.10 nmol L^{-1},) and quantification (LOQ, 10s method, 1.98-67.00 nmol L^{-1}) correspond to effective limits of 0.002-0.05 ng m^{-3} (ELOD) and 0.01-0.17 ng m^{-3} (ELOQ) for the detection and quantification of the investigated compounds in the coarse and fine aerosol samples, respectively. Measurement results for blank filter samples were generally below the LOD, except for adipic acid (C_6) and azelaic acid (C_9). For these two acids blank values larger than the LOQ, were observed and subtracted from the aerosol sample measurement results. The relative standard deviation of repeated measurements was generally less than 5 %. Therefore, the precision of the measurement accounting for imprecision of sample flow control and recovery (Winterhalter et al., 2009) is estimated to be less than 20 %.

Mass concentrations of the analytes in the investigated air samples were determined by scaling with the extract volume, filter aliquot fraction, and sampled air volume. Due to the operating principle of the dichotomous sampler, the coarse particle filter samples contained a contribution of fine particles corresponding to the ratio of air flow through the coarse filter to total air flow (~1/10). To correct for this interference, 1/10 of the concentration determined for fine particles was subtracted from the concentration determined for coarse particles. All measurement results are listed in sect. A2 (Table A1 and A2). Correlation analyses were performed for all investigated compounds, and the correlation coefficients obtained for coarse and fine particle samples are also listed in Table 2-3 and 2-4. Exponential fits were also performed between concentrations of investigated compounds and inverse temperature, and Arrhenius-type temperature dependence were found for 3-MBTCA and pinic acid, which is discussed below.

2.2.3 Supporting data and model calculations

Ambient temperature (daily mean values of recoded minimum and maximum temperature values, averaged over filter sampling period) and precipitation data were recorded on top of the 7–story building of the Institute of Atmospheric Physics of the University of Mainz, which is less than 500 m away from the sampling site.

Hydroxyl radical (OH) concentration data were obtained from a simulation (1998-2008) with the ECHAM/MESSy Atmospheric Chemistry model (EMAC, time resolution: 15 min, output frequency: 5 h, averaged over filter sampling period) (Jöckel et al., 2006). The OH concentration data were used for model calculations investigating the observed Arrhenius-type temperature dependence of 3-MBTCA as detailed in sect. A3 and discussed below.

2.3 Results and discussion

2.3.1 Concentration levels and seasonal variations

For all dicarboxylic acids, nitrophenols and pinene oxidation products investigated in this study, the observed concentration ranges, mean values and standard deviations are summarized in Table 2-2. For comparison we have also performed a comprehensive literature search and compiled data from other atmospheric aerosol studies and locations where these WSOCs have been analyzed.

The mean concentrations of individual dicarboxylic acids in fine particulate matter (PM_3, 0.09-3.76 ng m^{-3}) were generally lower than the values reported from polluted urban areas and megacity regions (Houston, USA; Hong Kong, and 14 economically developed or developing cities in China; 0.29-35.6 ng m^{-3})). With regard to total suspended particles (TSP, fine plus coarse particulate matter), the mean concentrations observed in Mainz (0.14-5.71 ng m^{-3}) were higher than values reported from Arctic regions (0.06-0.9 ng m^{-3}), similar to values reported from Philadelphia, USA (PM_{10}, 0.5-3.5 ng m^{-3}), and generally lower than the values reported from Tokyo, Japan, and Melpitz, Germany (PM_{10}, n.d.-25.8 ng m^{-3}). The highest mean concentrations in Mainz were observed for phthalic acid (PM_3: 3.76 ng m^{-3}; TSP: 5.71 ng m^{-3}) and for the pinene oxidation products pinic acid (PM_3: 1.51 ng m^{-3}; TSP: 2.32 ng m^{-3}) and 3-MBTCA (PM_3: 5.89 ng m^{-3}; TSP: 6.88 ng m^{-3}).

Seasonal variations of investigated compounds were studied (Fig. 2-1, 2-2 and 2-3), and, to our knowledge, this is the first study reporting a full annual cycle and characteristic differences in the seasonal variation of nitrophenols and 3-MBTCA. For most aliphatic dicarboxylic acids the seasonal mean concentration was highest in summer and spring, indicating biogenic or photochemical sources as discussed below (Fig. 2-1). Some of the lower seasonal values found in summer could be attributed to wet deposition of water-soluble compounds due to large amount of precipitation in summer (total precipitation of 186.5 mm in summer, 107.6 mm in autumn, 136.0 mm in winter, and 121.6 mm in spring). 4-Nitrocatechol and 2-nitrophenol also exhibited maximum concentrations in summer, whereas 4-nitrophenol exhibited maximum concentrations in winter (Fig. 2-2). The different seasonalities can be attributed to the different sources and formation pathways as discussed below. To our knowledge this is the first study reporting a full annual cycle and characteristic differences in the seasonal variation of nitrophenols and 3-MBTCA.

The most pronounced seasonal cycles and summertime maxima were observed for the pinene oxidation products 3-MBTCA, pinic acid and pinonic acid (Fig. 2-3), which exhibited also pronounced Arrhenius-type temperature dependencies that can be attributed to photochemistry and biogenic emissions as discussed below. The average particulate concentration level decreased with increasing volatility from 3-MBTCA (non-volatile) via pinic acid (low/semi-volatile) to pinonic acid (high/semi-volatile, see sect. A3).

The concentration of 3-MBTCA was generally higher in the fine particle fraction than in the coarse fraction. During summer and autumn the pinic acid concentration was also higher in the fine fraction than in the coarse fraction, but during winter and spring the concentration was similar in the fine and coarse fractions. The pinonic acid concentration was similar in the fine and coarse fractions during summer and autumns, but during winter and spring the concentration was higher in the coarse fraction. These differences may be related to the different volatilities and concentration levels of the three compounds, to seasonal differences in ambient temperature, and possibly also to seasonal differences in the overall aerosol particle size distribution and composition. Information about the latter parameters is unfortunately not available and further investigations would go beyond the scope of the present study. Nevertheless, we suggest and intend to investigate these effects and interactions in future studies, because they may be relevant for comprehensive characterisation, understanding and modelling of the sources and properties of organic aerosols.

Table 2- 2 Concentrations of WSOC measured in coarse and fine aerosols in this study and other studies.

Compound	Concentration (ng m^{-3})		Particle	Location, time	Publication
	Range	Mean±SD[a]			
Glutaric Acid (C_5)	0.16-6.15	1.28±0.99	PM_3[b]	Mainz, Germany 2006-2007	this study
		30	$PM_{2.5}$[c]	China 2003 summer	Ho et al., 2007
		22.1	$PM_{2.5}$	China 2003 winter	Ho et al., 2007
		35.56	$PM_{2.5}$	Hong Kong urban summer 2006	Hu et al., 2008
		7.73	$PM_{2.5}$	USA Houston area suburban 2000	Yue and Fraser, 2004
		2.3	PM_{10}[d]	Philadelphia, USA, July-August 1999	Ray and McDow, 2005
		6.8	PM_{10}	Melpitz, Germany/rural 2005	van Pinxteren and Herrmann, 2007
	1.24-18.41	2.56±1.27	TSP[e]	Mainz, Germany 2006-2007	this study
		0.9	TSP	Arctic July 1987 June 1988	Kawamura et al., 1996a
		11	TSP	Tokyo, Japan/urban July 1989	Kawamura and Yasui, 2005
		23.1	TSP	Tokyo, Japan/urban June 1989	Kawamura and Yasui, 2005
		18.2	TSP	Tokyo, Japan/urban Nov 1989	Kawamura and Yasui, 2005
Adipic Acid (C_6)	0.17-2.71	0.78±0.57	PM_3	Mainz, Germany 2006-2007	this study
		23.5	$PM_{2.5}$	China 2003 summer	Ho et al., 2007
		15	$PM_{2.5}$	China 2003 winter	Ho et al., 2007
		11.376	$PM_{2.5}$	Hong Kong urban summer 2006	Hu et al., 2008
		7.52	$PM_{2.5}$	USA Houston area suburban 2000	Yue and Fraser, 2004
		2	PM_{10}	Philadelphia, USA, July-August 1999	Ray and McDow, 2005
		13.8	PM_{10}	Melpitz, Germany/rural 2005	van Pinxteren and Herrmann, 2007
	0.59-4.69	1.51±0.84	TSP	Mainz, Germany 2006-2007	this study
		0.82	TSP	Arctic July 1987 June 1988	Kawamura et al., 1996a
		13	TSP	Tokyo, Japan/urban July 1989	Kawamura and Yasui, 2005
		25.8	TSP	Tokyo, Japan/urban June 1989	Kawamura and Yasui, 2005
		14.2	TSP	Tokyo, Japan/urban Nov 1989	Kawamura and Yasui, 2005
Pimelic Acid (C_7)	BDL[f]-1.77	0.32±0.31	PM_3	Mainz, Germany 2006-2007	this study

		6.34	$PM_{2.5}$	China 2003 summer	Ho et al., 2007
		6.7	$PM_{2.5}$	China 2003 winter	Ho et al., 2007
		4.564	$PM_{2.5}$	Hong Kong urban summer 2006	Hu et al., 2008
		2.58	$PM_{2.5}$	USA Houston area suburban 2000	Yue and Fraser, 2004
		1.6	PM_{10}	Melpitz, Germany/rural 2005	van Pinxteren and Herrmann, 2007
	BDL-2.05	0.58±0.39	TSP	Mainz, Germany 2006-2007	this study
		0.13	TSP	Arctic July 1987 June 1988	Kawamura et al., 1996a
		4.6	TSP	Tokyo, Japan/urban July 1989	Kawamura and Yasui, 2005
		9.9	TSP	Tokyo, Japan/urban June 1989	Kawamura and Yasui, 2005
		8.2	TSP	Tokyo, Japan/urban Nov 1989	Kawamura and Yasui, 2005
Suberic Acid (C_8)	0.11-1.87	0.44±0.35	PM_3	Mainz, Germany 2006-2007	this study
		9.06	$PM_{2.5}$	China 2003 summer	Ho et al., 2007
		5.98	$PM_{2.5}$	China 2003 winter	Ho et al., 2007
		5.43	$PM_{2.5}$	USA Houston area suburban 2000	Yue and Fraser, 2004
		0.5	PM_{10}	Philadelphia, USA, July-August 1999	Ray and McDow, 2005
		2.1	PM_{10}	Melpitz, Germany/rural 2005	van Pinxteren and Herrmann, 2007
	0.32-2.44	0.78±0.45	TSP	Mainz, Germany 2006-2007	this study
		0.15	TSP	Arctic July 1987 June 1988	Kawamura et al., 1996a
		2.4	TSP	Tokyo, Japan/urban July 1989	Kawamura and Yasui, 2005
		11	TSP	Tokyo, Japan/urban June 1989	Kawamura and Yasui, 2005
		9.1	TSP	Tokyo, Japan/urban Nov 1989	Kawamura and Yasui, 2005
Azelaic Acid (C_9)	0.12-4.64	1.60±1.04	PM_3	Mainz, Germany 2006-2007	this study
		31.6	$PM_{2.5}$	China 2003 summer	Ho et al., 2007
		28.9	$PM_{2.5}$	China 2003 winter	Ho et al., 2007
		10.07	$PM_{2.5}$	USA Houston area suburban 2000	Yue and Fraser, 2004
		1	PM_{10}	Philadelphia, USA, July-August 1999	Ray and McDow, 2005
		2.1	PM_{10}	Melpitz, Germany/rural 2005	van Pinxteren and Herrmann, 2007
	0.13-1.45	2.91±1.25	TSP	Mainz, Germany 2006-2007	this study

		0.26	TSP	Arctic July 1987 June 1988	Kawamura et al., 1996a
		11	TSP	Tokyo, Japan/urban July 1989	Kawamura and Yasui, 2005
		15.1	TSP	Tokyo, Japan/urban June 1989	Kawamura and Yasui, 2005
		20.6	TSP	Tokyo, Japan/urban Nov 1989	Kawamura and Yasui, 2005
Sebacic Acid (C_{10})	0.06-1.31	0.24±0.20	PM_3	Mainz, Germany 2006-2007	this study
		2.49	$PM_{2.5}$	China 2003 summer	Ho et al., 2007
		4.4	$PM_{2.5}$	China 2003 winter	Ho et al., 2007
		2.58	$PM_{2.5}$	USA Houston area suburban 2000	Yue and Fraser, 2004
		n.d.[g]	PM_{10}	Melpitz, Germany/rural 2005	van Pinxteren and Herrmann, 2007
	0.13-1.45	0.39±0.24	TSP	Mainz, Germany 2006-2007	this study
		1.1	TSP	Tokyo, Japan/urban July 1989	Kawamura and Yasui, 2005
		4.9	TSP	Tokyo, Japan/urban June 1989	Kawamura and Yasui, 2005
		7.3	TSP	Tokyo, Japan/urban Nov 1989	Kawamura and Yasui, 2005
Dodecanedioic Acid (C_{12})	BDL-1.24	0.09±0.17	PM_3	Mainz, Germany 2006-2007	this study
		0.91	$PM_{2.5}$	14 cities in China 2003 summer	Ho et al., 2007
		0.29	$PM_{2.5}$	14 cities in China 2003 winter	Ho et al., 2007
	BDL-1.34	0.15±0.18	TSP	Mainz, Germany 2006-2007	this study
Tridecanedioic Acid (C_{13})	BDL-2.04	0.09±0.27	PM_3	Mainz, Germany 2006-2007	this study
	BDL-2.11	0.14±0.29	TSP	Mainz, Germany 2006-2007	this study
Tetradecanedioic Acid (C_{14})	BDL-2.05	0.11±0.28	PM_3	Mainz, Germany 2006-2007	this study
	BDL-2.21	0.18±0.31	TSP	Mainz, Germany 2006-2007	this study
Hexadecanedioic Acid (C_{16})	BDL-2.05	0.13±0.29	PM_3	Mainz, Germany 2006-2007	this study
	BDL-2.18	0.20±0.31	TSP	Mainz, Germany 2006-2007	this study
Phthalic Acid (Ph)	0.69-13.38	3.76±2.87	PM_3	Mainz, Germany 2006-2007	this study
		3.36	$PM_{2.5}$	Hong Kong urban summer 2006	Hu et al., 2008
		12.4	PM_{10}	Melpitz, Germany/rural 2005	van Pinxteren and Herrmann, 2007
		3.5	PM_{10}	Philadelphia, USA, July-August 1999	Ray and McDow, 2005
	1.24-18.41	5.71±3.73	TSP	Mainz, Germany 2006-2007	this study

3-Methyl-1,2,3-butanetricarboxylic acid	1.6–99.3	13^{h}	PM_1	Hyytiälä, Finland, July-Aug 2005	Kourtchev et al., 2008a
(3-MBTCA)	1.9–74	15.8	PM_2	K-puszta, Hungary, summer 2003	Kourtchev et al., 2009
		5.2	$PM_{2.5}$	Jülich, Germany, July 2003	Kourtchev et al., 2008b
	n.d.–1.6		$PM_{2.5}$	Balbina, Brazil, Mar-Apr 1998	Kubatova et al., 2000
	15.8–130	41.95	$PM_{2.5}$	Research Triangle Park, NC, USA, summer 2003	Lewandowski et al., 2007
	0.13-26.00	5.89±6.15	PM_3	Mainz, Germany 2006-2007	this study
	0.13-29.72	6.88±7.04	TSP	Mainz, Germany 2006-2007	this study
	3.47-25.9		TSP	Mt. Tai, China, May to June 2006	Fu et al., 2009b
	0.005-2.613	0.647±0.786	TSP	Canadian high Arctic, Feb-Jun, 1991	Fu et al., 2009a
Pinic Acid	2–29.6	7.7^{h}	PM_1^{i}	Hyytiälä, Finland, July-Aug 2005	Kourtchev et al., 2008a
	0.6-135	12.2	PM_2	K-puszta, Hungary, summer 2003	Kourtchev et al., 2009
	1.1–21		$PM_{2.5}$	Tábua, Portugal Aug 1996	Kavouras et al., 1999b
		3.0	$PM_{2.5}$	Jülich, Germany, July 2003	Kourtchev et al., 2008b
	4.5-15.5	9.98	$PM_{2.5}$	Research Triangle Park, NC, USA, summer 2003	Lewandowski et al., 2007
	0.38–4.7		$PM_{2.5}$	Hyytiälä, Finland 2001	Warnke et al., 2006
	1.1–21		$PM_{2.5}$	Hyytiälä, Finland 2003	Warnke et al., 2006
	0.43–3.8		$PM_{2.5}$	Jülich, Germany 2002	Warnke et al., 2006
	0.94–12		$PM_{2.5}$	Jülich, Germany 2003	Warnke et al., 2006
	BDL-9.05	1.51±2.24	PM_3	Mainz, Germany 2006-2007	this study
	0.06-12.17	2.32±2.72	TSP	Mainz, Germany 2006-2007	this study
	0.36-6.27		TSP	Mt. Tai, China, May to June 2006	Fu et al., 2009b
	0.03-1.357	0.514±0.401	TSP	Canadian high Arctic, Feb-Jun, 1991	Fu et al., 2009a
		2.4±1.5	TSP	Pertouli, Greece Aug 1998	Kavouras and Stephanou, 2002
	0.4–82.7		TSP	Pertouli, Greece Aug 1997	Kavouras et al., 1999a
	0.48 - 0.59	0.54	TSP	Nova Scotia, Canada Jul 1996	Yu et al., 1999b
		0.5	TSP	San Bernadino, CA Sep 1998	Yu et al., 1999b
Pinonic Acid (PA)	7.1 - 98		$PM_{2.5}$	Tábua, Portugal Aug 1996	Kavouras et al., 1998; 1999b

	0.91–8.2		$PM_{2.5}$	Hyytiälä, Finland 2001	Warnke et al., 2006
	0.99–74		$PM_{2.5}$	Hyytiälä, Finland 2003	Warnke et al., 2006
	1.1–5.9		$PM_{2.5}$	Jülich, Germany 2002	Warnke et al., 2006
	1.4–78		$PM_{2.5}$	Jülich, Germany 2003	Warnke et al., 2006
	BDL-5.60	0.60±1.01	PM_3	Mainz, Germany 2006-2007	this study
	BDL-5.60	1.22±1.33	TSP	Mainz, Germany 2006-2007	this study
	0.21-21.8		TSP	Mt. Tai, China, May to June 2006	Fu et al., 2009b
	0.038-0.108	0.069±0.023	TSP	Canadian high Arctic, Feb-Jun, 1991	Fu et al., 2009b
		9.7±11	TSP	Pertouli, Greece Aug 1998	Kavouras and Stephanou, 2002
	1 - 25.7		TSP	Pertouli, Greece Aug 1997	Kavouras et al., 1999a
	0.13 - 0.39	0.26	TSP	Nova Scotia, Canada Jul 1996	Yu et al., 1999b
		0.8	TSP	San Bernadino, CA Sep 1998	Yu et al., 1999b
4-Nitrocatechol	BDL-26.30	6.40±17.55	PM_3	Mainz, Germany 2006-2007	this study
	BDL-28.72	4.49±5.32	TSP	Mainz, Germany 2006-2007	this study
2-Nitrophenol	BDL-8.51	1.57±1.45	PM_3	Mainz, Germany 2006-2007	this study
		3.5±1.5	PM_5	Rome, Italy, Spring 2003	Cecinato et al., 2005
	BDL-8.51	1.81±1.70	TSP	Mainz, Germany 2006-2007	this study
4-Nitrophenol	BDL-10.22	2.48±2.12	PM3	Mainz, Germany 2006-2007	this study
		17.8±5.6	PM5	Rome, Italy, Spring 2003	Cecinato et al., 2005
	BDL-12.52	3.78±2.89	TSP	Mainz, Germany 2006-2007	this study

[a] standard deviation;

[b] particles of aerodynamic diameters less than 3 µm (the cut-off of the dichotomous sampler in this study);

[c] particles of aerodynamic diameters less than 2.5 µm;

[d] particles of aerodynamic diameters less than 10 µm;

[e] total suspended particles, in this study, it's the sum of the particle contents in both coarse and fine mode;

[f] below detection limit (limit of quantification listed in table 2-1);

[g] not detected;

[h] is median value;

[i] particles of aerodynamic diameter less than 1 µm.

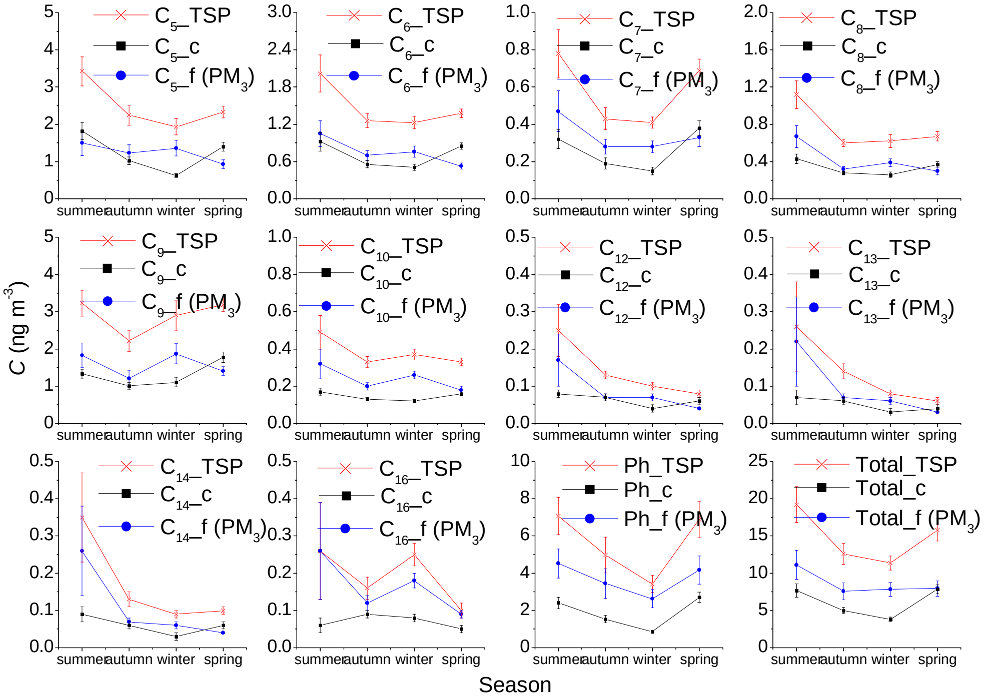

Figure 2- 1 Seasonal variations of dicarboxylic acid mass concentrations in fine, coarse, and total particulate matter (TSP). The data points are mean values for different seasons (summer: JJA, autumn: SON, winter: DJF, spring: MAM). The error bars are standard errors of the mean, and the lines are to guide the eye.

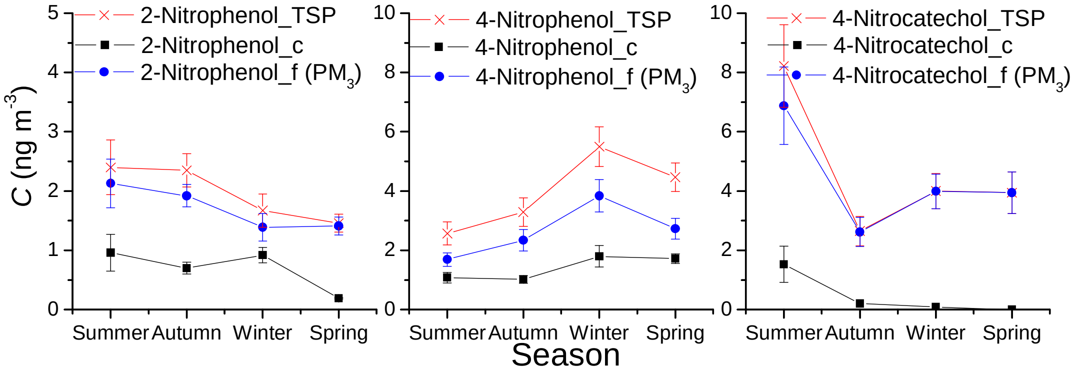

Figure 2- 2 Seasonal variations of 2-nitrophenol, 4-nitrophenol and 4-nitrocatechol mass concentrations in fine, coarse, and total particulate matter (TSP). The data points are mean values for different seasons (summer: JJA, autumn: SON, winter: DJF, spring: MAM). The error bars are standard errors of the mean, and the lines are to guide the eye.

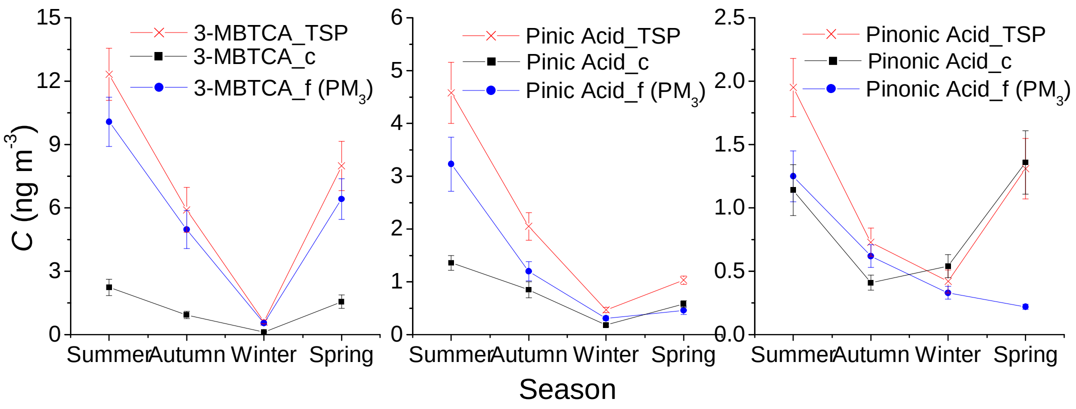

Figure 2- 3 Seasonal variation of pinene oxidation products: mass concentrations of 3-MBTCA, pinic acid and pinonic acid in fine, coarse, and total particulate matter (TSP). The data points are mean values for different seasons (summer: JJA, autumn: SON, winter: DJF, spring: MAM). The error bars are standard errors of the mean, and the lines are to guide the eye.

2.3.3 Source attribution of dicarboxylic acids and nitrophenols

Atmospheric photo-oxidation of volatile and semi-volatile organic compounds is considered to be the main source of dicarboxylic acids in air particulate matter. Mochida et.al. (2003a) proposed that small dicarboxylic acids containing up to 7 carbon atoms originate mostly from anthropogenic precursors. Glutaric acid is formed upon oxidation of cyclopentene cyclohexene and glutardialdehyde (Winterhalter et al., 2009). Adipic acid (C_6) originates from the oxidation of cyclohexene in the atmosphere (Hatakeyama et al., 1987; Koch et al., 2000), and from the ozonolysis of polycyclic aromatic hydrocarbons (PAHs) like methylene-cyclohexane and 1-methyl-cyclohexene (Koch et al., 2000). As an aromatic compound, phthalic acid is also considered to originate mostly from anthropogenic sources, including direct emission from automobile, industrial and other anthropogenic sources sources (manufacturing of plastics, hydrolysis of phthalate esters in the ageing of plastics), and the oxidation of PAHs (Kawamura and Ikushima, 1993). The correlation coefficients between phthalic acid and the sum of C_5-C_7 dicarboxylic acids (R^2 = 0.65 for coarse particles PM and 0.47 for fine particles) suggest that these compounds originate indeed from related sources.

According to Mochida et al. (2003a), the oxidation of biogenic precursors like unsaturated fatty acids is the main source of C_8-C_{10} dicarboxylic acids (Kawamura and Gagosian, 1987; Stephanou and Stratigakis, 1993). The most abundant of these compounds was azelaic acid (C_9, 2.9 ng m^{-3} in TSP). It originates from the oxidation of unsaturated fatty acids containing a double bond at position 9 (Kawamura and Gagosian, 1987), including oleic acid which is relatively abundant in air particulate matter and has been studied extensively (Shiraiwa et al., 2010; Zahardis and Petrucci, 2007). The concentrations of suberic acid (C_8, 0.8 ng m^{-3} in TSP) and sebacic acid (C_{10}, 0.4 ng m^{-3} in TSP) were substantially lower than that of azelaic acid. The correlation coefficients suggest that the sources of C_8 and C_{10} are similar ($R^2 = 0.71$ and 0.81 for coarse and fine PM), and related but not identical to the sources of C_9 ($R^2 = 0.36$-0.52, Tables 2-3 and 2-4).

Long-chain dicarboxylic acids (C_{12}-C_{16}) are generally attributed to the oxidation of ω-hydroxy fatty acids from vascular plants or other biogenic sources. The correlation coefficients suggest that the sources of C_{12}-C_{16} are more closely related to each other ($R^2 = 0.33$-0.97) than to C_8-C_{10} ($R^2 = 0.07$-0.75) or C_9 ($R^2 = 0.00$-0.19, Tables 2-3 and 2-4).

Table 2- 3 Correlation coefficients (R^2) between investigated compounds in coarse particulate matter. Abbreviations are the same as Table 2-1.

	Ph	C_5	C_6	C_7	C_8	C_9	C_{10}	C_{12}	C_{13}	C_{14}	C_{16}	C_{5-7}	C_{8-10}	C_{12-16}	Di_total[a]
Ph	1.00														
C_5	0.63	1.00													
C_6	0.45	0.60	1.00												
C_7	0.62	0.62	0.60	1.00											
C_8	0.49	0.75	0.54	0.56	1.00										
C_9	0.38	0.31	0.19	0.41	0.40	1.00									
C_{10}	0.48	0.61	0.39	0.39	0.71	0.36	1.00								
C_{12}	0.16	0.35	0.16	0.12	0.49	0.09	0.67	1.00							
C_{13}	0.08	0.26	0.13	0.11	0.39	0.04	0.45	0.68	1.00						
C_{14}	0.12	0.34	0.14	0.12	0.40	0.05	0.47	0.66	0.83	1.00					
C_{16}	0.01	0.01	0.00	0.00	0.07	0.00	0.23	0.46	0.44	0.33	1.00				
C_{5-7}	0.65				0.75	0.32	0.58	0.29	0.22	0.28	0.00	1.00			
C_{8-10}	0.49	0.49	0.31	0.53				0.22	0.13	0.14	0.01	0.55	1.00		
C_{12-16}	0.07	0.24	0.11	0.09	0.38	0.04	0.53					0.23	0.17	1.00	
Di_total	0.66											0.93	0.78	0.31	1.00
3-MBTCA	0.53	0.64	0.26	0.51	0.44	0.17	0.36	0.30	0.21	0.28	0.01	0.55	0.28	0.20	0.55
Pinic acid	0.28	0.51	0.21	0.26	0.39	0.04	0.37	0.42	0.44	0.53	0.08	0.43	0.13	0.43	0.40
Pinonic acid	0.55	0.44	0.26	0.42	0.45	0.20	0.39	0.21	0.18	0.27	0.01	0.43	0.31	0.18	0.46
Sum	0.57	0.72	0.34	0.52	0.58	0.19	0.52	0.42	0.35	0.47	0.04	0.65	0.35	0.37	0.64
4-Nitrocatechol	0.20	0.03	0.00	0.00	0.00	0.05	0.00	0.02	0.02	0.05	0.05	0.00	0.03	0.05	0.02
2-Nitrophenol	0.00	0.00	0.01	0.22	0.01	0.02	0.01	0.02	0.07	0.04	0.05	0.01	0.01	0.05	0.02
4-Nitrophenol	0.05	0.01	0.05	0.03	0.00	0.06	0.04	0.01	0.06	0.03	0.06	0.03	0.05	0.04	0.03
Nitrophenols	0.02	0.00	0.01	0.00	0.00	0.04	0.02	0.00	0.08	0.06	0.06	0.01	0.05	0.03	0.02

To be continued

Continued

	3-MBTCA	Pinic acid	Pinonic acid	Sum[b]	4-Nitrocatechol	2-Nitrophenol	4-Nitrophenol	Nitrophenols
Ph								
C_5								
C_6								
C_7								
C_8								
C_9								
C_{10}								
C_{12}								
C_{13}								
C_{14}								
C_{16}								
C_{5-7}								
C_{8-10}								
C_{12-16}								
Di_total								
3-MBTCA	1.00							
Pinic acid	0.62	1.00						
Pinonic acid	0.38	0.23	1.00					
Sum				1.00				
4-Nitrocatechol	0.06	0.05	0.01	0.00	1.00			
2-Nitrophenol	0.02	0.10	0.14	0.09	0.01	1.00		
4-Nitrophenol	0.01	0.03	0.02	0.00	0.00	0.27	1.00	
Nitrophenols	0.02	0.04	0.00	0.00	0.00			1.00

[a] the total of aliphatic dicarboxylic acids and phthalic acids;

[b] the sum of pinene oxidation products (3-MBTCA, pinic acid and pinonic acid).

Table 2- 4 Correlation coefficients (R^2) between investigated compounds in fine particulate matter. Abbreviations are the same as Table 2-1.

	Ph	C_5	C_6	C_7	C_8	C_9	C_{10}	C_{12}	C_{13}	C_{14}	C_{16}	C_{5-7}	C_{8-10}	C_{12-16}	Di_total[a]
Ph	1.00														
C_5	0.40	1.00													
C_6	0.35	0.56	1.00												
C_7	0.41	0.35	0.63	1.00											
C_8	0.36	0.25	0.68	0.70	1.00										
C_9	0.17	0.28	0.49	0.37	0.52	1.00									
C_{10}	0.19	0.13	0.57	0.72	0.82	0.49	1.00								
C_{12}	0.08	0.08	0.41	0.64	0.59	0.19	0.75	1.00							
C_{13}	0.03	0.03	0.27	0.52	0.44	0.11	0.66	0.95	1.00						
C_{14}	0.06	0.06	0.38	0.60	0.53	0.18	0.73	0.97	0.97	1.00					
C_{16}	0.01	0.02	0.27	0.51	0.41	0.12	0.68	0.86	0.91	0.89	1.00				
C_{5-7}	0.47				0.52	0.43	0.38	0.27	0.16	0.24	0.15	1.00			
C_{8-10}	0.24	0.29	0.62	0.55				0.37	0.24	0.34	0.26	0.52	1.00		
C_{12-16}	0.04	0.04	0.33	0.57	0.49	0.15	0.72					0.20	0.30	1.00	
Di_total	0.34											0.81	0.83	0.51	1.00
3-MBTCA	0.41	0.01	0.12	0.22	0.26	0.03	0.18	0.13	0.09	0.13	0.05	0.07	0.09	0.10	0.11
Pinic acid	0.13	0.08	0.37	0.41	0.51	0.16	0.45	0.41	0.30	0.39	0.24	0.23	0.29	0.33	0.38
Pinonic acid	0.12	0.33	0.22	0.12	0.17	0.22	0.09	0.08	0.03	0.07	0.01	0.31	0.22	0.04	0.26
Sum	0.41	0.05	0.25	0.35	0.42	0.09	0.31	0.24	0.17	0.24	0.10	0.18	0.21	0.18	0.26
4-Nitrocatechol	0.02	0.04	0.01	0.02	0.06	0.11	0.06	0.03	0.01	0.02	0.01	0.03	0.11	0.00	0.07
2-Nitrophenol	0.52	0.14	0.44	0.36	0.59	0.32	0.51	0.28	0.02	0.17	0.01	0.27	0.43	0.09	0.41
4-Nitrophenol	0.13	0.10	0.20	0.27	0.16	0.22	0.32	0.02	0.00	0.00	0.15	0.17	0.25	0.04	0.24
Nitrophenols	0.22	0.11	0.11	0.04	0.07	0.19	0.04	0.01	0.04	0.03	0.02	0.13	0.17	0.02	0.09

To be continued

Continued

	3-MBTCA	Pinic acid	Pinonic acid	Sum^b	4-Nitrocatechol	2-Nitrophenol	4-Nitrophenol	Nitrophenols
Ph								
C_5								
C_6								
C_7								
C_8								
C_9								
C_{10}								
C_{12}								
C_{13}								
C_{14}								
C_{16}								
C_{5-7}								
C_{8-10}								
$C_{\_12-16}$								
Di_total								
3-MBTCA	1.00							
Pinic acid	0.34	1.00						
Pinonic acid	0.02	0.14	1.00					
Sum				1.00				
4-Nitrocatechol	0.00	0.00	0.51	0.01	1.00			
2-Nitrophenol	0.24	0.18	0.06	0.31	0.01	1.00		
4-Nitrophenol	0.01	0.00	0.00	0.02	0.00	0.33	1.00	
Nitrophenols	0.00	0.01	0.00	0.00	0.01			1.00

[a] the total of aliphatic dicarboxylic acids and phthalic acids;

[b] the sum of pinene oxidation products (3-MBTCA, pinic acid and pinonic acid).

According to Ho et al. (2006), the ratios of adipic acid (C_6) and phthalic acid (Ph) to azelaic acid (C_9) can be used to estimate the relative influence of anthropogenic and biogenic sources of organic aerosol. The lower values of the two ratios represent typically biogenic emission; whreas the higher values indicate influence of anthropogenic origin. Comparisons of the two ratios in this study and other location around the world were performed (Table 2-5).

Table 2- 5 Ratios between the mass concentrations of adipic acid, phthalic acid and azelaic acid (C_6/C_9 and Ph/C_9) in comparison to other studies.

Location	Time	C_6/C_9	Ph/C_9	Particle	Publication
Mainz, Germany	June, 2006-May, 2007	0.65	3.13	PM_3	this study
14 cities in China	summer 2003	0.74		$PM_{2.5}$	Ho et al., 2007
14 cities in China	winter 2003	0.52		$PM_{2.5}$	Ho et al., 2007
Hoston area, USA	2000	0.75		$PM_{2.5}$	Yue and Fraser, 2004
Melpitz, Germany	2005	6.57	5.90	PM_{10}	van Pinxteren and Herrmann, 2007
Philadelphia, USA	July-August 1999	2.00	3.50	PM_{10}	Ray and McDow, 2005
Mainz, Germany	June, 2006-May, 2007	0.58	2.16	TSP	this study
Arctic	July, 1987 June, 1988	3.15		TSP	Kawamura et al., 1996a
Tokyo, Japan	summer, 1989	1.19-1.71		TSP	Kawamura and Yasui, 2005
Tokyo, Japan	winter, 1989	0.69		TSP	Kawamura and Yasui, 2005

The mean C_6/C_9 ratio in PM_3 (0.65, ranged from 0.21 to 4.35) were generally comparable with the values reported from Houston, USA and 14 economically developed or developing cities in China (0.52-0.75).. With regard to TSP, the mean ratio observed in Mainz (0.58, ranged from 0.23 to 1.81) were generally lower than the other region around the world (TSP: Tokyo, Japan and Arctic, 0.69-3.15; PM_{10}: Melpitz, Germany and Philadelphia, USA, 2.00-6.57). 84 % of samples in PM_3 and 91 % in TSP had the ratio lower than 1.

The mean Ph/C_9 value in PM_3 was 3.13 (ranged from 0.76 to 11.78). In TSP, the mean ratio (2.16, ranged from 0.60 to 11.78) were lower than the values in other region (PM_{10}, Melpitz, Germany and Philadelphia, USA, 3.50-5.90). The low values of the two ratios indicate that aerosols in Mainz were mainly influenced by biogenic sources.

2-Nitrophenol and 4-nitrophenol can be directly emitted as primary pollutants in combustion exhaust (Tremp et al., 1993), and they can also be formed as secondary pollutants by nitration of phenols in the atmosphere (Atkinson et al., 1992; Dumdei and Obrien, 1984; Grosjean, 1985; Nojima et al., 1975; Olariu et al.,2002). 2-Nitrophenol and 4-nitrophenol can originate from the irradiation of benzene-NO-air mixture (Nojima et al.,1975), whereas only 2-nitrophenol can form from various reaction including OH initiated reaction in the presence of NO_x, NO_3 initiated reaction and OH initiated reaction in the presence of NO_3 (Atkinson et al., 1992; Olariu et al.,2002). The distinctly different seasonal variations and low correlation coefficients of the two isomers of nitrophenol (($R^2 = 0.27$ and 0.33 for coarse and fine PM) indicate that their main sources are different.

The observed summer maximum and correlations with phthalic acid and various aliphatic dicarboxylic acids (R^2 up to 0.59, Table 2-4) suggest that atmospheric photochemistry is a major source of 2-nitrophenol. In contrast, the winter maximum of

4-nitrophenol and low correlation coefficients of with dicarboxylic acids ($R^2 < 0.32$, Table 2-4) suggest that primary emissions are more important for this compound than secondary formation. Interestingly, 4-nitrocatechol exhibits a summer maximum like 2-nitrophenol but no correlation with dicarboxylic acids ($R^2 < 0.11$, Table 2-4). These observations indicate primary sources that are enhanced during summer, which could be evaporation from soil as proposed by Gelencser et al. (2002) for humic-like substances (HULIS, Graber and Rudich, 2006). We suggest that further analyses of nitrophenols, nitrocatechol and other nitrated and oxygenated aromatic compounds by HPLC-MS may help to unravel combustion- and soil-related sources of organic particulate matter (Letzel et al., 2001; Schauer et al., 2004).

2.3.4 Temperature dependence of pinene oxidation products

In Fig. 2-4 the concentrations of 3-MBTCA, pinic acid and pinonic acid observed in the coarse and fine particle fractions and in total plotted against the inverse of ambient temperature (275 – 300 K).

Each of the data sets was fitted with an Arrhenius-type expression of the form *X* = A exp(E_a/RT), and the fit parameters are summarized in Table 2-6. The results obtained for coarse, fine particulate matter and TSP (fine plus coarse particles) were in overall agreement (Fig. 2-4), and for simplicity the following discussion is focused on the TSP results.

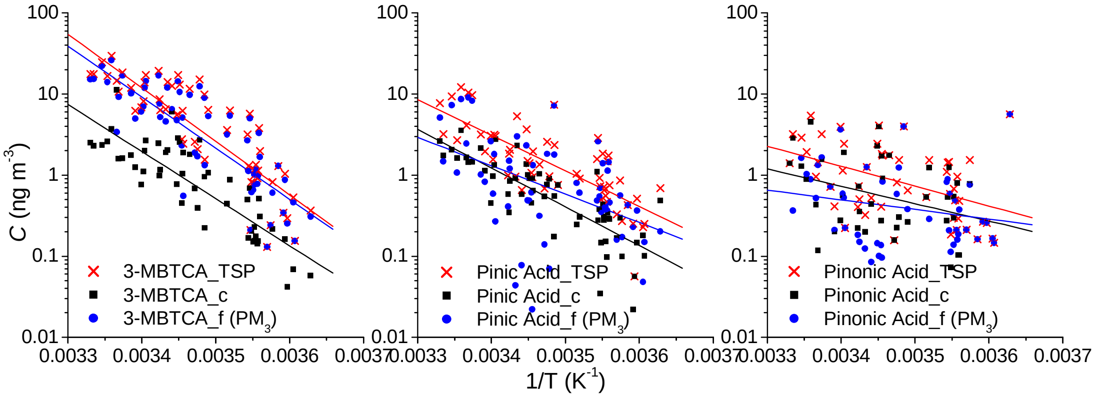

Figure 2- 4 Arrhenius-type temperature dependencies observed for pinene oxidation products (275–300 K): mass concentrations of 3-MBTCA, pinic acid and pinonic acid in fine, coarse and total particulate matter (TSP) plotted against inverse temperature. The data points represent individual samples, the lines are exponential fits, and the corresponding Arrhenius parameters are listed in Table 2-6.

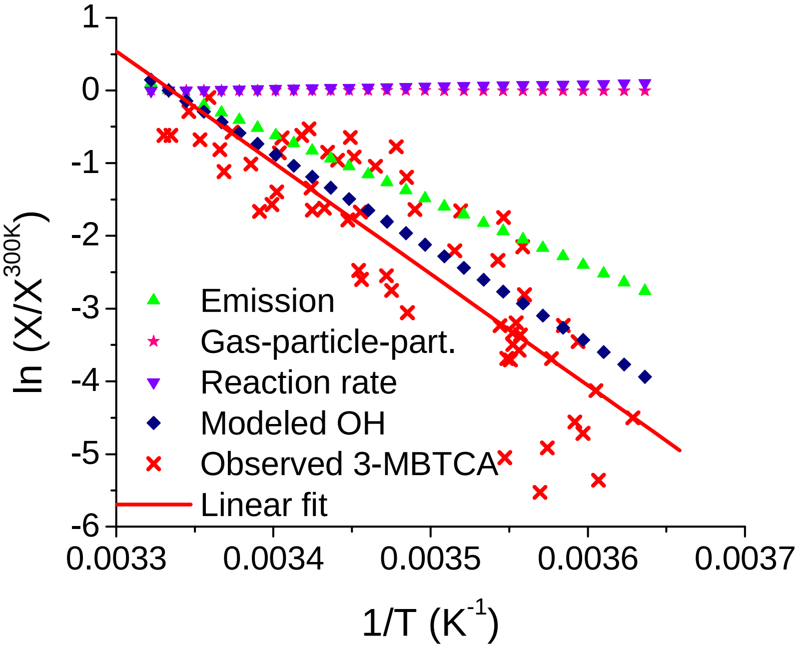

Figure 2- 5 Normalized Arrhenius-type plot of the temperature dependencies (275–300 K) observed for the concentration of 3-MBTCA ($C_{\text{3-MBTCA,TSP}}$, data points and solid line) and modeled for the emission of pinene (C_{PE}), the gas-particle partitioning of pinonic acid (FGP_{PA}), and the concentration of OH radicals (C_{OH}, dotted lines). For each parameter, X_{300} is the fit value at 300 K. The model assumptions and calculations are described in sect. A3.

Table 2- 6 Arrhenius parameters for observed and modeled temperature dependencies (275–300 K): pinene oxidation product mass concentrations (3-MBTCA, pinic acid, pinonic acid) in fine, coarse and total particulate matter (TSP) as shown in Fig. 2-4; emission of pinene, gas-particle partitioning of pinonic acid, and concentration of OH radicals as described in sect. A3 and shown in Fig. 2-5.

	A[a]	E_a (kJ mol^{-1})[b]	R^2 [c]	n[d]
3-MBTCA (TSP)	3.29×10^{23} ng m^{-3}	126±10	0.74	52
(fine)	2.41×10^{22} ng m^{-3}	121±11	0.69	58
(coarse)	1.05×10^{20} ng m^{-3}	111±10	0.72	52
Pinonic acid (TSP)	2.82×10^{8} ng m^{-3}	46.9±12.7	0.21	35
(fine)	5.49×10^{3} ng m^{-3}	22.8±15.0	0.05	36
(coarse)	1.45×10^{7} ng m^{-3}	41.1±18.3	0.12	35
Pinic acid (TSP)	2.54×10^{15} ng m^{-3}	83.9±9.1	0.60	56
(fine)	9.78×10^{11} ng m^{-3}	66.8±16.3	0.24	56
(coarse)	2.05×10^{16} ng m^{-3}	91.3±8.9	0.66	57
Pinene emission	6.31×10^{14} ng m^{-3}	75.6±3.3	-	-
Pinonic acid gas-particle-partitioning	1.09	0.213±0.011	0.95	27
OH concentration	4.52×10^{24} cm^{-3}	110±8	0.79	59

[a] pre-exponential factor (Fig. 2-4 and sect. A3);

[b] activation energy (Fig. 2-4 and sect. A3)

[c] correlation coefficient;

[d] number of data points.

3-MBTCA exhibited a strong Arrhenius-type temperature dependence with high activation energy and correlation coefficient (E_a = 126±10 kJ mol^{-1}, R^2 = 0.74, Table 2-6). Pinic acid also exhibited a pronounced temperature dependence albeit with lower activation energy and correlation coefficient (E_a = 84±9 kJ mol^{-1}, R^2 = 0.60, Table 2-6), whereas the temperature dependence of pinonic acid was very weak (E_a = 47±13 kJ mol^{-1}, R^2 = 0.21, Table 2-6).To explain the observed temperature dependencies and differences, we considered the following steps involved in the atmospheric oxidation of pinene and formation of pinic acid, pinonic acid and 3-MBTCA: (1) Emission of pinene; (2) Oxidation of pinene and formation of pinic and pinonic acid; (3) Oxidation of pinonic acid and formation of 3-MBTCA.

As detailed in sect. A3 and illustrated in Table 2-6, the temperature dependence (275 – 300 K) of the pinene emission rate can be described by an Arrhenius activation energy of ~84 kJ mol^{-1}.

The oxidation rate of pinene depends primarily on the concentration of oxidants (ozone, OH, etc.) and on rate coefficients of the involved gas phase reactions (Szmigielski et al., 2007). For typical atmospheric conditions and oxidant concentration levels, however, the lifetime of pinene is relatively short (~5 hours for α-pinene and ~3.5 h for β-pinene, k(OH) = $5.3*10^{-11}$ cm^3 $molecule^{-1}$ s^{-1} for α-pinene and k(OH) = $7.9*10^{-11}$ cm^3 $molecule^{-1}$ s^{-1} for β-pinene (Atkinson et al., 2006) and typical average $C_{OH} = 1*10^6$ radical cm^{-3}) compared to the transport, mixing and averaging times involved in the collection of air samples in this study (of the order of one week). Thus, we assume that the oxidation of pinene is not rate-limiting and that the temperature dependence of the formation of pinic and pinonic acid can be approximated by the temperature dependence of pinene emission. The plausibility of this assumption is confirmed by the agreement between the observed temperature dependence of pinic acid concentration and the calculated temperature dependence of pinene emission (Table 2-6).

The oxidation rate of pinonic acid depends primarily on gas-particle partitioning, on the concentration of OH radicals, and on the OH reaction rate coefficient (Jimenez et al., 2009; Hallquist et al., 2009). As detailed in sect. A3 and illustrated in Fig. 2-5, the temperature dependence of gas-particle partitioning of pinonic acid is very weak and can be approximated by an Arrhenius activation energy of ~0.21 kJ mol^{-1} (Table 2-6). Moreover, pinonic acid is expected to reside almost exclusively in the gas phase (> 99%, sect. A3) under the conditions relevant for this study, and thus gas-particle partitioning should have little influence on the observed temperature dependencies.

As detailed in sect. A3, the E_a of OH reaction rate coefficient cause insignificant temperature dependence of overall OH oxidation of pinonic acid.

The atmospheric concentration of OH radicals depends on a wide range of processes, including the photolysis of ozone by solar UV radiation (Crutzen et al., 1999; Rohrer and Berresheim, 2006). Due to radiative heating, the intensity of solar radiation at a given location usually varies in conjunction with diurnal and seasonal variations of temperature. To explore the effective dependence of OH radical concentration on ambient temperature at our sampling location, we used model data from the ECHAM/MESSy Atmospheric Chemistry Model (EMAC, Jöckel et al., 2006). As detailed in sect. A3, these data could be fitted with an Arrhenius-type expression (R^2 = 0.79) and with an apparent Arrhenius activation energy of 110 kJ mol^{-1}.

As illustrated in Fig. 2-5, the model-derived effective temperature dependence (in the range of 275 – 300 K) of OH radical concentration is similar to the observed temperature dependence of 3-MBTCA concentration and shows only 16 kJ mol^{-1} difference, which is within the error range. The agreement suggests that the OH-initiated oxidation of pinonic acid is indeed the rate-limiting step in the formation of 3-MBTCA, because the temperature dependence of a process consisting of multiple steps is generally dominated by the temperature dependence of the rate-limiting step. None of the other temperature dependencies considered above and illustrated in Fig. 2-5 appears strong enough to explain the observed temperature dependence of 3-MBTCA, and the it appears plausible that the formation and concentration of 3-MBTCA is limited by the OH-initiated oxidation of pinonic acid. The result is also consistent with regard to the very weak temperature dependence observed for the pinonic acid concentration, which may results from an effective cancelation of the temperature dependencies of the formation from pinene emission and oxidation (in analogy to pinic acid) and the loss by OH oxidation. Due to aldehyde group, k(OH) is larger for pinonic acid (1.04 x 10^{-11} cm^3 $molecule^{-1}$ s^{-1}) than for pinic acid (8.7 x 10^{-12} cm^3 $molecule^{-1}$ s^{-1}) at 298 K (Vereecken and Peeters, 2002), resulting in an OH-lifetime of ~27 h for pinonic acid and ~32 h for pinic acid, using a typical average OH-concentration of 1*10^6 radical cm^{-3}. It appears not very likely that potential temperature dependencies of other relevant processes like dry and wet deposition of the investigated compounds would be more important and better suited to explain the observations.

Nevertheless, the above considerations have to be regarded as a first approximation and simple conceptual model approach to explain the observations. A full mechanistic understanding and quantification will require detailed numerical model studies including potential effects of atmospheric transport and deposition. This would go beyond the scope of the present study, but we suggest and intend to pursue such investigations in follow-up studies. Similarity of E_a for observed Arrhenius concentration and model OH concentration suggests that OH initiated oxidation is rate limited step of 3-MBTCA formation. The difference of 16 kJ mol^{-1} is within the range of uncertainties and might also be related to sink processes (chemical loss, dry/wet deposition).

2.4 Conclusions and outlook

Based on the dicarboxylic acid and nitrophenol measurement data of this study we suggest that further analyses of nitrated and oxygenated aromatic compounds by HPLC-MS may help to unravel combustion- and soil-related sources of organic particulate matter in comparison to primary biological aerosols containing fatty acids and SOA formed from gaseous biogenic precursors like pinene.

From on the analysis of pinene oxidation products including pinic acid, pinonic acid and 3-MBTCA and accompanying model calculations we conclude that the emission of pinene appears to limit the formation and explain the observed Arrhenius-type temperature dependence (275 – 300 K) of pinic acid. The OH radical concentration and the OH-initiated oxidation of pinonic acid seem to limit the formation and explain the observed Arrhenius-type temperature dependence (275 – 300 K) of 3-MBTCA, whereas the influence of gas-particle partitioning appears negligible. Thus, 3-MBTCA may be a suitable tracer for the chemical aging of biogenic SOA by OH radicals.

WSOCs collected and studied in this study were mainly influenced by biogenic sources. Biogenic volatile organic compounds such as monoterpenes react directly with O_3, OH etc., forming low volatility oxidation products that are important sources for SOA formation and growth. It is evident that with reducing anthropogenic emissions of both volatile organic compounds (VOC) and NO_x, biogenic sources become increasingly important in atmospheric chemical processes. For better control of the air quality, not only anthropogenic source but also the present or even enhanced biogenic emission in particular at high temperatures and high solar radiation should be taken into account. At present, study on isoprene and monoterpene emission has progressed substantially, and the importance of oxygenated VOC and sesquiterpenes has been appreciated. However, observation data of biogenic emission are still species limited and spatial sparse (Monks et al. 2009). An improved understanding of the processes is required for accurate predictions of future natural emissions. Global observation of different species should be launched. Knowledge on emission processes and SOA formation will help to improve the controlling of biogenic emission, thus, controls the air quality.

2.5 References

Atkinson, R. and J. Arey (2003). "Gas-phase tropospheric chemistry of biogenic volatile organic compounds: a review." Atmospheric Environment **37**: S197-S219.

Atkinson, R., S. M. Aschmann and J. Arey (1992). "Reactions of OH and NO_3 radicals with phenol, cresols, and 2-nitrophenol at 296 K±2 K." Environmental Science & Technology **26**(7): 1397-1403.

Atkinson, R., D. L. Baulch, R. A. Cox, J. N. Crowley, R. F. Hampson, R. G. Hynes, M. E. Jenkin, M. J. Rossi and J. Troe (2006). "Evaluated kinetic and photochemical data for atmospheric chemistry: Volume II - gas phase reactions of organic species." Atmospheric Chemistry and Physics **6**: 3625-4055.

Belloli, R., B. Barletta, E. Bolzacchini, S. Meinardi, M. Orlandi and B. Rindone (1999). "Determination of toxic nitrophenols in the atmosphere by high-performance liquid chromatography." Journal of Chromatography A **846**(1-2): 277-281.

Cecinato, A., V. Di Palo, D. Pomata, M. C. T. Sciano and M. Possanzini (2005). "Measurement of phase-distributed nitrophenols in Rome ambient air." Chemosphere **59**(5): 679-683.

Crutzen, P. J., M. G. Lawrence and U. Poschl (1999). "On the background photochemistry of tropospheric ozone." Tellus Series a-Dynamic Meteorology and Oceanography **51**(1): 123-146.

Dumdei, B. E. and R. J. Obrien (1984). "Toluene Degradation Products in Simulated Atmospheric Conditions." Nature **311**(5983): 248-250.

Frohlich-Nowoisky, J., D. A. Pickersgill, V. R. Despres and U. Poschl (2009). "High diversity of fungi in air particulate matter." Proceedings of the National Academy of Sciences of the United States of America **106**(31): 12814-12819.

Fu, P., K. Kawamura, J. Chen and L. A. Barrie (2009a). "Isoprene, monoterpene, and sesquiterpene oxidation products in the High Arctic Aerosols during late winter to early summer." Environmental Science & Technology **43**(11): 4022-4028.

Fu, P. Q., K. Kawamura, P. Pochanart, H. Tanimoto, Y. Kanaya and Z. F. Wang (2009b). "Summertime contributions of isoprene, monoterpenes, and sesquiterpene oxidation to the formation of secondary organic aerosol in the troposphere over Mt. Tai, Central East China during MTX2006." Atmospheric Chemistry and Physics Discussion **9**(4): 16941-16972.

Gelencser, A., A. Hoffer, Z. Krivacsy, G. Kiss, A. Molnar and E. Meszaros (2002). "On the possible origin of humic matter in fine continental aerosol." Journal of Geophysical Research-Atmospheres **107**(D12): 4137, Doi 10.1029/2001jd001299.

Graber, E. R. and Y. Rudich (2006). "Atmospheric HULIS: How humic-like are they? A comprehensive and critical review." Atmospheric Chemistry and Physics **6**: 729-753.

Grosjean, D. (1985). "Reactions of o-cresol and nitrocresol with NO_X in sunlight and with ozone nitrogen-dioxide mixtures in the dark." Environmental Science & Technology **19**(10): 968-974.

Hallquist, M., J. C. Wenger, U. Baltensperger, Y. Rudich, D. Simpson, M. Claeys, J. Dommen, N. M. Donahue, C. George, A. H. Goldstein, J. F. Hamilton, H. Herrmann, T. Hoffmann, Y. Iinuma, M. Jang, M. E. Jenkin, J. L. Jimenez, A. Kiendler-Scharr, W. Maenhaut, G. McFiggans, T. F. Mentel, A. Monod, A. S. H. Prevot, J. H. Seinfeld, J. D. Surratt, R. Szmigielski and J. Wildt (2009). "The formation, properties and impact of secondary organic aerosol: current and emerging issues." Atmospheric Chemistry and Physics **9**(14): 5155-5236.

Hatakeyama, S., K. Izumi, T. Fukuyama and H. Akimoto (1989). "Reactions of ozone with alpha-pinene and beta-pinene in air - yields of gaseous and particulate products." Journal of Geophysical Research-Atmospheres **94**(D10): 13013-13024.

Hatakeyama, S., K. Izumi, T. Fukuyama, H. Akimoto and N. Washida (1991). "Reactions of OH with alpha-pinene and beta-pinene in air - estimate of global CO production from the atmospheric oxidation of terpenes." Journal of Geophysical Research-Atmospheres **96**(D1): 947-958.

Hatakeyama, S., M. Ohno, J. H. Weng, H. Takagi and H. Akimoto (1987). "Mechanism for the Formation of Gaseous and Particulate Products from Ozone-Cycloalkene Reactions in Air." Environmental Science & Technology **21**(1): 52-57.

Herterich, R. (1991). "Gas-chromatographic determination of nitrophenols in atmospheric liquid water and airborne-particulates." Journal of Chromatography **549**(1-2): 313-324.

Ho, K. F., J. J. Cao, S. C. Lee, K. Kawamura, R. J. Zhang, J. C. Chow and J. G. Watson (2007). "Dicarboxylic acids, ketocarboxylic acids, and dicarbonyls in the urban atmosphere of China." Journal of Geophysical Research-Atmospheres **112:** D22S27, Doi:10.1029/2006JD008011.

Ho, K. F., S. C. Lee, J. J. Cao, K. Kawamura, T. Watanabe, Y. Cheng and J. C. Chow (2006). "Dicarboxylic acids, ketocarboxylic acids and dicarbonyls in the urban roadside area of Hong Kong." Atmospheric Environment **40**(17): 3030-3040.

Hoffmann, T., J. R. Odum, F. Bowman, D. Collins, D. Klockow, R. C. Flagan and J. H. Seinfeld (1997). "Formation of organic aerosols from the oxidation of biogenic hydrocarbons." Journal of Atmospheric Chemistry **26**(2): 189-222.

Hu, D., Q. Bian, T. W. Y. Li, A. K. H. Lau and J. Z. Yu (2008). "Contributions of isoprene, monoterpenes, beta-caryophyllene, and toluene to secondary organic aerosols in Hong Kong during the summer of 2006." Journal of Geophysical Research-Atmospheres **113:** D22206, doi:10.1029/2008JD010437.

Jaoui, M., T. E. Kleindienst, M. Lewandowski, J. H. Offenberg and E. O. Edney (2005). "Identification and quantification of aerosol polar oxygenated compounds bearing carboxylic or hydroxyl groups. 2. Organic tracer compounds from monoterpenes." Environmental Science & Technology **39**(15): 5661-5673.

Kavouras, I. G., J. Lawrence, P. Koutrakis, E. G. Stephanou and P. Oyola (1999a). "Measurement of particulate aliphatic and polynuclear aromatic hydrocarbons in Santiago de Chile: source reconciliation and evaluation of sampling artifacts." Atmospheric Environment **33**(30): 4977-4986.

Kavouras, I. G., N. Mihalopoulos and E. G. Stephanou (1998). "Formation of atmospheric particles from organic acids produced by forests." Nature **395**(6703): 683-686.

Kavouras, I. G., N. Mihalopoulos and E. G. Stephanou (1999b). "Secondary organic aerosol formation vs primary organic aerosol emission: In situ evidence for the chemical coupling between monoterpene acidic photooxidation products and new particle formation over forests." Environmental Science & Technology **33**(7): 1028-1037.

Kavouras, I. G. and E. G. Stephanou (2002). "Direct evidence of atmospheric secondary organic aerosol formation in forest atmosphere through heteromolecular nucleation." Environmental Science & Technology **36**(23): 5083-5091.

Kawamura, K. and R. B. Gagosian (1987a). "Implications of omega-oxocarboxylic acids in the remote marine atmosphere for photooxidation of unsaturated fatty-acids." Nature **325**(6102): 330-332.

Kawamura, K. and K. Ikushima (1993a). "Seasonal-changes in the distribution of dicarboxylic-acids in the urban atmosphere." Environmental Science & Technology **27**(10): 2227-2235.

Kawamura, K. and I. R. Kaplan (1987b). "Motor exhaust emissions as a primary source for dicarboxylic-acids in Los-Angeles ambient air." Environmental Science & Technology **21**(1): 105-110.

Kawamura, K., H. Kasukabe and L. A. Barrie (1996a). "Source and reaction pathways of dicarboxylic acids, ketoacids and dicarbonyls in arctic aerosols: one year of observations." Atmospheric Environment **30**(10-11): 1709-1722.

Kawamura, K., R. Semere, Y. Imai, Y. Fujii and M. Hayashi (1996b). "Water soluble dicarboxylic acids and related compounds in Antarctic aerosols." Journal of Geophysical Research-Atmospheres **101**(D13): 18721-18728.

Kawamura, K. and K. Usukura (1993b). "Distributions of low molecular weight dicarboxylic acids in the North Pacific aerosol samples." Journal of Oceanography **49**(3): 271-283.

Kawamura, K. and O. Yasui (2005). "Diurnal changes in the distribution of dicarboxylic acids, ketocarboxylic acids and dicarbonyls in the urban Tokyo atmosphere." Atmospheric Environment **39**(10): 1945-1960.

Koch, S., R. Winterhalter, E. Uherek, A. Kolloff, P. Neeb and G. K. Moortgat (2000). "Formation of new particles in the gas-phase ozonolysis of monoterpenes." Atmospheric Environment **34**(23): 4031-4042.

Komenda, M., K. Kobel, R. Koppmann and J. Wildt (2003). "Comparability of biogenic VOC emission rate measurements under laboratory and ambient conditions at the example of monoterpene emissions from Scots pine (Pinus sylvestris)." Journal of Atmospheric Chemistry **45**(1): 1-23.

Kourtchev, I., I. Bejan, J. R. Sodeau and J. C. Wenger (2009). "Gas-phase reaction of (E)-beta-farnesene with ozone: Rate coefficient and carbonyl products." Atmospheric Environment **43**(20): 3182-3190.

Kourtchev, I., T. M. Ruuskanen, P. Keronen, L. Sogacheva, M. Dal Maso, A. Reissell, X. Chi, R. Vermeylen, M. Kulmala, W. Maenhaut and M. Claeys (2008a). "Determination of isoprene and alpha-/beta-pinene oxidation products in boreal forest aerosols from Hyytiala, Finland: diel variations and possible link with particle formation events." Plant Biology **10**(1): 138-149.

Kourtchev, I., J. Warnke, W. Maenhaut, T. Hoffmann and M. Claeys (2008b). "Polar organic marker compounds in $PM_{2.5}$ aerosol from a mixed forest site in western Germany." Chemosphere **73**(8): 1308-1314.

Kubatova, A., R. Vermeylen, M. Claeys, J. Cafmeyer and W. Maenhaut (2002). "Organic compounds in urban aerosols from Gent, Belgium: characterization, sources, and seasonal differences." Journal of Geophysical Research-Atmospheres **107**(D21): 8343, doi:10.1029/2001JD000556.

Kubatova, A., R. Vermeylen, M. Claeys, J. Cafmeyer, W. Maenhaut, G. Roberts and P. Artaxo (2000). "Carbonaceous aerosol characterization in the Amazon basin, Brazil: novel dicarboxylic acids and related compounds." Atmospheric Environment **34**(29-30): 5037-5051.

Kundu, S., K. Kawamura, T. W. Andreae, A. Hoffer and M. O. Andreae (2010). "Molecular distributions of dicarboxylic acids, ketocarboxylic acids and α-dicarbonyls in biomass burning aerosols: implications for photochemical production and degradation in smoke layers." Atmospheric Chemistry and Physics **10**(5): 2209-2225.

Lefer, B. L., R. W. Talbot, R. C. Harriss, J. D. Bradshaw, S. T. Sandholm, J. O. Olson, G. W. Sachse, J. Collins, M. A. Shipham, D. R. Blake, K. I. Klemm, O. Klemm, K. Gorzelska and J. Barrick (1994). "Enhancement of acidic gases in biomass burning impacted air masses over Canada." Journal of Geophysical Research-Atmospheres **99**(D1): 1721-1737.

Legrand, M. and M. DeAngelis (1996). "Light carboxylic acids in Greenland ice: a record of past forest fires and vegetation emissions from the boreal zone." Journal of Geophysical Research-Atmospheres **101**(D2): 4129-4145.

Letzel, T., U. Poschl, R. Wissiack, E. Rosenberg, M. Grasserbauer and R. Niessner (2001). "Phenyl-modified reversed-phase liquid chromatography coupled to atmospheric pressure chemical ionization mass spectrometry: a universal method for the analysis of partially oxidized aromatic hydrocarbons." Analytical Chemistry **73**(7): 1634-1645.

Leuenberger, C., M. P. Ligocki and J. F. Pankow (1985). "Trace organic-compounds in rain .4. Identities, concentrations, and scavenging mechanisms for phenols in urban air and rain." Environmental Science & Technology **19**(11): 1053-1058.

Lewandowski, M., M. Jaoui, T. E. Kleindienst, J. H. Offenberg and E. O. Edney (2007). "Composition of $PM_{2.5}$ during the summer of 2003 in Research Triangle Park, North Carolina." Atmospheric Environment **41**(19): 4073-4083.

Luttke, J. and K. Levsen (1997a). "Occurrence and formation of nitrated phenols in clouds at two European sites." Proceedings of Eurotrac Symposium '96 - Transport and Transformation of Pollutants in the Troposphere, Vol 1: 101-107.

Luttke, J., V. Scheer, K. Levsen, G. Wunsch, J. N. Cape, K. J. Hargreaves, R. L. StoretonWest, K. Acker, W. Wieprecht and B. Jones (1997b). "Occurrence and formation of nitrated phenols in and out of cloud." Atmospheric Environment **31**(16): 2637-2648.

Mochida, M., A. Kawabata, K. Kawamura, H. Hatsushika and K. Yamazaki (2003a). "Seasonal variation and origins of dicarboxylic acids in the marine atmosphere over the western North Pacific." Journal of Geophysical Research-Atmospheres **108**(D6): 4193, doi:10.1029/2002JD002355.

Mochida, M., N. Umemoto, K. Kawamura and M. Uematsu (2003b). "Bimodal size distribution of C_2-C_4 dicarboxylic acids in the marine aerosols." Geophysical Research Letters **30**(13): 13, 1672, doi:10.1029/2003GL017451.

Monks, P. S., C. Granier, S. Fuzzi, A. Stohl, M. L. Williams, H. Akimoto, M. Amann, A. Baklanov, U. Baltensperger, I. Bey, N. Blake, R. S. Blake, K. Carslaw, O. R. Cooper, F. Dentener, D. Fowler, E. Fragkou, G. J. Frost, S. Generoso, P. Ginoux, V. Grewe, A. Guenther, H. C. Hansson, S. Henne, J. Hjorth, A. Hofzumahaus, H. Huntrieser, I. S. A. Isaksen, M. E. Jenkin, J. Kaiser, M. Kanakidou, Z. Klimont, M. Kulmala, P. Laj, M. G. Lawrence, J. D. Lee, C. Liousse, M. Maione, G. McFiggans, A. Metzger, A. Mieville, N. Moussiopoulos, J. J. Orlando, C. D. O'Dowd, P. I. Palmer, D. D. Parrish, A. Petzold, U. Platt, U. Poschl, A. S. H. Prevot, C. E. Reeves, S. Reimann, Y. Rudich, K. Sellegri, R. Steinbrecher, D. Simpson, H. ten Brink, J. Theloke, G. R. van der Werf, R. Vautard, V. Vestreng, C. Vlachokostas and R. von Glasow (2009). "Atmospheric composition change - global and regional air quality." Atmospheric Environment **43**(33): 5268-5350.

Narukawa, M., K. Kawamura, N. Takeuchi and T. Nakajima (1999). "Distribution of dicarboxylic acids and carbon isotopic compositions in aerosols from 1997 Indonesian forest fires." Geophysical Research Letters **26**(20): 3101-3104.

Nojima, K., A. Kawaguchi, T. Ohya, S. Kanno and M. Hirobe (1983). "Studies on photochemical-reaction of air-pollutants .10. Identification of nitrophenols in suspended particulates." Chemical & Pharmaceutical Bulletin **31**(3): 1047-1051.

Nojima, M., T. Nagata and N. Tokura (1975). "Deoxygenation of sulfoxides to sulfides in an iodine-pyridine sulfur dioxide system." Bulletin of the Chemical Society of Japan **48**(4): 1343-1344.

Olariu, R. I., B. Klotz, I. Barnes, K. H. Becker and R. Mocanu (2002). "FT-IR study of the ring-retaining products from the reaction of OH radicals with phenol, o-, m-, and p-cresol." Atmospheric Environment **36**(22): 3685-3697.

Pöschl, U. (2005). "Atmospheric aerosols: composition, transformation, climate and health effects." Angewandte Chemie-International Edition **44**(46): 7520-7540.

Ray, J. and S. R. McDow (2005). "Dicarboxylic acid concentration trends and sampling artifacts." Atmospheric Environment **39**(40): 7906-7919.

Rohrer, F. and H. Berresheim (2006). "Strong correlation between levels of tropospheric hydroxyl radicals and solar ultraviolet radiation." Nature **442**(7099): 184-187.

Rompp, A., R. Winterhalter and G. K. Moortgat (2006). "Oxodicarboxylic acids in atmospheric aerosol particles." Atmospheric Environment **40**(35): 6846-6862.

Schauer, C., R. Niessner and U. Poschl (2004). "Analysis of nitrated polycyclic aromatic hydrocarbons by liquid chromatography with fluorescence and mass spectrometry detection: air particulate matter, soot, and reaction product studies." Analytical and Bioanalytical Chemistry **378**(3): 725-736.

Shafer, W. E. and J. Schonherr (1985). "Accumulation and transport of phenol, 2-nitrophenol, and 4-nitrophenol in plant cuticles." Ecotoxicology and Environmental Safety **10**(2): 239-252.

Shiraiwa, M., C. Pfrang and U. Pöschl (2010). "Kinetic multi-layer model of aerosol surface and bulk chemistry (KM-SUB): the influence of interfacial transport and bulk diffusion on the oxidation of oleic acid by ozone." Atmospheric Chemistry and Physics Discussions **10**: 281-326.

Solomon, P. A., J. L. Moyers and R. A. Fletcher (1983). "High-volume dichotomous virtual impactor for the fractionation and collection of particles according to aerodynamic size." Aerosol Science and Technology **2**(4): 455-464.

Stephanou, E. G. and N. Stratigakis (1993). "Oxocarboxylic and alpha, omega-dicarboxylic acids - photooxidation products of biogenic unsaturated fatty-acids present in urban aerosols." Environmental Science & Technology **27**(7): 1403-1407.

Szmigielski, R., J. D. Surratt, Y. Gomez-Gonzalez, P. Van der Veken, I. Kourtchev, R. Vermeylen, F. Blockhuys, M. Jaoui, T. E. Kleindienst, M. Lewandowski, J. H. Offenberg, E. O. Edney, J. H. Seinfeld, W. Maenhaut and M. Claeys (2007). "3-Methyl-1,2,3-butanetricarboxylic acid: an atmospheric tracer for terpene secondary organic aerosol." Geophysical Research Letters **34**(24): L24811, doi:10.1029/2007GL031338.

Tremp, J., P. Mattrel, S. Fingler and W. Giger (1993). "Phenols and nitrophenols as tropospheric pollutants - emissions from automobile exhausts and phase-transfer in the atmosphere." Water Air and Soil Pollution **68**(1-2): 113-123.

van Pinxteren, D. and H. Herrmann (2007). "Determination of functionalised carboxylic acids in atmospheric particles and cloud water using capillary electrophoresis/mass spectrometry." Journal of Chromatography A **1171**(1-2): 112-123.

Vereecken, L. and J. Peeters (2002). "Enhanced H-atom abstraction from pinonaldehyde, pinonic acid, pinic acid, and related compounds: theoretical study of C-H bond strengths." Physical Chemistry Chemical Physics **4**(3): 467-472.

Warnke, J., R. Bandur and T. Hoffmann (2006). "Capillary-HPLC-ESI-MS/MS method for the determination of acidic products from the oxidation of monoterpenes in atmospheric aerosol samples." Analytical and Bioanalytical Chemistry **385**(1): 34-45.

Winterhalter, R., M. Kippenberger, J. Williams, E. Fries, K. Sieg and G. K. Moortgat (2009).

"Concentrations of higher dicarboxylic acids C_5-C_{13} in fresh snow samples collected at the High Alpine Research Station Jungfraujoch during CLACE 5 and 6." Atmospheric Chemistry and Physics **9**(6): 2097-2112.

Yu, J. Z., D. R. Cocker, R. J. Griffin, R. C. Flagan and J. H. Seinfeld (1999a). "Gas-phase ozone oxidation of monoterpenes: gaseous and particulate products." Journal of Atmospheric Chemistry **34**(2): 207-258.

Yu, J. Z., R. J. Griffin, D. R. Cocker, R. C. Flagan, J. H. Seinfeld and P. Blanchard (1999b). "Observation of gaseous and particulate products of monoterpene oxidation in forest atmospheres." Geophysical Research Letters **26**(8): 1145-1148.

Yue, Z. W. and M. P. Fraser (2004). "Polar organic compounds measured in fine particulate matter during TexAQS 2000." Atmospheric Environment **38**(20): 3253-3261.

Zahardis, J. and G. A. Petrucci (2007). "The oleic acid-ozone heterogeneous reaction system: products, kinetics, secondary chemistry, and atmospheric implications of a model system - a review." Atmospheric Chemistry and Physics **7**: 1237-1274.

3. Protein analysis by HPLC-DAD-MS

3.1 Introduction

The nitration of biomolecules, including proteins, desoxyribonucleic acid (DNA) and lipids, plays an important role in biological systems and human diseases. It can trigger cellular responses ranging from subtle modulations of cell signaling to oxidative injury, committing cells to necrosis or apoptosis (Halliwell et al., 2004; Pacher et al., 2007). Protein nitration is a protein post-translational modification occurring under the action of a nitrating agent. The nitration of tyrosine has been extensively investigated (Abello et al., 2009). 3-nitrotyrosine, with an addition of a nitro group (-NO_2) in ortho position to the phenolic hydroxyl group (as shown in figure 3-1), is the main product of protein tyrosine nitration.

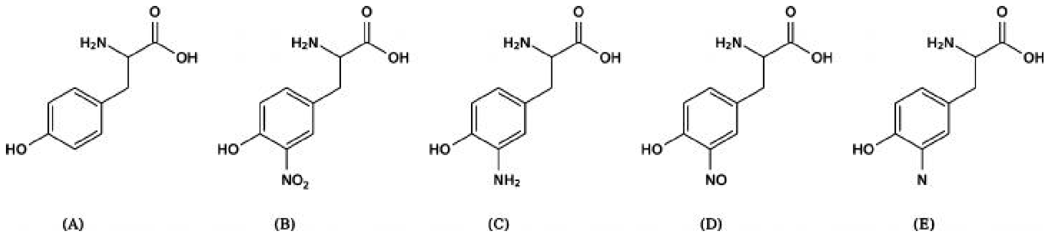

Figure 3- 1 Molecular structures of tyrosine, nitrotyrosine, and other derivatives. (A) Tyrosine, (B) nitrotyrosine, (C) aminotyrosine, (D) nitrosotyrosine and (E) nitrenetyrosine (Abello et al., 2009)

There are two major pathways of protein nitration in literatures: one is with tetranitromethane (TNM) and the other is with peroxynitrite and derivatives. In 1960s, TNM has been widely used to nitrate tyrosine residues in proteins (Riordan et al., 1966; 1967; Sokolovs.M et al., 1970; Sokolovs.M et al., 1966). 3-nitrotyrosine is the main product of this experiment, but other modifications of tyrosine residues were also found, e.g., tyrosine nitrosylation (i.e., the addition of -NO, see Figure 3-1) by a radical-mediated reaction (Lee et al., 2007). Although still being used in the later studies, nitration with peroxynitrite is more preferred because of its supposedly greater biological relevance. Peroxynitrite ($ONOO^-$) forms from the reaction between free radicals nitrogen oxide ($NO^\bullet$) and superoxide ($O_2^{\bullet-}$) under physiological conditions (Beckman et al., 1990; Beckman et al., 1992; Beckmann et al., 1994). It can react with various amino acids in protein especially tyrosine, tryptophan, cysteine and methionine (Alvarez et al., 1999). Besides, the possibility of its in-house production also makes it more useful in protein nitration studies. It can be formed by the reaction of nitroxyl anion (NO^-) with molecular oxygen and stored under basic conditions prior to use (Kirsch et al., 2002). For studies on the selectivity and the biological consequence of protein nitration, nitrated proteins were usually prepared using the mentioned pathways.

Elevated concentrations of nitrated proteins, i.e. protein containing 3-nitrotyrosine residues, have been detected in biological tissues, body fluids and cells. Nitrotyrosine in its free or protein-bound form has been detected in association with at least 50 diseases and more than 80 animal models or cell culture systems (Greenacre et al., 2001), e.g. asthma ((Kaminsky et al., 1999; Saleh et al., 1998). On the other hand, some studies suggested the traffic-related air pollution with high concentration of nitrogen oxides and ozone tend to be related to allergic diseases (Brunekreef, 2001; Brunekreef et al., 2003). Franze et al. (Franze et al., 2005) found both synthetic gas mixtures of nitrogen oxides and ozone and polluted urban air (summer smog) can lead to protein nitration. In this study, he proposed that the nitration of airborne allergens, such as Bet v 1, by traffic-related air pollution promotes allergies. Gruijthuijsen et al. (Gruijthuijsen et al., 2006) found that functional IgE specific for nitrated Bet v 1a, which does not bind unmodified Bet v 1 or nitrated unrelated proteins, is detected in serum samples of patients who are allergic to birch pollen. The experiment suggested that nitration generates novel allergenic epitopes and allergen nitration is relevant in vivo and can contribute to allergenicity in polluted environments. Thus, further investigations of protein nitration by air pollutants are under way, and suitable analytical techniques are required. In particular, laboratory studies characterizing the reaction kinetics of protein nitration under a wide range of well defined experimental conditions require efficient ways of quantifying nitrotyrosine in protein molecules.

The detection and quantification methods for nitrotyrosine reported in the reference are: immunohistochemistry including western blot, Enzyme-linked immunosorbent assay (ELISA) and immunoprecipitation followed by western blot, ultraviolet-visible photometry (UV-Vis), gas chromatography (GC) coupled to a thermal energy analyzer (TEA) or mass spectrometer (MS), and high-performance liquid chromatography (HPLC) coupled to UV-Vis absorption, fluorescence, electrochemical (ECD), and MS (Duncan, 2003; Herce-Pagliai et al., 1998). Immunochemistry has been applied extensively but is generally regarded as semi-quantitative (Duncan, 2003; Franze et al., 2003; Franze et al., 2004; Greenacre et al., 2001). UV-Vis photometry enables the detection of nitrotyrosine as a free amino acid as well as in peptides and proteins. As illustrated in Fig. 3-2, tyrosine and nitrotyrosine both exhibit an absorption peak at 280 nm, and nitrotyrosine has an additional peak at ~357 nm in acidic solutions ($pH \leq 3.5$) or at ~430 nm in basic solutions ($pH \geq 9.5$) (Crow et al., 1995). Due to low sensitivity and low specificity the application of simple photometers is restricted to relatively pure and large amount of substance (Crow et al., 1996).

The advantages and disadvantages of various GC and HPLC methods and related sample preparation techniques have been reviewed by Duncan (Duncan, 2003) and Herce-Pagliai, Kotecha et al. (Herce-Pagliai et al., 1998). In the reported GC and HPLC methods, proteins had to undergo hydrolysis or enzymatic digestion to release nitrotyrosine as a free amino acid, whereby artificial formation or loss of nitrotyrosine are of concern. Methods that account for artificial formation or loss of nitrotyrosine have been developed, but they tend to be highly labor and cost-intensive. For example, Yi et al. (Yi et al., 2000) developed gas phase HCl hydrolysis followed by LC-MS/MS analysis using isotopomeric $[^{13}C_6]$-tyrosine as an internal standard.

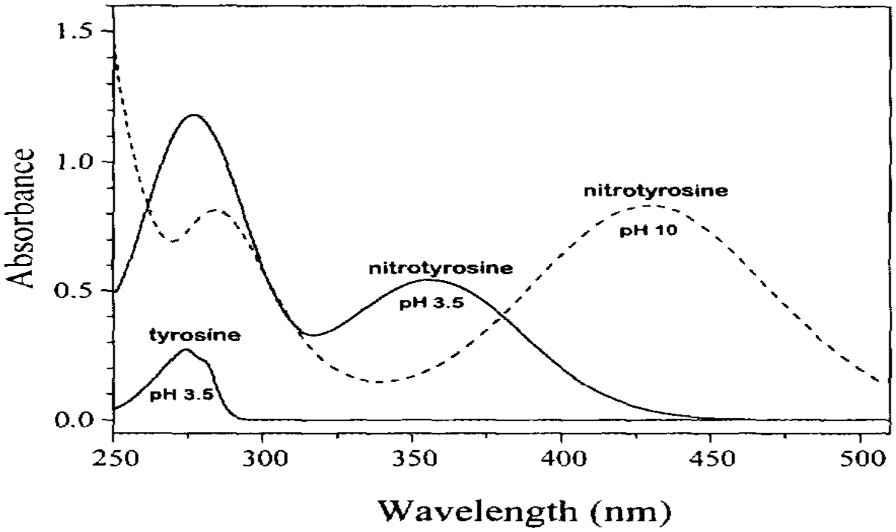

Figure 3- 2 UV-visible spectra of tyrosine and nitrotyrosine (Crow and Beckman (1995))

In this study, TNM was used to prepare the standard nitrated proteins including bovine serum albumin (BSA) and ovalbumin (OVA). To determine the nitration degrees (ND) of the nitrated proteins, we develop a simple, inexpensive and robust HPLC-UV-Vis-DAD method, which is based on the one developed by Crow and Beckman (1995) for free nitrotyrosine. Here, ND is defined as the number of nitrotyrosine residues divided by the total number of tyrosine residues. As will be demonstrated below, it is applicable for characterizing the reaction kinetics of protein nitration by nitrogen oxides and ozone. Besides, mass spectra of native and nitrated proteins were acquired and analyzed using deconvolution software.

3.2 Methods

3.2.1 Chemicals

Bovine serum albumin (BSA) (05473-50G) was obtained from Fluka. Ovalbumin (Grade V, A5503-5G), tetranitromethane (TNM) (T25003-5G), phosphate buffered saline (PBS) tablet (P4417-50TAB) and bicinchoninic acid assay (BCA) kit (BCA1-1KT) were obtained from Sigma-Aldrich, Schnelldorf, Germany. L-3-Nitrotyrosine (ALX-106-020-G001) was obtained from Alexis, Grünberg, Germany. Water for chromatography (LiChrosolv) was obtained from Merck, Damstadt, Germany. For all other purposes, high purity water (18.2 MΩ m was taken from an ELGA LabWater system (PURELAB Ultra, ELGA LabWater Global Operations, UK). Synthetic air, nitrogen (99.9995 %) and ~5 ppmv NO_2 in N_2 99.9995 % were obtained from AIR LIQUIDE Deutschland GmbH, Germany.

Size exclusion chromatography columns PD-10, Sephadex G-25M (17-0851-01) and PD MiniTrap G-25 (28-9180-08) were obtained from GE Healthcare, Freiburg, Germany.Syringe filters (cellulose acetate membrane, 1.2 µm pore size, 30 mm diameter, sterile. FP 30) were obtained from Whatman (Whatman GmbH, Dassel, Germany).

3.2.2 Nitration of proteins and determination of nitration degree

The preparation of nitrated protein standards basically followed the optimized nitration procedure described by Franze et al. (Franze et al., 2003). Briefly, the protein was dissolved in PBS (50 mg/mL BSA or 10 mg/mL OVA). Aliquots of the protein solution (2.5 mL) were pipetted into 20 mL glass vials with screw caps. TNM dissolved in methanol (4 % v/v) was added in different amounts corresponding to the tetranitromethane/tyrosine ratios listed in Table 1. The reaction mixtures were stirred with Teflon-coated magnetic bars at room temperature (~298 K), and the reaction times were varied in the range of 35-230 min (Table 1). Each reaction mixture was then pipetted onto a PD-10 size exclusion chromatography column and eluted with water. The columns had been pre-washed with 40 mL of water, and upon elution of the reaction mixtures the first 2.5 mL of the eluate were discarded, and the subsequent ~ 3.5 mL were collected. Two aliquots of the eluate were taken to determine the protein concentration (50 µL) and the concentration of nitrotyrosine residues (150 µL), respectively. The remaining eluate was dried under a high purity N_2 stream or in a freeze drier (ALPHA 2-4 LDplus, Martin Christ Gefriertrocknungsanlagen GmbH, Germany) and stored in a refrigerator at 4 ºC (Yang et al., 2010).

The protein concentration in the eluate was determined with a bicinchoninic acid (BCA) assay. The 50 µL eluate aliquot was diluted with water (to 2 mL) to a concentration in the range of 200-1000 µg/mL, and 0.1 mL of this diluted solution was then mixed with 2 mL of the BCA working reagent. After incubation at room temperature for 3-6 hours, the absorbance of the solution was measured at 562 nm using an UV-Vis Spectrometer (Perkin Elmer, Lambda 25). The determined concentration was used to calculate the total amount of protein in the eluate and the recovery of protein from the nitration reaction, respectively.

The concentration of nitrotyrosine residues in the eluate was determined by dilution of the 150 µL eluate with 0.05 N NaOH into 1.5 mL solution and measurement of absorbance at 425 nm calibrated against 3-nitrotyrosine in 0.05 N NaOH (Perkin Elmer, Lambda 25 UV/VIS Spectrometer). The average nitrotyrosine residue number per protein molecule (NTN) was then determined from the amount-of-substance (mol) of nitrotyrosine divided by the amount-of-substance of protein. Based on the NTN value, the nitrated protein standards were designated as nitro-(NTN)-BSA or nitro-(NTN)-OVA (Table 1). The ND was calculated by NTN divided by the total number of tyrosine residues in one protein molecule (Yang et al., 2010).

3.2.3 Analysis of nitrated proteins with HPLC-DAD-MS

The dilute protein solutions applied in the BCA assay were also analyzed with the HPLC-DAD system (Agilent Technologies 1200 Series) consisting of a binary pump (G1312B), a 4-channel micro-vacuum degasser (G1379B), a column thermostat (G1316B), an auto-sampler with thermostat (G1330B), a photo-diode array detector (DAD, G1315C) and a quadropole mass spectrometer (6130). Chemstation software (Version B.03.01, Agilent) was used for system control and data analysis.

A monomerically bonded C18 column (Vydac 238TP, 250 mm × 2.1mm i.d., particle size: 5µm. Grace Vydac, Alltech) was used for the chromatographic separation. Gradient elution was applied with 0.1 % (v/v) trifluoroacetic acid in water and acetonitrile (ACN) at the flow rate of 300 µL min^{-1}. The chromatographic run started with 0.1 % (v/v) trifluoroacetic acid in water and then the ACN content was increased to 20 % within 4 min, and to 100 % within the next 16 min. The mobile phase composition was reset to initial conditions within 10 min, and the column was equilibrated for 2 min before the next run. The absorbance was monitored with the DAD at 280 nm and 357 nm. The sample injection volume was 100 µL (Yang et al., 2010).

Electrospray (ESI) was interfaced to the quadrupole mass spectrometer, and all the mass spectra were acquired in the positive mode. The ionization voltage was 4000 V, and the mass range of acquired mass spectra was 500-2000 Da. Mass calibration and tuning were done using the tuning standard provided by Agilent.

3.2.5 Gas phase nitration

Syringe filters were prewashed with autoclaved high purity water (18.2 MΩ m) and dried with freeze-dryer. 100 μL of BSA aqueous solution (~5 g L^{-1}) was pipetted onto the prewashed filter and dried by lyophilisation (~0.2 mbar for 40~60 min). The BSA-loaded syringe filters were then exposed to a synthetic gas flow containing variable amounts of nitrogen dioxide, ozone and water vapor. NO_2 was supplied from a gas cylinder (~5 ppmv NO_2 in N_2 99.9995 %) at a flow rate of 10-70 mL/min. Ozone was produced from synthetic air passing through a mercury vapor lamp (Jelight Company, Inc., Irvine, USA) at ~1.5 L/min. At the end of a dark flow tube (~ 4 L) inside which NO_2 in N_2 and O_3 in synthetic air have been mixed (residence time ~2.5 min) water vapor was introduced by passing a N_2 flow at ~1.0 L/min through a washing bottle filled with autoclaved high purity water. The relative humidity achieved in the gas mixtures was between 30 % ~ 50 %. The concentrations of the trace gases and water vapor were measured with commercial monitoring systems (NO_x analyzer, 42i-TL, Thermo SCIENTIFIC; ozone analyzer, 49i, Thermo SCIENTIFIC; the humidity detector, ALMEMO 2390-3, AHLBORN, Mess und Regelungstechnik GmbH, Germany).

The BSA-loaded syringe filters were exposed to the gas mixtures for 1 - 7 days and then extracted with water (6 mL). The extract was dried by lyophilisation (at ~0.8 mbar for ~24 hours), re-dissolved in water (0.5 mL), pipetted onto a PD MiniTrap G-25 column, that had been pre-washed with 8 mL of water, and eluted the column with 1 mL of water. The eluate was collected and used for analysis with HPLC-DAD to determine NTN values for the products of the exposure experiments and for analysis of protein concentration by BCA assay to subsequently calculate the protein recovery rate. Because the amount of the sample is small, BCA assay based on 96 well plate was employed. Briefly, 200 µL BCA working reagent was added into 25 µL eluate. Sealed the 96 well plate (Product #9017, Corning Incorporated, Corning, NY 14831, USA) with sealing film (SealPlate®, EXCEL Scientific, Inc., Wringtwood, CA 92397, USA), incubated the samples for 3-6 hours and measured the absorbance of the solutions with MULTISKAN EX (Thermo Electron Corporation) at 560 nm (Yang et al., 2010).

3.3 Results and discussion

3.3.1 Nitrotyrosine detection with UV-Vis spectrometer and quantification of standard nitrated protein

Nitrated protein standards with ND were obtained by reaction between protein and TNM at different molar ratios and for different lengths of time. As shown in Table 3-1 and Fig. 3-3, generally the ND increased with increasing TNM:tyrosine molar ratio (TNM/Tyr) and reaction time. Within the investigated range of experimental conditions (Table 3-1), the ND values exhibited only a weak dependence on reaction time but a strong dependence on the molar ratio of TNM to tyrosine residues (TNM/Tyr). As illustrated in Fig. 3-3, the observed increase of ND with increasing TNM/Tyr ratio was near-logarithmic for BSA (R^2 = 0.941) and near-linear for OVA (R^2 = 0.992).

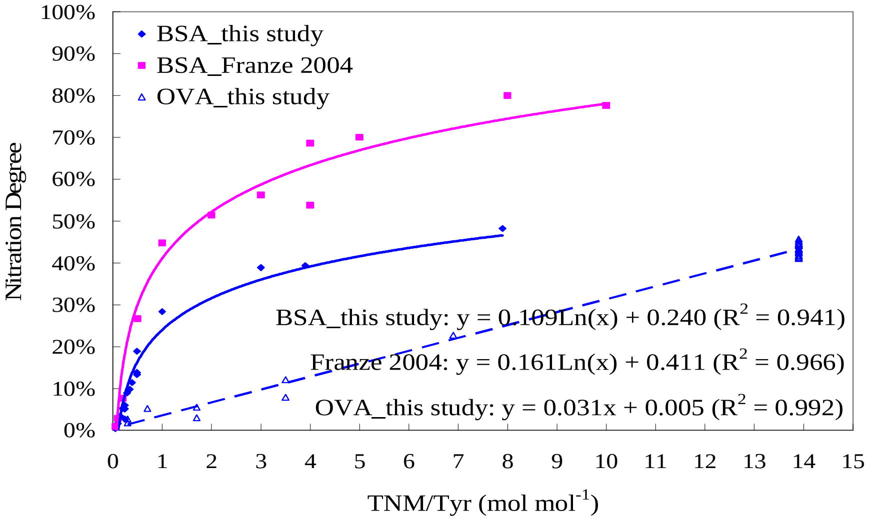

Figure 3- 3 the relationships between ND and TNM/Tyrosine molar ratios of nitrated BSA and nitrated OVA

For nitrated BSA, the ND increase linearly with TNM/Tyr before ND reaches ~30 % and it reaches a plateau gradually with increasing TNM/tyrosine ratio after ND reaches 30 %. This indicates that for steric reason only the tyrosine residues at the surface of the protein molecule can be nitrated by TNM in the liquid solution. Data from the previous study (Franze et al., 2004) shows the similar correlation (Fig. 1), but their nitrated BSAs produced at the same TNM/tyrosine ratio and for the same reaction time as ours have systematically higher ND than those of our products. Possible reason might be that their lab temperatures were generally higher than our lab temperatures, but it can not be proved without the temperature data. For nitrated OVA, the ND has a good linear correlation with the TNM:tyrosine molar ratio.

The average recovery rate of nitrated BSA is 74.6 %±15.2 % (average±standard deviation) and that of nitrated OVA is 91.3 %±12.4 %. Precipitation was observed during the reactions when TNM:TYR molar ratio was 7.9 for BSA and 20.7 for OVA, which were the highest in our experiments. The precipitation seemed to be caused by decrease of solubility as a result of cross-linking of protein molecules when TNM:protein ratio is high. There are studies reporting the similar phenomena. Bristow and Virden observed partial loss of enzymatic activity during the nitration of tyrosine residues of staphylococcal penicillinase using TNM as nitration agent (Bristow et al., 1978). They found the loss of activity was correlated with low recovery of tyrosine plus nitrotyrosine and suggested that the loss of enzymatic activity was caused by covalent cross-linking through tyrosine, rather than by nitration. Williams and Lowe also suggested a possible mode of cross-linking might be responsible for the polymerization of some proteins on treatment with TNM based on their preliminary experiments on the formation of biphenyl and terphenyl derivatives from the tyrosine residues of proteins (Williams et al., 1971).

The ND were then determined by the nitrotyrosine measured with UV-Vis and protein concentration determined by BCA assay. 3-Nitrotyrosine can be quantified by UV-Vis spectrometer using its characteristic spectral shift in alkaline solutions. Both tyrosine and 3-nitrotyrosine have an absorption peak at 280 nm, but 3-nitrotyrosine has a secondary maximum at ~357 nm in acidic solutions ($pH \leq 3.5$) or at ~430 nm in basic solutions ($pH \geq 9.5$) (Crow et al., 1995) (Fig. 3-2). Thus, 3-nitrotyrosine can be quantified by detections of absorption at 357 nm or 430 nm depending on the acidity of the solution. This method is also reliable for quantization of 3-nitrotyrosine residues in a protein or peptide. In our study, absorption of the basic standard solution at 425 nm was detected to quantify the amount of 3-nitrotyrosine residues in the synthesized nitrated BSA and nitrated OVA standards. The reliability of this method was checked and confirmed by Franze et al. (Franze et al., 2003; Franze et al., 2004). They measured the NTN of their nitrated BSA standard by spectrophotometry at 429 nm in 0.05 M NaOH calibrated against 3-nitrotyrosine. They also hydrolyzed their nitrated BSA and analyzed the released free 3-nitrotyrosine by HPLC with UV-Vis absorption detection. The results from the two independent methods were comparable. Moreover, their immunoassay results were also consistent with their UV-Vis photometric results.

Table 3- 1 Nitrated protein standards prepared by reaction of tetranitromethane (TNM) with bovine serum albumin (BSA) or ovalbumin (OVA) in phosphate buffered saline (PBS). TNM/Tyr is the molar ratio of TNM to tyrosine residues in the reaction mixture; NTN is the number of nitrated tyrosine residues per protein molecule, and ND is the nitration degree.

Protein standards	TNM/Tyr (mol mol^{-1})	Reaction time (min)	NTN	ND (%)
BSA				
nitro-(0.08)-BSA	0.05	120	0.08	0.4
nitro-(0.3)-BSA	0.10	120	0.34	1.6
nitro-(0.6)-BSA	0.24	35	0.57	2.7
nitro-(0.7)-BSA	0.15	120	0.71	3.4
nitro-(1.1)-BSA-1	0.24	140	1.1	5.1
nitro-(1.1)-BSA-2	0.20	120	1.1	5.2
nitro-(1.3)-BSA	0.24	120	1.3	6.0
nitro-(1.9)-BSA	0.29	120	1.9	9.0
nitro-(2.1)-BSA	0.34	120	2.1	9.8
nitro-(2.4)-BSA	0.39	120	2.4	11.4
nitro-(2.8)-BSA	0.49	70	2.8	13.3
nitro-(2.9)-BSA	0.49	140	2.9	13.8
nitro-(4.0)-BSA	0.49	140	4.0	18.9
nitro-(6.0)-BSA	1.0	140	6.0	28.4
nitro-(8.2)-BSA	3.0	170	8.2	38.9
nitro-(8.3)-BSA	3.9	200	8.3	39.4
nitro-(10.1)-BSA	7.9	230	10.1	48.2
OVA				
nitro-(0.2)-OVA	0.3	35	0.18	1.8
nitro-(0.3)-OVA-1	0.3	70	0.27	2.7
nitro-(0.3)-OVA-2	1.7	35	0.30	3.0
nitro-(0.5)-OVA	0.7	70	0.52	5.2
nitro-(0.6)-OVA	1.7	70	0.55	5.5
nitro-(0.8)-OVA	3.5	70	0.79	7.9
nitro-(1.2)-OVA	3.5	140	1.2	12.1
nitro-(2.3)-OVA	6.9	140	2.3	22.7
nitro-(4.1)-OVA-1	13.9	180	4.1	41.1
nitro-(4.1)-OVA-2	13.9	180	4.1	41.2
nitro-(4.1)-OVA-3	13.9	180	4.1	41.5
nitro-(4.2)-OVA-1	13.9	180	4.2	41.8
nitro-(4.2)-OVA-2	13.9	180	4.2	42.4
nitro-(4.3)-OVA-1	13.9	180	4.3	42.6
nitro-(4.3)-OVA-2	13.9	180	4.3	42.9
nitro-(4.3)-OVA-3	13.9	180	4.3	43.2
nitro-(4.3)-OVA-4	13.9	180	4.3	43.4
nitro-(4.4)-OVA-1	13.9	180	4.4	44.1
nitro-(4.4)-OVA-2	13.9	180	4.4	44.1
nitro-(4.4)-OVA-3	13.9	180	4.4	44.3
nitro-(4.4)-OVA-4	13.9	180	4.4	44.4
nitro-(4.5)-OVA-1	13.9	180	4.5	44.6
nitro-(4.5)-OVA-2	13.9	180	4.5	44.7
nitro-(4.5)-OVA-3	13.9	180	4.5	45.2
nitro-(4.6)-OVA	13.9	180	4.6	45.7

3.3.2 Correlation between nitration degree and absorption peak area ratio A_{357}/A_{280}

Fig. 3-4 shows the HPLC-DAD calibration curves obtained with the nitrated protein standards. The relations between ND and the ratio of absorbance peak areas at 357 nm and 280 nm (A_{357}/A_{280}) can be described by second order polynomials ($R^2 > 0.99$). At low ND (ND < 0.2) they are near-identical for both BSA and OVA (relative deviations < 2 %). Even at high ND (ND ~ 0.5) the deviations between the BSA and OVA calibration curves did not exceed the measurement uncertainties of ~6 %, suggesting that one single calibration curve can be applied for determining the ND of different types of nitrated proteins.

At the low ND that are most relevant for kinetic experiments with nitrating gas mixtures (ND <= 0.1; Sect. 3.3.4), the calibration curves can be fitted by linear regression ($R^2 > 0.99$).

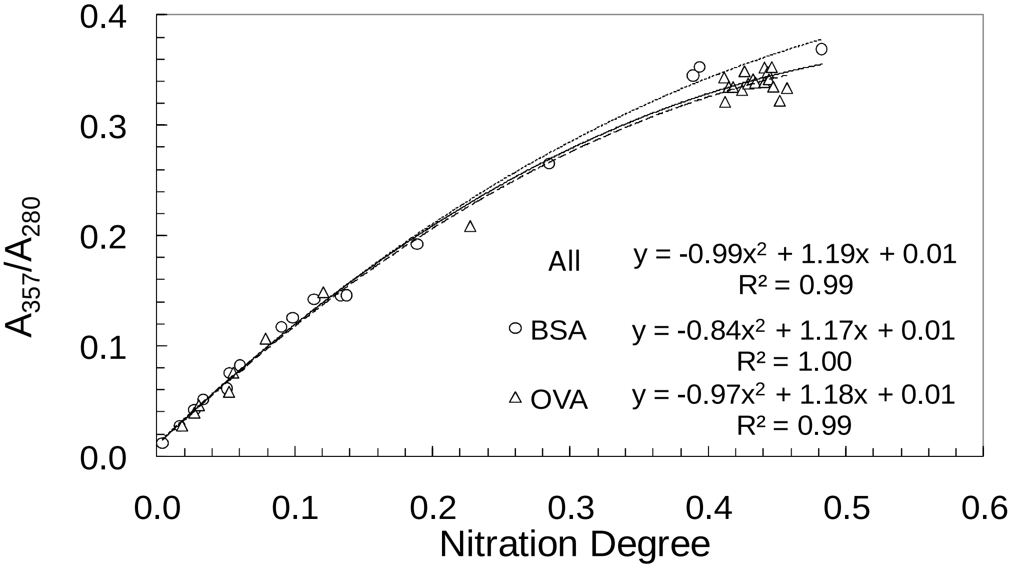

Figure 3- 4 Calibration curves plotting the ratio of absorbance peak areas at 357 nm and 280 nm (A_{357}/A_{280}) against the nitration degree (ND) of nitrated protein standards for BSA (···), for OVA (---), and for all samples (—), respectively

As illustrated in Fig. 3-5a the calibration curve of absorbance peak area ratio A_{357}/A_{280} vs. ND remained essentially unchanged when the chromatographic column of the HPLC system was exchanged, which demonstrates high robustness of our method. In contrast, an alternative calibration approach using only the peak area at 357 nm instead of the peak area ratio A_{357}/A_{280} was strongly influenced by the change of chromatographic column (Fig. 3-5b).

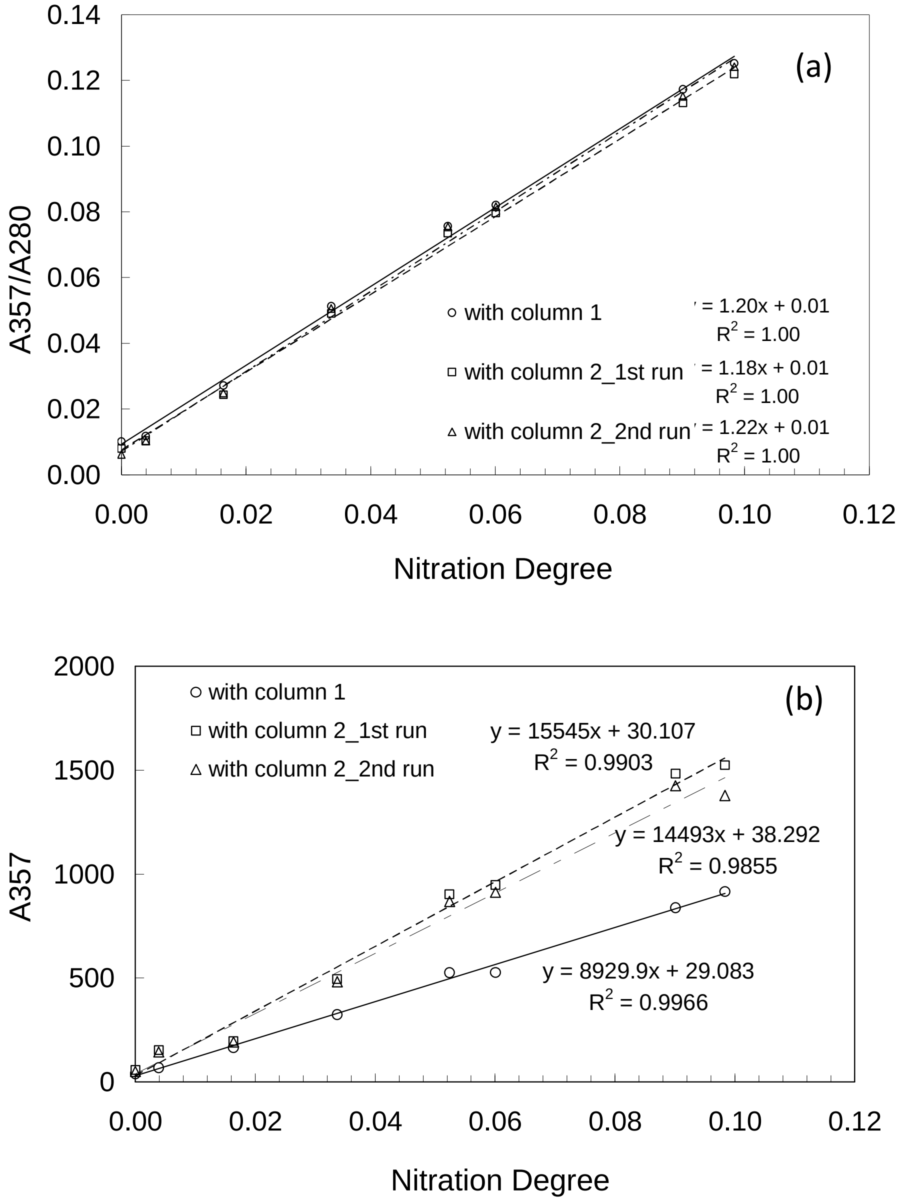

Figure 3- 5 Calibration lines plotting the ratio of absorbance peak areas at 357 nm and 280 nm (A_{357}/A_{280}, panel a) or just the absorbance peak area at 357 nm (A_{357}, panel b) against the nitration degree (ND) of nitrated BSA standards measured with different chromatographic columns

With regard to ND, the detection limit of our method is 0.0035 based on the standard deviation of measurements with unnitrated BSA (3s method), corresponding to ~0.51 pmol/µL nitrotyrosine (41 pmol in 80 µL) of the absolute concentration of nitrotyrosine in the investigated protein solution samples, which is comparable to 16 pmol nitrotyrosine per 80 µL injection by Crow and Beckmann for free nitrotyrosine (Crow and Beckmann 1995).

3.3.3 Application in kinetic experiments

An example of application of this analysis method in our kinetic study of BSA exposed to synthetic gas mixtures of NO_2 and O_3 was shown in Fig. 3-7. Two series of experiment data were shown. In one series, BSA samples were exposed to 102±1.9 ppb NO_2 and 110±3.5 ppb O_3 for 1-7 days. In another series BSA samples were exposed to 212±8.5 ppb NO_2 and 209±5.7 ppb O_3 for 1-7 days. The NO_2 and O_3 concentrations were the mean values averaged over the whole exposure period. The relative humidities in the two experiments were 41 %±0.8 % and 37%±0.4 % respectively. The exposures were carried on at room temperature with the mean values of 22.5 °C and 21.3°C, respectively.

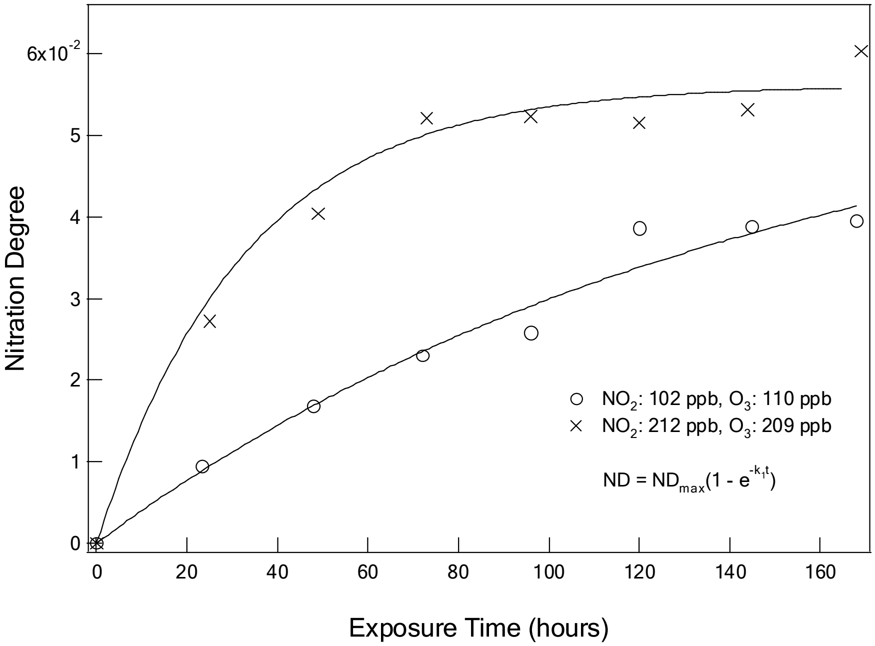

Figure 3- 6 Nitration degrees plotted against exposure time for bovine serum albumin (BSA) exposed to synthetic gas mixtures of NO_2 and O_3 at ~ 40% relative humidity.

The results show that when the concentrations of NO_2 and O_3 were both around 100 ppb the ND of nitrated BSA molecules produced after one day exposure is ~ 1 % and the ND increased steadily along the time before it reaches a maximum at around 4 % after 5 days. Similar phenomena were also observed when the concentrations of NO_2 and O_3 were increased to ~210 ppb and higher ND was obtained. This application example shows that our analysis method can directly quantify the ND of the products from the gas exposure nitration experiments.

3.3.4 Interpretation of mass spectra of native and nitrated protein

For better understanding the properties of native and nitrated proteins, e.g. the molecular weight of native and nitrated protein, MS was also applied in this study. The attachment of nitro group ($-NO_2$) will lead to a mass shift of 45 Da. If the molecular weights of native and nitrated protein are obtained, using the difference between the two values to divide 45 will get an accurate ND of the nitrated proteins. A typical mass spectrum of intact protein (BSA) was showed in Fig. 3-7. Because the multiplicity of organic functional groups in a biological molecule, e.g. the 20 different base groups composing protein, can attract protons in positive mode, proteins are multiple charged. It provides the possibility of calculating the accurate molecular weight of proteins using deconvolution. The principle of deconvolution is using the m/z of two neighboring peaks of protein mass spectra (m_1, m_2, and $m_2>m_1$) and assuming continuity of charge states and proton ionization, then we will have the following equations:

$m_1 = (M+n_1)/n_1$;

$m_2 = (M+n_2)/n_2$;

$n_2 = n_1-1$

Using these equations, we will have the equations for deconvolution:

$$n2 = \frac{m1-1}{m2-m1}\text{; } M = n_2*(m_2-1).$$

m denotes the m/z measured by MS; M denotes the molecular weight of the analyzed protein; n denotes the charge state z.

Deconvolution provides independent M value for each peak, and average the M calculated from each peak. If a good quality mass spectrum has been obtained, the averaged M value is close to the average molecular weight of biomolecule. For example, the molecular weight of BSA is determined as 66430 Da in our study.

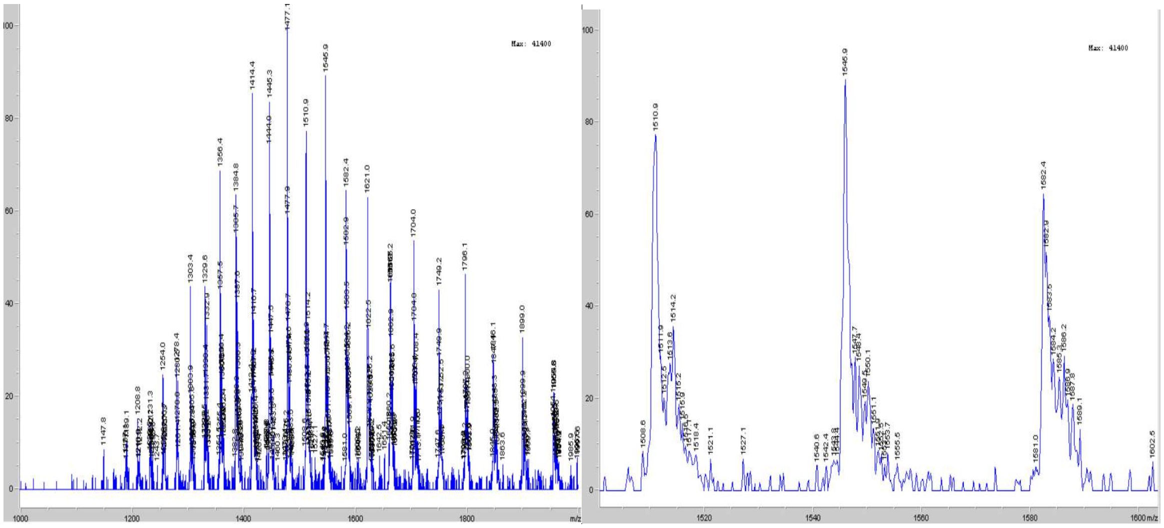

Figure 3- 7 The mass spectrum of native BSA (panel a) and the zoomed view of the mass spectrum (panel b).

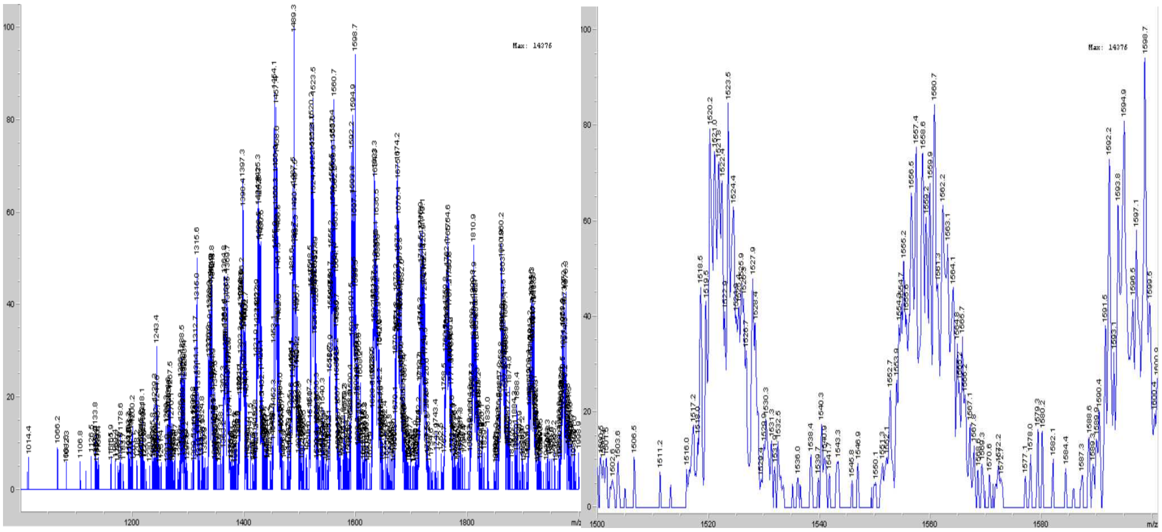

Figure 3- 8 The mass spectrum of nitrited BSA (panel a) and the zoomed view of the mass spectrum (panel b).

Figure 3-8 showed a mass spectrum of the nitrated BSA, and it showed a more complex spectrum compared to native BSA showed in figure 3-6. There are more signals in one peak in the nitrated BSA than in the native BSA. It indicats that the protein nitration causes the mass shift in the mass spectrum and the nitrated BSA analyzed is a mixture of nitrated BSA at different ND. After deconvolution, not only mass shift of 45 Da but also mass shift of 29 Da was found, which suggests that there are nitration and nitrosylation reactions during the reaction between protein and TNM. Therefore, the ND determined using the HPLC- DAD method is the average value. Because of the complexity of the mass spectrum, it failed to identify the molecular weight of the nitrated BSA. It suggested that better identification is acquired for further studying on the nitration mechanism.

3.4 Conclusions

Series of nitrated BSA and nitrated OVA standards were synthesized at different TNM/tyrosine molar ratio in liquid phase by TNM. Different relationships between ND and TNM/tyrosine molar ratio indicate different nitration mechanisms for BSA and OVA.

An HPLC-DAD method has been developed and applied to investigate the nitration of proteins after exposure to synthetic gas mixtures of NO_2, O_3 and water vapor. Good correlation has been found between ND and the ratios of chromatography absorption peak area at 357 nm to that at 280 nm (A_{357}/A_{280}) and used as the calibration curve to calculate the nitration degrees of gas phase nitrated proteins. The calibration curve is very stable and not affected by the change of analytical column. This method requires no hydrolysis or digestion of proteins and thus avoids introduction of artifacts and saves time.

The HPLC-DAD method has been applied to detect and quantify the ND of the products of the gas exposure experiments. Apparent correlations were observed between the nitration degrees of the exposed BSA and exposure time at different gas concentration levels. This confirms the applicability and consistency of our measurement method.

Mass spectrometer has also been applied to obtain the accurate molecular weight of the proteins and nitrated proteins. The molecular weight of BSA is determined as 66430 Da in our study.

3.5 References

Abello, N., H. A. M. Kerstjens, D. S. Postma and R. Bischoff (2009). "Protein tyrosine nitration: selectivity, physicochemical and biological consequences, denitration, and proteomics methods for the identification of tyrosine-nitrated proteins." Journal of Proteome Research **8**(7): 3222-3238.

Alvarez, B., G. Ferrer-Sueta, B. A. Freeman and R. Radi (1999). "Kinetics of peroxynitrite reaction with amino acids and human serum albumin." Journal of Biological Chemistry **274**(2): 842-848.

Beckman, J. S., T. W. Beckman, J. Chen, P. A. Marshall and B. A. Freeman (1990). "Apparent hydroxyl radical production by peroxynitrite - implications for endothelial injury from nitric-oxide and superoxide." Proceedings of the National Academy of Sciences of the United States of America **87**(4): 1620-1624.

Beckman, J. S., H. Ischiropoulos, L. Zhu, M. Vanderwoerd, C. Smith, J. Chen, J. Harrison, J. C. Martin and M. Tsai (1992). "Kinetics of superoxide dismutase-catalyzed and iron-catalyzed nitration of phenolics by peroxynitrite." Archives of Biochemistry and Biophysics **298**(2): 438-445.

Beckmann, J. S., Y. Z. Ye, P. G. Anderson, J. Chen, M. A. Accavitti, M. M. Tarpey, C. R. White and J. S. Beckman (1994). "Extensive nitration of protein tyrosines in human atherosclerosis detected by immunohistochemistry." Biological Chemistry Hoppe-Seyler **375**(2): 81-88.

Bristow, A. F. and R. Virden (1978). "Preferential nitration with tetranitromethane of a specific tyrosine residue in penicillinase from Staphylococcus aureus PCl: evidence that the preferentially nitrated residue is not part of the active site but that loss of activity is due to intermolecular cross-linking." Biochem. J. **169**: 381-388.

Brunekreef, B. (2001). "NO_2: the gas, that won't go away." Clinical and Experimental Allergy **31**(8): 1170-1172.

Brunekreef, B. and J. Sunyer (2003). "Asthma, rhinitis and air pollution: is traffic to blame?" European Respiratory Journal **21**(6): 913-915.

Crow, J. P. and J. S. Beckman (1995). "Quantitation of protein tyrosine, 3-nitrotyrosine, and 3-aminotyrosine utilizing HPLC and intrinsic ultraviolet absorbance." Methods (Orlando) **7**(1): 116-120.

Crow, J. P. and H. Ischiropoulos (1996). Detection and quantitation of nitrotyrosine residues in proteins: In vivo marker of peroxynitrite. Nitric Oxide, Pt B. San Diego, Academic Press Inc. **269:** 185-194.

Duncan, M. W. (2003). "A review of approaches to the analysis of 3-nitrotyrosine." Amino Acids

25(3-4): 351-361.

Franze, T., M. G. Weller, R. Niessner and U. Pöschl (2003). "Enzyme immunoassays for the investigation of protein nitration by air pollutants." Analyst **128**(7): 824-831.

Franze, T., M. G. Weller, R. Niessner and U. Pöschl (2004). "Comparison of nitrotyrosine antibodies and development of immunoassays for the detection of nitrated proteins." Analyst **129**(7): 589-596.

Franze, T., M. G. Weller, R. Niessner and U. Pöschl (2005). "Protein Nitration by Polluted Air." Environ. Sci. Technol. **39**(6): 1673-1678.

Greenacre, S. A. B. and H. Ischiropoulos (2001). "Tyrosine nitration: localisation, quantification, consequences for protein function and signal transduction." Free Radical Research **34**(6): 541-581.

Gruijthuijsen, Y. K., I. Grieshuber, A. Stoecklinger, U. Tischler, T. Fehrenbach, M. G. Weller, L. Vogel, S. Vieths, U. Pöschl and A. Duschl (2006). "Nitration enhances the allergenic potential of proteins." International Archives of Allergy and Immunology **141**: 265-275.

Halliwell, B. and M. Whiteman (2004). "Measuring reactive species and oxidative damage *in vivo* and in cell culture: how should you do it and what do the results mean?" British Journal of Pharmacology **142**(2): 231-255.

Herce-Pagliai, C., S. Kotecha and D. E. G. Shuker (1998). "Analytical methods for 3-nitrotyrosine as a marker of exposure to reactive nitrogen species: a review." Nitric Oxide **2**(5): 324-336.

Kaminsky, D. A., J. Mitchell, N. Carroll, A. James, R. Soultanakis and Y. Janssen (1999). "Nitrotyrosine formation in the airways and lung parenchyma of patients with asthma." Journal of Allergy and Clinical Immunology **104**(4): 747-754.

Kirsch, M. and H. de Groot (2002). "Formation of peroxynitrite from reaction of nitroxyl anion with molecular oxygen." Journal of Biological Chemistry **277**(16): 13379-13388.

Lee, S. J., J. R. Lee, Y. H. Kim, Y. S. Park, S. I. Park, H. S. Park and K. P. Kim (2007). "Investigation of tyrosine nitration and nitrosylation of angiotensin II and bovine serum albumin with electrospray ionization mass spectrometry." Rapid Communications in Mass Spectrometry **21**(17): 2797-2804.

Pacher, P., J. S. Beckman and L. Liaudet (2007). "Nitric oxide and peroxynitrite in health and disease." Physiological Reviews **87**(1): 315-424.

Riordan, J. F., Sokolovs.M and B. L. Vallee (1966). "Tetranitromethane. A reagent for nitration of tyrosine and tyrosyl residues of proteins." Journal of the American Chemical Society **88**(17): DOI: 10.1021/bi00875a029.

Riordan, J. F., Sokolovs.M and B. L. Vallee (1967). "Environmentally sensitive tyrosyl residues . nitration with tetranitromethane." Biochemistry **6**(1): DOI: 10.1021/bi00853a053.

Saleh, D., P. Ernst, S. Lim, P. J. Barnes and A. Giaid (1998). "Increased formation of the potent oxidant peroxynitrite in the airways of asthmatic patients is associated with induction of nitric oxide synthase: effect of inhaled glucocorticoid." Faseb Journal **12**(11): 929-937.

Sokolovs.M and J. F. Riordan (1970). "On use of tetranitromethane as a nitration reagent for tyrosyl residues." Febs Letters **9**(4): 239-241.

Sokolovs.M, J. F. Riordan and B. L. Vallee (1966). "Tetranitromethane: a reagent for nitration of tyrosyl residues in proteins." Biochemistry **5**(11): DOI: 10.1021/bi00875a029.

Williams, J. and J. M. Lowe (1971). "The cross-Linking of tyrosine by treatment with tetranitromethane." Biochem. J. **121**: 203-209.

Yang, H., Zhang, Y. and Pöschl, U. (2010): Quantification of nitrotyrosine in nitrated proteins, Analytical and Bioanalytical Chemistry, doi:10.1007/s00216-010-3557-3.

Yi, D., B. A. Ingelse, M. W. Duncan and G. A. Smythe (2000). "Quantification of 3-nitrotyrosine in biological tissues and fluids: generating valid results by eliminating artifactual formation." Journal of the American Society for Mass Spectrometry **11**(6): 578-586.

4. Protein digestion and analysis by HPLC-chip-MS/MS

4.1 Introduction

Protein nitration, a protein post-translational modification occurring under the action of nitrating agents, has been extensively investigated (Abello et al., 2009). The nitration of biomolecules, including proteins, desoxyribonucleic acid (DNA) and lipids, plays an important role in biological systems and human diseases. It can trigger cellular responses ranging from subtle modulations of cell signalling to oxidative injury, committing cells to necrosis or apoptosis (Halliwell et al., 2004; Pacher et al., 2007).

Protein nitration has been reported in association with at least 50 diseases and more than 80 animal models or cell culture systems (Greenacre et al., 2001), e.g. asthma (Kaminsky et al., 1999; Saleh et al., 1998). On the other hand, some studies suggested the traffic-related air pollution with high concentrations of nitrogen oxides and ozone tend to be related to allergic diseases (Brunekreef, 2001; Brunekreef et al., 2003). Franze et al. (Franze et al., 2005) found that nitration of proteins can occur upon exposure to synthetic gas mixtures of nitrogen oxides and ozone, and polluted urban air (summer smog). He proposed that protein nitration by traffic-related air pollution promotes allergies. This hypothesis was supported by the Gruijthuijsen's immunological experiments (Gruijthuijsen et al., 2006), which triggers the further studies of protein nitration by traffic-related air pollution, mainly the gas mixtures of nitrogen oxides (NO_X) and ozone (O_3). In these studies, suitable analytical methods are required. Most of the studies on protein nitration focused on the detection and /or quantification of free nitrotyrosine either in its circulating free form or in protein hydrolyzates (Duncan, 2003; Greenacre et al., 2001; Herce-Pagliai et al., 1998; Ryberg et al., 2007; Tsikas et al., 2005). We have presented a high performance liquid chromatography coupled to diode-array detection (HPLC-DAD) method without complex sample preparation, e.g., hydrolysis, to determine the nitration degrees (ND) of the proteins nitrated by either tetranitromethane (TNM) or nitration gases nitrogen oxides and ozone. Quantification of total nitrotyrosine is useful for identifying ND of protein exposed to nitration agent, which is suitable for kinetic study of gas phase nitration. However, for understanding the mechanism of protein nitration, site-specific information is acquired. Moreover, the ND of individual nitrated residues (i.e., quantity of nitrotyrosine vs. tyrosine residues), which could infer the extent of nitration-evoked change in the function of a given protein, is also important for this purpose. Suitable analytical methods need to be developed.

With introduction of soft ionization methods suitable for proteins and peptides, namely matrix-assisted laser desorption/ionization (MALDI) (Karas et al., 1988) and electrospray (ESI) (Fenn et al., 1989; Whitehouse et al., 1985), mass spectrometry (MS), especially tandem mass spectrometry (MS/MS), could be used to study protein nitration at peptide or protein level (Walcher et al., 2003). The two most powerful approaches provided by MS/MS are peptide mass fingerprinting (Ling et al., 1991) and peptide fragment fingerprinting upon collision induced fragmentation (Biemann, 1986; Biemann et al., 1994; Martin et al., 2000), which make MS (/MS) a suitable analytical method for studying post-translational modification, e.g., protein nitration (Aebersold et al., 2001). Mass fingerprinting determines protein nitration based on a mass increase of 45 Da, and peptide fragment fingerprinting can localize the modified amino acid in the protein sequence.

With ESI as the interface of MS, reversed-phase high performance liquid chromatography (RP-HPLC) provides good separations of the peptide generated from tryptic digestion. Lots of studies indicated HPLC-ESI-MS (/MS) is one of the most successful techniques for studying protein nitration and accomplishes the identification of nitration sites in proteins and peptides nitrated by different nitration agents (Curcuruto et al., 1999; Delatour et al., 2002; Greis et al., 1996; Jiao et al., 2001; Sharov et al., 2002). Walcher et al. (Walcher et al., 2003) reported that, after tryptic digestion, protein nitrated by both TNM and gas mixtures of nitrogen dioxide (NO_2) and O_3 could be analyzed using HPLC-ESI-MS/MS. In his study, he also discussed the differences of the nitrotyrosine residues found in BSA nitrated by TNM and gas mixtures: less nitrotyrosine residues were found in gas mixtures nitrated BSA than in TNM nitrated BSA; the ND of nitrotyrosine residue in gas mixtures nitrated BSA were generally the same as those found in TNM nitrated BSA. Therefore, Walcher et al. suggested protein gas phase nitration is highly site-selective.

In this study, nitrated protein standard series were prepared using the TNM method as nitrated protein standard series and the ND of them were determined using the HPLC-DAD method described in Chapter 3 and by Yang et al (2010). Gas phase nitrated BSA was prepared upon exposure to synthetic gas mixture of NO_2 and O_3 and ND was determined using the same HPLC-DAD. HPLC-chip-MS/MS was used to analyze nitrated protein after tryptic digestion. The correlations between nitration degrees of each nitrotyrosine residues found (ND_Y) and ND of nitrated protein determined by HPLC-DAD have been studied. The correlation of ND of nitrated proteins between from HPLC-chip-MS/MS and from HPLC-DAD has been studied as well. The difference between the nitrotyrosine residues found in different nitration pathways has also been discussed.

4.2 Methods

4.2.1 Chemicals and samples

Bovine serum albumin (BSA) (05473-50G) was obtained from Fluka. Ovalbumin (Grade V, A5503-5G), tetranitromethane (TNM) (T25003-5G) and phosphate buffered saline (PBS) tablet (P4417-50TAB) were obtained from Sigma-Aldrich, Schnelldorf, Germany. Ammonium bicarbonate (A6141, Sigma), dithiothreitol (DTT) (D5545, Sigma), iodoacetamide (IAM) (I6125, Sigma-Aldrich), trifluoroethanol (TFE) (T63002, Sigma-Aldrich), and sequencing grade trypsin (T6567, Sigma-Aldrich) were purchased from Sigma-Aldrich and dissolved in autoclaved ultra-pure water to prepare stock solutions prior to use. 0.1 N acetic acid (34254, Sigma-Aldrich,) was diluted to 50 mN solution to prepare trypsin stock solution. Formic acid (28905, Perbio Science Deutschland) was obtained from Perbio Science. C18 spin tube used for desalting was obtained from Pierce (Thermo, Germany). Water for chromatography (LiChrosolv) was obtained from Merck, Damstadt, Germany. For all other purposes, high purity water (18.2 MΩ m was prepared by an ELGA LabWater system (PURELAB Ultra, ELGA LabWater Global Operations, UK).

Nitrated proteins (BSA and OVA) were synthesized using the method described in Chapter 3. In brief, standard proteins reacted with TNM at different TNM/Tyr ratio under the same condition for different length of reaction time. Gas phase nitrated BSA was obtained upon the exposure of synthetic gas mixture of NO_2 and O_3. The ND of the nitrated protein standard series and the gas phase nitrated BSA were determined using the HPLC-DAD method described in Chapter 3. After analysis, nitrated proteins were dried under nitrogen stream and stored at 4 °C before tryptic digestion and HPLC-chip-MS/MS analysis.

4.2.2 Digestion and desalting of native and nitrated proteins

About 0.1 mg of dried nitrated proteins was dissolved in 0.1 mL water in 1.5 mL Eppendorf tube. 5 µL 100 mN ammonium bicarbonate solution, 5 µL TFE denaturizing agent and 0.5 µL 200 mN DTT solution were used to denature the 0.1 mL protein solution at 60 ºC for 1 hour. After 1 hour, 2 µL 200 mN IAM solution was then added to the mixture to alkylate the protein at room temperature in dark for 1 hour. After alkylation, another 0.5 µL 200 mN DTT solution was added to the solution to destroy excess IAM at room temperature in dark for another 1 hour. 60 µL water and 20 µL 100 mN ammonium bicarbonate solution were added to solution to dilute denaturant and raised the pH value of the solution before digestion with trypsin. 2 µg trypsin in 2 µL 50mN acetic acid (1:50 enzyme: substrate) was then used to digest the proteins. The mixture was incubated at 37 ºC overnight. 0.4 µL formic acid was used to stop the digestion. After digestion, samples were desalted by conditioned C18 spin tube before HPLC-chip-MS/MS analysis.

4.2.3 HPLC-chip-MS/MS analysis and data processing

The desalted digested protein samples were loaded to an HPLC-MS/MS chip cube system consisting of a nano pump (G2226A, Agilent), a 4-channel micro-vacuum degasser (G1379B, Agilent), and a Q-ToF mass spectrometer (6520, Agilent) by a capillary pump (G1376A, Agilent) with degasser (G1379B, Agilent) and an auto-sampler with thermostat (G1377A, Agilent). The control of all modules was performed using the Mass Hunter software (version B.02.00, Agilent). The data were then submitted to the Spectrum Mill software (version A.03.03.084, Agilent) for database search to locate the tyrosine and nitrotyrosine residues.

A µ-fluidic HPLC chip cube system (Zorbax 300SB-C18, 5 µm particle size, 75 µm i.d., and 150 mm length) interfaced to a Q-TOF MS instrument was used for peptide separation. Formic acid (the volume fraction is 0.1 %) in water (Chromasolv, Sigma, Seelze, Germany) was used as elute A and acetonitrile (Chromasolv, Sigma, Seelze, Germany) as elute B. The gradient used for separation started with 3 % elute B, increased to 40 % in 23 min, then increased to 70 % in 5 min, decreased to 3 % at 28.1 min, and kept for 2 min before starting new run. Spray voltage was set to 1750 V and fragmentor voltage was 175 V. Drying gas was 300 °C and 4 L min^{-1}. The acquisition mode was auto MS/MS, and the collision energy started with 2.5 V and increased 3.7 V per 100 Da. The mass range (m/z) were 300 to 2400 Da in the MS mode and 59 to 3000 Da in the MS/MS mode. Scan rates were 4 spectra per second for MS mode and 3 spectra per second for MS/MS mode. In each cycle, the MS would select the three highest peaks to fragment and the rule would be excluded after 2 spectra and released after 0.08 min. Reference correction was enable during the acquisition.

All the acquired data were submitted to Spectrum Mill for database search to identify peptides and nitrated peptides. Swiss-Prot was used as the database. Except carbamidomethylation, nitration was included in the modification. All the ions of the range 600 to 4000 Da would be extracted and the ions appearing in the chromatogram within 15 seconds and having the m/z within 1.4 Da would be considered as one peak and merged in the extraction. All the exported data should be with the score higher than 11 for protein identification and 6 for peptide identification.

4.3 Results and discussion

4.3.1 HPLC-chip-MS/MS analysis of digested native and nitrated proteins

After tryptic digestion, the digested peptides were separated and identified using HPLC-chip-MS/MS. The location of tyrosine and nitrotyrosine sites and the intensities of peptides containing tyrosine and nitrotyrosine were reported by Spectrum Mill. BSA nitrated by TNM and gas mixtures of NO_2 and O_3 as well as OVA nitrated by TNM have been studied.

BSA, a protein consisting of 607 amino acids, produces 87 different peptides when digested with proteolytic enzyme trypsin. A total of 54 native and nitrated peptides were found in the native and TNM nitrated BSA, and the amino acid coverage is 67 %. In native BSA, 17 out of 21 tyrosine residues were located; in BSA nitrated by TNM, 17 out of 21 tyrosine residues were located, and 10 tyrosine residues were found in both nitrated and unnitrated forms. A total of 62 native and nitrated peptides were found in NO_2 and O_3 nitrated BSA, and the amino acid coverage is 82 %. In BSA nitrated by NO_2 and O_3, 18 out of 21 tyrosine residues were located, and 3 tyrosine residues were found in both nitrated and unnitrated forms. The information of the located peptides in TNM nitrated BSA including retention time, measured mass (m/z) and corresponding molecular weight was listed in Table 4-1 and the information of the located peptides in NO_2 and O_3 nitrated BSA was listed in Table 4-2. The phenomenon observed in this study that less nitrotyrosine residues were found in proteins nitrated by NO_2 and O_3 than that in protein nitrated by TNM is similar to that observed by Walcher (Walcher et al. 2003). This could be due to the large excess of TNM in the liquid phase nitration, which generates larger nitration stress to protein and leads to more sufficient protein nitration. As a result, more nitrotyrosine residues were found in TNM nitrated BSA.

OVA is a protein consisting of 386 amino acids. A total of 21 native and nitrated peptides were found in native and nitrated OVA, and the amino acid coverage is 44 %. 7 out of 10 tyrosine sites were located for OVA and nitrated OVA, and 5 tyrosine residues were found in both nitrated and unnitrated forms. The large percentage of nitrated tyrosine out of unnitrated tyrosine could be attributed to the large nitration stress generated by TNM. The retention time, measured mass (m/z) and corresponding molecular weight of the located peptides were listed in Table 4-3.

Table 4- 1 Identification of tryptic peptides of BSA nitrated by tetranitromethane (TNM) by Spectrum Mill. RT denotes retention time; z denotes charge states; m/z denotes mass over charge state measured by HPLC-chip-MS/MS; theoretical mass is the theoretical molecular weight of the corresponding peptides.

position	Sequence	RT (min)	z	m/z (Da)	Theoretical mass (Da)	native tyrosine	nitrated tyrosine
35-44	(R)FKDLGEEHFK(G)	8.54	3	417.2139	1249.6212		
37-44	(K)DLGEEHFK(G)	6.64	3	325.4917	974.4578		
45-65	(K)GLVLIAFSQYLQQCPFDEHVK(L)	19.76	3	831.4249	2492.2642	Y_{54}	
66-75	(K)LVNELTEFAK(T)	13.09	2	582.321	1163.6307		
89-100	(K)SLHTLFGDELCK(V)	13.48	3	473.9048	1419.6937		
106-117	(R)ETYGDMADCCEK(Q)	7.19	2	739.7661	1478.5232	Y_{108}	
123-138	(R)NECFLSHKDDSPDLPK(L)	9.27	4	476.2251	1901.8698		
131-138	(K)DDSPDLPK(L)	6.23	2	443.7144	886.4153		
139-151	(K)LKPDPNTLCDEFK(A)	11.03	3	526.261	1576.7676		
139-155	(K)LKPDPNTLCDEFKADEK(K)	10.93	4	505.7488	2019.9692		
156-160	(K)KFWGK(Y)	6.17	2	333.1924	665.377		
161-167	(K)YLYEIAR(R)	10.67	2	464.2511	927.4934	Y_{161}, Y_{163}	
161-167	(K)yLYEIAR(R)	11.96	2	486.744	927.4934	Y_{163}	Y_{161}
168-183	(R)RHPYFYAPELLYYANK(Y)	15.59	3	682.3473	2045.028	Y_{171}, Y_{173}, Y_{179}, Y_{180}	
168-183	(R)RHPYFyAPELLYYANK(Y)	15.90	3	697.3389	2045.028	Y_{171}, Y_{179}, Y_{180}	Y_{173}
169-183	(R)HPYFYAPELLYYANK(Y)	16.55	3	630.3152	1888.9268	Y_{171}, Y_{173}, Y_{179}, Y_{180}	
169-183	(R)HPYFyAPELLYYANK(Y)	17.73	3	645.3103	1888.9268	Y_{171}, Y_{179}, Y_{180}	Y_{173}
169-183	(R)HPyFYAPELLYYANK(Y)	17.73	3	645.3103	1888.9268	Y_{173}, Y_{179}, Y_{180}	Y_{171}
169-183	(R)HPyFYAPELLYyANK(Y)	18.35	3	660.2954	1888.9268	Y_{173}, Y_{179}	Y_{171}, Y_{180}
184-197	(K)YNGVFQECCQAEDK(G)	8.59	2	874.3518	1747.705	Y_{184}	
198-204	(K)GACLLPK(I)	8.15	2	379.7168	758.4229		
205-209	(K)IETMR(E)	3.33	2	325.1694	649.3338		
249-256	(K)AEFVEVTK(L)	8.98	2	461.7453	922.488		
257-263	(K)LVTDLTK(V)	7.46	2	395.2401	789.4716		
267-280	(K)ECCHGDLLECADDR(A)	8.97	3	583.8953	1749.6625		
286-298	(K)YICDNQDTISSK(L)	6.47	2	722.3238	1443.642	Y_{286}	
286-298	(K)yICDNQDTISSK(L)	7.45	2	744.8188	1443.642		Y_{286}
298-309	(K)LKECCDKPLLEK(S)	6.87	3	511.6009	1532.7811		
299-309	(K)ECCDKPLLEK(S)	6.44	3	431.205	1291.6021		
310-340	(K)SHCIAEVEKDAIPENLPPLTADFAEDKDVCK(N)	15.46	5	703.1415	3511.672		
319-336	(K)DAIPENLPPLTADFAEDK(D)	15.50	2	978.4879	1955.9597		
319-340	(K)DAIPENLPPLTADFAEDKDVCK(N)	14.96	3	820.0651	2458.1806		
347-359	(K)DAFLGSFLYEYSR(R)	18.12	2	784.3769	1567.7427	Y_{355}, Y_{357}	
347-359	(K)DAFLGSFLYEySR(R)	19.76	2	806.868	1567.7427	Y_{355}	Y_{357}
360-371	(R)RHPEYAVSVLLR(L)	12.45	3	480.6101	1439.8118	Y_{364}	
360-371	(R)RHPEyAVSVLLR(L)	13.38	3	495.6038	1439.8118		Y_{364}
361-371	(R)HPEYAVSVLLR(L)	12.92	3	428.576	1283.7106	Y_{364}	
387-399	(K)DDPHACYSTVFDK(L)	10.19	3	518.8914	1554.6529	Y_{393}	
402-412	(K)HLVDEPQNLIK(Q)	11.02	2	653.3626	1305.7161		
421-433	(K)LGEYGFQNALIVR(Y)	15.05	2	740.4009	1479.7954	Y_{424}	
421-433	(K)LGEyGFQNALIVR(Y)	16.70	2	762.8949	1479.7954		Y_{424}
437-451	(R)KVPQVSTPTLVEVSR(S)	12.01	3	547.3183	1639.9377		
469-482	(R)MPCTEDYLSLILNR(L)	17.99	3	575.624	1724.8346	Y_{475}	
469-482	(R)MPCTEDyLSLILNR(L)	19.59	3	590.6113	1724.8346		Y_{475}
483-489	(R)LCVLHEK(T)	6.34	3	300.167	898.4815		
498-507	(K)CCTESLVNR(R)	6.24	2	569.754	1138.498		
508-523	(R)RPCFSALTPDETYVPK(A)	12.71	3	627.6472	1880.9211	Y_{520}	
508-523	(R)RPCFSALTPDETyVPK(A)	13.39	3	642.6325	1880.9211		Y_{520}

529-544	(K)LFTFHADICTLPDTEK(Q)	14.50	3	636.6458	1907.9208		
538-551	(K)VPQVSTPTLVEVSR(S)	11.99	2	756.4218	1511.8428		
548-557	(K)KQTALVELLK(H)	13.16	3	381.5764	1142.7143		
549-557	(K)QTALVELLK(H)	14.65	2	507.8132	1014.6194		
569-580	(K)TVMENFVAFVDK(C)	16.55	2	700.3544	1399.6926		
598-607	(K)LVVSTQTALA(-)	10.78	2	501.7968	1002.583		

Table 4- 2 Identification of tryptic peptides of BSA nitrated by NO_2 and O_3 by Spectrum Mill. RT denotes retention time; z denotes charge states; m/z denotes mass over charge state measured by HPLC-chip-MS/MS; theoretical mass is the theoretical molecular weight of the corresponding peptides.

position	Sequence	RT (min)	z	m/z (Da)	Theoretical mass (Da)	native tyrosine	nitrated tyrosine
29-34	(K)SEIAHR(F)	1.63	2	356.6901	712.3737		
35-44	(R)FKDLGEEHFK(G)	8.82	3	417.2112	1249.6212		
37-44	(K)DLGEEHFK(G)	7.71	2	487.7313	974.4578		
45-65	(K)GLVLIAFSQYLQQCPFDEHVK(L)	20.30	3	831.4278	2492.2642	Y_{54}	
66-75	(K)LVNELTEFAK(T)	13.24	2	582.32	1163.6307		
76-88	(K)TCVADESHAGCEK(S)	4.71	3	488.534	1463.589		
89-100	(K)SLHTLFGDELCK(V)	13.65	3	473.9024	1419.6937		
106-117	(R)ETYGDMADCCEK(Q)	7.50	2	739.7633	1478.5232	Y_{108}	
118-130	(K)QEPERNECFLSHK(D)	7.66	4	419.1992	1673.77		
118-138	(K)QEPERNECFLSHKDDSPDLPK(L)	10.00	4	636.0504	2541.1674		
123-130	(R)NECFLSHK(D)	7.37	2	517.739	1034.4724		
123-138	(R)NECFLSHKDDSPDLPK(L)	10.21	3	634.628	1901.8698		
131-138	(K)DDSPDLPK(L)	7.30	2	443.7113	886.4153		
139-151	(K)LKPDPNTLCDEFK(A)	11.84	3	526.2601	1576.7676		
139-155	(K)LKPDPNTLCDEFKADEK(K)	11.72	4	505.7478	2019.9692		
139-156	(K)LKPDPNTLCDEFKADEKK(F)	11.17	4	537.7738	2148.0641		
156-160	(K)KFWGK(Y)	7.42	2	333.1928	665.377		
161-167	(K)YLYEIAR(R)	10.85	2	464.2504	927.4934	Y_{161}, Y_{163}	
161-167	(K)yLYEIAR(R)	11.94	2	486.7433	927.4934	Y_{163}	Y_{161}
168-183	(R)RHPYFYAPELLYYANK(Y)	15.59	4	512.0139	2045.028	Y_{171}, Y_{173}, Y_{179}, Y_{180}	
169-183	(R)HPYFYAPELLYYANK(Y)	16.64	3	630.3145	1888.9268	Y_{171}, Y_{173}, Y_{179}, Y_{180}	
184-197	(K)YNGVFQECCQAEDK(G)	9.43	2	874.3552	1747.705	Y_{184}	
198-204	(K)GACLLPK(I)	9.26	2	379.7142	758.4229		
205-209	(K)IETMR(E)	4.99	2	325.1701	649.3338		
236-241	(K)AWSVAR(L)	7.91	2	345.1902	689.3729		
249-256	(K)AEFVEVTK(L)	9.13	2	461.7474	922.488		
257-263	(K)LVTDLTK(V)	8.48	2	395.2392	789.4716		
267-280	(K)ECCHGDLLECADDR(A)	9.33	3	583.8915	1749.6625		
267-285	(K)ECCHGDLLECADDRADLAK(Y)	10.78	4	562.7422	2247.9427		
286-298	(K)YICDNQDTISSK(L)	7.52	2	722.3273	1443.642	Y_{286}	
298-309	(K)LKECCDKPLLEK(S)	7.82	3	511.5977	1532.7811		
299-309	(K)ECCDKPLLEK(S)	7.41	3	431.2052	1291.6021		
310-318	(K)SHCIAEVEK(D)	6.13	2	536.7583	1072.5092		
310-340	(K)SHCIAEVEKDAIPENLPPLTADFAEDKDVCK(N)	15.49	5	703.1435	3511.672		
310-346	(K)SHCIAEVEKDAIPENLPPLTADFAEDK(D)	16.04	4	753.1231	3009.451		
319-336	(K)DAIPENLPPLTADFAEDK(D)	15.78	2	820.0675	2458.1806		
347-359	(K)DAFLGSFLYEYSR(R)	16.19	2	978.4891	1955.9597	Y_{355}, Y_{357}	
360-371	(R)RHPEYAVSVLLR(L)	12.51	3	480.6092	1439.8118	Y_{364}	
360-371	(R)RHPEyAVSVLLR(L)	14.03	3	495.6012	1439.8118		Y_{364}
361-371	(R)HPEYAVSVLLR(L)	13.60	3	428.5744	1283.7106	Y_{364}	
375-386	(K)EYEATLEECCAK(D)	8.57	2	751.8121	1502.6138	Y_{376}	
387-399	(K)DDPHACYSTVFDK(L)	10.28	3	518.8892	1554.6529	Y_{393}	

402-412	(K)HLVDEPQNLIK(Q)	11.10	2	653.3621	1305.7161		
413-420	(K)QNCDQFEK(L)	5.22	2	534.7242	1068.4415		
421-433	(K)LGEYGFQNALIVR(Y)	15.20	2	740.4026	1479.7954	Y_{424}	
423-428	(R)CASIQK(F)	2.21	2	353.6812	706.3552		
437-451	(R)KVPQVSTPTLVEVSR(S)	12.10	3	547.3183	1639.9377		
469-482	(R)MPCTEDYLSLILNR(L)	18.62	3	575.6163	1724.8346	Y_{475}	
483-489	(R)LCVLHEK(T)	7.48	2	449.7432	898.4815		
490-495	(K)TPVSEK(V)	1.76	2	330.6817	660.3563		
498-507	(K)CCTESLVNR(R)	7.36	2	569.7522	1138.498		
508-523	(R)RPCFSALTPDETYVPK(A)	12.80	3	627.6452	1880.9211	Y_{520}	
508-523	(R)RPCFSALTPDETyVPK(A)	14.05	3	642.6426	1880.9211		Y_{520}
524-528	(K)AFDEK(L)	3.07	2	305.1478	609.2879		
538-551	(K)VPQVSTPTLVEVSR(S)	12.90	3	504.6218	1511.8428		
548-557	(K)KQTALVELLK(H)	13.21	3	381.5761	1142.7143		
549-557	(K)QTALVELLK(H)	14.81	2	507.8138	1014.6194		
562-568	(K)ATEEQLK(T)	4.26	2	409.7146	818.4254		
569-580	(K)TVMENFVAFVDK(C)	17.29	2	700.3492	1399.6926		
571-597	(K)CCAADDKEACFAVEGPK(L)	9.56	3	643.2715	1927.7983		
588-597	(K)EACFAVEGPK(L)	9.48	2	554.2596	1107.5139		
598-607	(K)LVVSTQTALA(-)	11.62	2	501.7952	1002.583		

Table 4- 3 Identification of tryptic peptides of OVA nitrated by tetranitromethane (TNM) by Spectrum Mill. RT denotes retention time; z denotes charge states; m/z denotes mass over charge state measured by HPLC-chip-MS/MS; theoretical mass is the theoretical molecular weight of the corresponding peptides.

position	Sequence	RT (min)	z	m/z (Da)	Theoretical mass (Da)	native tyrosine	nitrated tyrosine
52-59	(R)TQINKVVR(F)	4.83	3	319.8684	957.584		
86-105	(R)DILNQITKPNDVYSFSLASR(L)	15.93	3	761.0665	2281.1823	Y_{98}	
86-105	(R)DILNQITKPNDVySFSLASR(L)	17.76	3	776.0608	2281.1823		Y_{98}
106-123	(R)LYAEERYPILPEYLQCVK(E)	15.63	3	762.0595	2284.1682	Y_{107}, Y_{112}, Y_{118}	
106-123	(R)LYAEERyPILPEYLQCVK(E)	16.86	3	777.053	2284.1682	Y_{107}, Y_{118}	Y_{112}
112-123	(R)YPILPEYLQCVK(E)	15.26	2	761.9033	1522.7974	Y_{112}, Y_{118}	
112-127	(R)YPILPEYLQCVKELYR(G)	17.73	3	695.3683	2084.0885	Y_{112}, Y_{118}, Y_{126}	
124-143	(K)ELYRGGLEPINFQTAADQAR(E)	13.45	3	750.3816	2249.1309	Y_{126}	
124-143	(K)ELyRGGLEPINFQTAADQAR(E)	15.04	3	765.3795	2249.1309		Y_{126}
128-143	(R)GGLEPINFQTAADQAR(E)	12.67	2	844.4248	1687.8398		
144-159	(R)ELINSWVESQTNGIIR(N)	15.61	2	929.9873	1858.9658		
160-182	(R)NVLQPSSVDSQTAMVLVNAIVFK(G)	20.33	3	820.7784	2460.3167		
160-187	(R)NVLQPSSVDSQTAMVLVNAIVFKGLWEK(A)	22.37	3	1025.2175	3073.6391		
183-187	(K)GLWEK(A)	7.37	2	316.6757	632.3402		
188-200	(K)AFKDEDTQAMPFR(V)	10.10	3	519.2462	1555.721		
201-229	(R)VTEQESKPVQMMYQIGLFR(V)	16.69	3	762.0558	2284.1464	Y_{213}	
201-229	(R)VTEQESKPVQMMyQIGLFR(V)	18.27	3	777.0503	2284.1464		Y_{213}
265-277	(K)LTEWTSSNVMEER(K)	10.95	2	791.3673	1581.7213		
281-285	(K)VYLPR(M)	7.54	2	324.1989	647.3875	Y_{282}	
281-285	(K)VyLPR(M)	9.38	2	346.6912	647.3875		Y_{282}
371-382	(K)HIATNAVLFFGR(C)	13.95	3	449.2537	1345.7375		

4.3.2 Nitration degree of nitrotyrosine residues in nitrated proteins

The observation of peptides in both native and nitrated forms in the same analytical run enabled a quantitative estimation of the nitration degree of each nitrotyrosine. The nitration degree of each nitrotyrosine residue ($\mathrm{ND_Y}$) was calculated using the equation:

$$\mathrm{ND_Y} = \frac{Intensity_{nitratedpeptide}}{Intensity_{nitratedpeptide} + Intensity_{unnitratedpeptide}}$$

As shown in Table 1-3, the nitrated peptides were eluted slightly later than the native peptides, indicative of an increase in hydrophobicity with the addition of a nitro group to the tyrosine. This will cause a slight increase of acetonitrile in the mobile phase. The quantization of the $\mathrm{ND_Y}$ was based on the assumption that ionization efficiencies were similar for native and nitrated peptides and that the signal intensities were not affected by the slight change of mobile phases (Walcher et al., 2003).

As shown in Figure 4-1, the $\mathrm{ND_Y}$ determined by HPLC-chip-MS/MS are proportional to the ND of the nitrated BSA. All $\mathrm{ND_Y}$ show linear correlations with the ND of nitrated BSA, with different slopes.

As we discussed above, not all the nitrotyrosine residues found in TNM nitrated BSA could be found nitrated in NO_2 and O_3 nitrated BSA. Only tyrosine residues 161, 364 and 520 were found nitrated in gas phase nitration. The nitrotyrosine residues found in gas mixture nitrated BSA were of very low $\mathrm{ND_Y}$. The $\mathrm{ND_{Y161}}$, $\mathrm{ND_{Y364}}$ and $\mathrm{ND_{Y520}}$ were 100 %, 0.3 % and 0.6 %, respectively. $\mathrm{ND_{Y161}}$ and $\mathrm{ND_{Y520}}$ measured by HPLC-chip-MS/MS were higher than $\mathrm{ND_{Y161}}$ and $\mathrm{ND_{Y520}}$ calculated using the nitration curve obtained from TNM nitrated BSA (calculated $\mathrm{ND_{Y161}}$: 10.1 % and $\mathrm{ND_{Y520}}$: 0 %) , while $\mathrm{ND_{Y364}}$ were lower (calculated $\mathrm{ND_{Y364}}$: 1.9 %).

As shown in Figure 4-2, the $\mathrm{ND_Y}$ determined by HPLC-chip-MS/MS are proportional to the ND of nitrated OVA. Same as nitrated BSA, all $\mathrm{ND_Y}$ show strong linear correlations with the ND of nitrated OVA, with different slopes.

The finding that $\mathrm{ND_Y}$ both in nitrated BSA and OVA showed linear correlation with the ND of nitrated proteins with different slopes suggests that, in general, all $\mathrm{ND_Y}$ increase as the ND of nitrated BSA increase. However, some of the tyrosine sites with high slope values are the more preferred nitration sites in TNM protein nitration, indicating that nitration is site-selective.

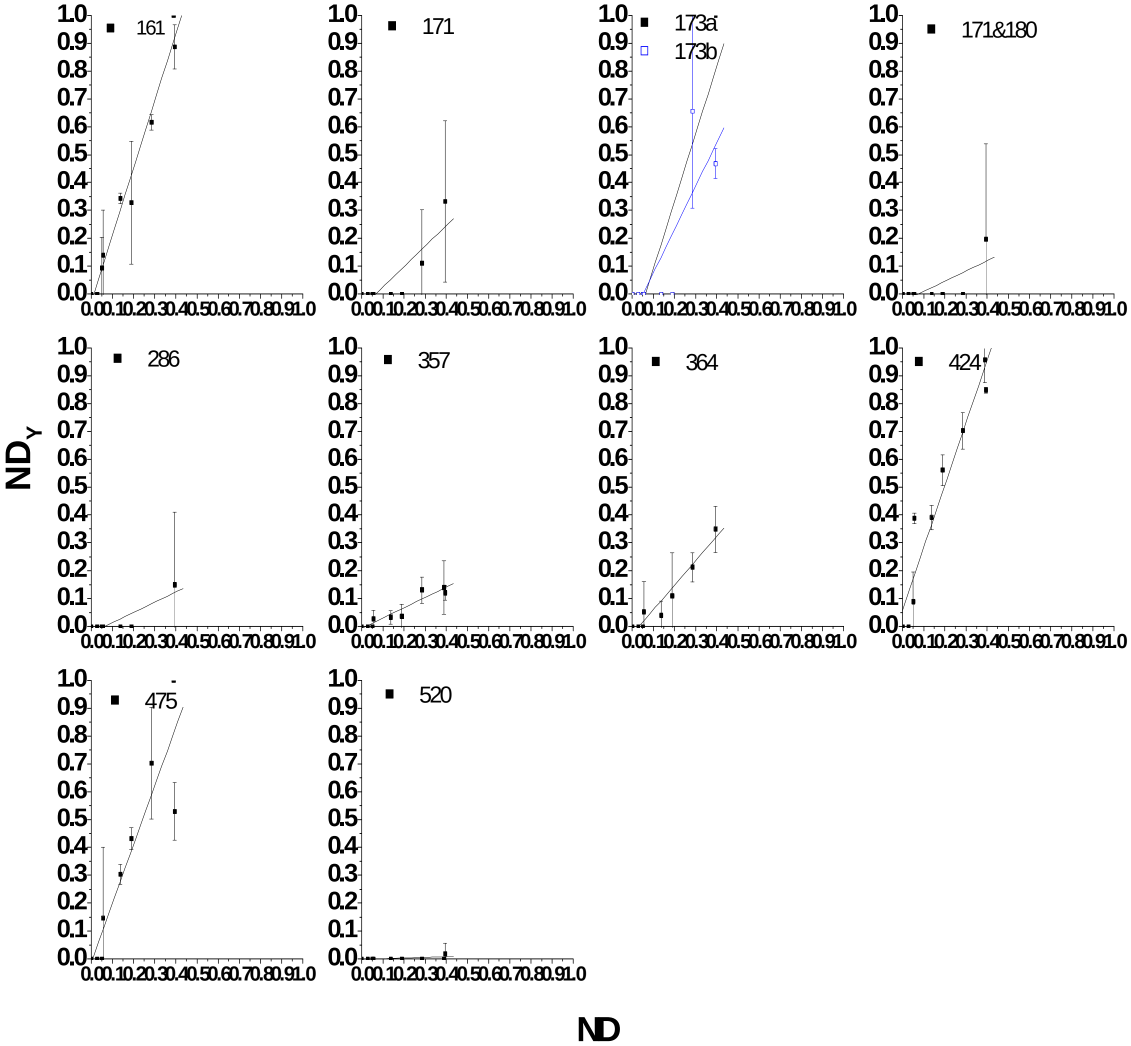

Figure 4- 1 Correlations between the nitration degree of each nitrotyrosine residues (ND_Y) found in BSA nitrated by TNM (161, 171, 173, 171&180, 286, 357, 364, 424, 475 and 520) determined by HPLC-chip-MS/MS (y axis) and the nitration degree (ND) of nitrated BSA determined by HPLC-DAD (x axis). The error bars are standard deviations, and the lines are linear fits. The correlations of each nitrotyrosine residues are as followed: 161: y = 2.417x-0.031 (R^2 = 0.978, n = 9); 171: y = 0.737x-0.049 (R^2 = 0.744, n = 8); 173a: y = 2.427x-0.153 (R^2 = 0.770, n = 7), 173b: y = 1.564x-0.082 (R^2 = 0.669, n = 8); 171&180: y = 0.367x-0.028 (R^2 = 0.536, n = 8); 286: y = 0.366x-0.023 (R^2 = 0.770, n = 7); 357: y = 0.372x-0.008 (R^2 = 0.910, n = 9); 364: y = 0.881x-0.029 (R^2 = 0.940, n = 8); 424: y = 2.245x+0.057 (R^2 = 0.920, n = 9); 475: y = 2.118x-0.013 (R^2 = 0.850, n = 9); 520: y = 0.023x-0.002 (R^2 = 0.299, n = 9).

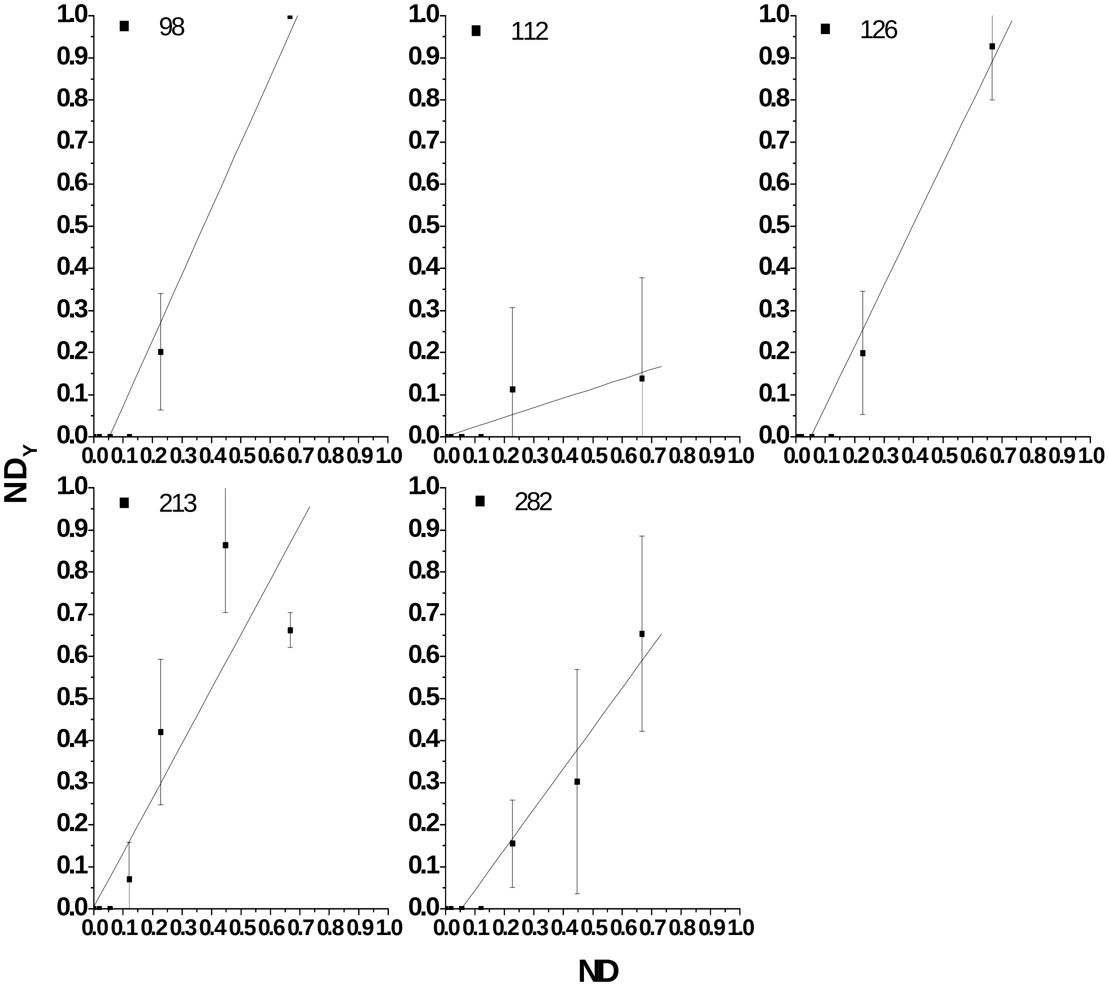

Figure 4- 2 Correlations between the nitration degree of each nitrotyrosine residues (ND_Y) found in OVA nitrated by TNM (98, 107, 126, 112, 213 and 282) determined by HPLC-chip-MS/MS (y axis) and the nitration degree (ND) of nitrated OVA determined by HPLC-DAD (x axis). The error bars are standard deviations, and the lines are linear fits. The correlations of each nitrotyrosine residues are as followed: 98: y = 1.561x-0.082 (R^2 = 0.966, n = 6); 112: y = 0.227x (R^2 = 0.775, n = 6); 126: y = 1.448x-0.075 (R^2 = 0.968, n = 6); 213: y = 1.296x+0.004 (R^2 = 0.808, n = 7); 282: y = 0.961x-0.052 (R^2 = 0.951, n = 7).

4.3.3 Selectivity of nitrated tyrosine residues

In this study, we could not observe specific sequence of the nitrotyrosine residues in TNM and gas mixture nitrated BSA and TNM nitrated OVA (Table 4-4), which suggests that protein nitration was not promoted by specific consensus sequence.

Table 4- 4 Nitrotyrosine residues found in nitrated BSA by TNM as well as NO_2 and O_3 and nitrated OVA by TNM, the bold wide character is the target nitrotyrosine, the underlined characters are glutamate (E) and aspartate (D), the one with dots is glycine (G) and ,and the grey one is tryptophan (W).

n-Tyr position	Sequence from -10 to +10 amino acids relative to the nitrated tyrosine	helice/loop	steric hindrance (disulfide bonds)
TNM nitrated BSA			
161	KADEKKFWGK**Y**LYEIARRHPY	helice	
171	YLYEIARRHP**Y**FYAPELLYYA	loop	
173	YEIARRHPYF**Y**APELLYYANK	loop	
180	PYFYAPELLY**Y**ANKYNGVFQE	helice	
286	CADDRADLAK**Y**ICDNQDTISS	helice	YIC
357	DAFLGSFLYE**Y**SRRHPEYAVS	helice	
364	LYEYSRRHPE**Y**AVSVLLRLAK	loop	
424	NCDQFEKLGE**Y**GFQNALIVRY	helice	
475	ESERMPCTED**Y**LSLILNRLCV	helice	
520	CFSALTPDET**Y**VPKAFDEKLF	loop	
NO_2 and O_3 nitrated BSA			
161	KADEKKFWGK**Y**LYEIARRHPY	helice	
364	LYEYSRRHPE**Y**AVSVLLRLAK	loop	
520	CFSALTPDET**Y**VPKAFDEKLF	loop	
TNM nitrated OVA			
98	LNQITKPNDV**Y**SFSLASRLYA	loop	
112	LASRLYAEER**Y**PILPEYLQCV	loop	
126	PEYLQCVKEL**Y**RGGLEPINFQ	helice	
213	EQESKPVQMM**Y**QIGLFRVASM	helice	
282	NVMEERKIKV**Y**LPRMKMEEKY	helice	

Souza et al. (Souza et al., 1999) suggested there was no apparent sequence to predict the protein nitration but the nearby negative charged amino acids (glutamate (E) and aspartate (D)) will promote nitration. Ischiropoulos (Ischiropoulos, 2003) also suggested the presence of a nearby negative charge (usually in position -1 before the tyrosine residue or several acidic residues within five residues on either side of the tyrosine) is required in protein tyrosine nitration. Souza et al. (Souza et al., 1999) proposed a hypothesis that the electrostatic repulsion of negatively charged nitrating agents by the carboxyl group directs the nitrating agent toward the aromatic ring of the neighbouring tyrosine, which will effectively increase the local concentration of the nitrating agent over that of the bulk solvent in the vicinity of the tyrosine residue leading to selective nitration. Among the nitrotyrosine residues found, there are four with either a glutamate or a aspartate at -1 position: 357, 364, 424 and 475 nitrotyrosine resides in TNM nitrated BSA. Nitrotyrosine residue 364 can also be found in the gas phase nitrated BSA, which suggests a negative charged amino acid at -1 position will promote the nitration not only in liquid phase but also in gas phase. Except 213 and 282 nitrotyrosine residues in TNM nitrated OVA, most of the other found nitrotyrosine residues were found with 1 to 2 glutamate or aspartate residues within 5 residues on either side.

Souza et al. (Souza et al., 1999) and Ischiropoulos (Ischiropoulos, 2003) pointed out that the secondary structure of protein is also important for predicting the preferred nitration sites. Souza et al. (Souza et al., 1999) found in their study nearly all the nitrotyrosine located on loop structures. Ischiropoulos (Ischiropoulos, 2003) examined the nitrotyrosine and found a preference for nitration of tyrosine residues located on loop structures and paucity of nitration of tyrosine residues located on β-strands. In this study, nitrotyrosine residues 171, 173, 364 and 520 in TNM nitrated BSA and nitrotyrosine residues 98 and 112 in TNM nitrated OVA were found on loop structures. This suggests that tyrosine residues located on loop structure are the preferred nitrated target in TNM nitration. Nitrotyrosine residues 364 and 520 were also found in NO_2 and O_3 nitrated BSA. That 2 out of 3 nitrotyrosine found in NO_2 and O_3 nitrated BSA were located on loop structure suggests that, in gas phase nitration, the tyrosine residues located on loop structure are also the preferred nitrated target. No nitrotyrosine residues were found on β-strands. This supports the hypothesis that paucity of nitrated tyrosine residues were located on β-strands..

It is also suggested that one important factor influencing nitration was steric hindrance (disulfide bonds) (Souza et al., 1999). Disulfide bonds in proteins are formed between the thiol groups of cysteine residues. Protein structure prediction found that only one nitrotyrosine residue with disulfide bonds within five residues on either sites, which can only found in TNM nitrated BSA but not in gas mixture nitrated BSA. Protein structure prediction also found that other 4 tyrosine residues with disulfide bonds within 5 residues on other tyrosine residues were not nitrated.

Besides the factor mentioned above, Souza et al. (Souza et al. 1999) suggested nitrating agents would also influence the nitration selectivity because the reactivity of tyrosine residues might rely on the nature of the reactive species. Greis (Greis et al. 1996) found that peroxynitrite and TNM nitrated certain proteins in a comparable manner. However, in later studies ((Batthyany et al. 2005; Lennon et al. 2007), different protein nitration patterns were found in other proteins. The nitrotyrosine residues found in both TNM nitrated and nitration gas mixtures BSA are 161, 364 and 520, and the slopes of these residues are 2.417, 0.881 and 0.023. Among these nitrotyrosine residues, the slope of 161 is the highest values but those of 364 and 520 are low values. This suggests the pattern observed from the TNM nitrated BSA reveals some preferred nitrated sites in gas phase nitration. However, not all the preferred nitration sites found in TNM nitrated BSA and gas phase nitration are the same.

4.3.4 Comparison of nitration degree from HPLC-DAD and HPLC-chip-MS/MS

The ND determined by HPLC-chip-MS/MS were plotted against the ND determined by HPLC-DAD (Figure 3). The ND from HPLC-chip-MS/MS were calculated using the sum of all ND_Y to the total tyrosine numbers of the proteins. The ND from

HPLC-DAD and HPLC-chip-MS/MS analysis showed good linear correlations for both BSA and OVA ($R^2 = 0.964$ and $R^2 = 0.901$ for BSA and OVA, respectively). However, the slopes of the linear correlations were not 1 but about 0.5, which means only 50 % of nitrotyrosine residues were found in the nitrated proteins using the HPLC-MS/MS method.

Delatour et al. (Delatour et al., 2007) pointed out that the autolysis of the enzyme(s) leads to an incomplete digestion of the substrate. Furthermore, the activity of some enzymes may be too specific to completely cleave proteins/peptides, leading to a trend in the measurement. That only one enzyme was used in this protocol may be the reason that only 50 % of nitrotyrosine residues were found in the nitrated proteins.

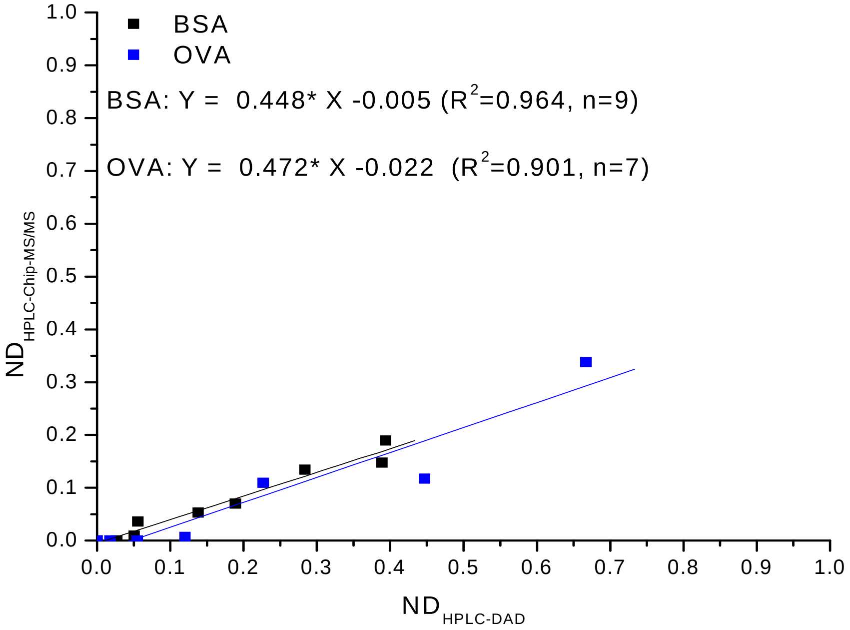

Figure 4- 3 ND determined by HPLC-DAD ($ND_{HPLC-DAD}$) vs. the ND determined by HPLC-chip-MS/MS ($ND_{HPLC-chip-MS/MS}$) of nitrated BSA (●) and OVA (●). ND denotes nitration degrees. Lines are linear fit.

4.4 Conclusions and outlook

After tryptic enzymatic digestion, an HPLC-chip-MS/MS method was applied to separate and analyze the digested peptides of native and nitrated BSA and OVA series. With high sequence coverage by the HPLC-chip-MS/MS and successful database searching by software Spectrum Mill (TNM nitrated BSA: 67 %, NO_2 and O_3 nitrated BSA: 82 %, and TNM nitrated OVA: 44 %), 17 out of 21 tyrosine residues in TNM nitrated BSA as well as 18 out of 21 tyrosine residues in NO_2 and O_3 nitrated BSA, and 7 out of 10 tyrosine residues in TNM nitrated OVA were located. Among these tyrosine residues, 10 in TNM nitrated BSA, 3 in NO_2 and O_3 nitrated BSA, and 5 in TNM nitrated OVA were found in both native and nitrated forms.

The nitration patterns of nitrotyrosine residues in both TNM nitrated BSA and TNM nitrated OVA were studied. The ND_Y of all nitrotyrosine residues were found well correlated with the ND of nitrated protein with different slope, indicating protein nitration is site-selective. The factors influencing site selectivity including primary sequence, secondary structure and nitrating agents were discussed. No apparent sequence favours the protein nitration. However, a nearby negative charge amino acids glutamate and aspartate will promote protein tyrosine nitration. Tyrosine residues located on loop structures were found to be preferred nitration target not only in TNM nitration but also in NO_2 and O_3 nitration. No nitrotyrosine residues were found located on β-strands. The nitration patterns of nitrated BSA were different in TNM nitration and NO_2 and O_3 nitration.

The ND of nitrated proteins detected using this method linearly correlated with those detected using the HPLC-DAD method. The slopes for both nitrated BSA and nitrated OVA were about 0.5.

Many analytical methods have been developed for the analysis of nitrotyrosine, either in its free form or after its release by protein hydrolysis. HPLC-chip-MS/MS provides an LC separation and allows an absorbance detector prior to MS. Moreover, it generates better fragmentation in MS/MS, which allows the localization of the modified amino acids in protein sequence. Therefore, HPLC-chip-MS/MS supported by database search has been widely used in the analysis of nitrotyrosine in its protein binding form after digestion. However, the disadvantage of this method is the nitration position can not be localized if the digested peptides contain more than one nitrotyrosine. To label the nitrotyrosine using isotope could be one protential way to solve the problem. Another problem of this method was found in this study: the ND determined by HPLC-chip-MS/MS is only 0.5 of ND determined by HPLC-DAD. Possible reason could be that only trypsin is not enough to digest and multiple enzymatic digestion is needed. Another possible reason is that the nitration of tryptophan has been ignored. Further study on protein nitration should include not only protein tyrosine nitration but also tryptophan nitration.

4.5 References

Abello, N., H. A. M. Kerstjens, D. S. Postma and R. Bischoff (2009). "Protein tyrosine nitration: selectivity, physicochemical and biological consequences, denitration, and proteomics methods for the identification of tyrosine-nitrated proteins." Journal of Proteome Research **8**(7): 3222-3238.

Aebersold, R. and D. R. Goodlett (2001). "Mass spectrometry in proteomics." Chemical Reviews **101**(2): 269-295.

Batthyany, C., J. M. Souza, R. Duran, A. Cassina, C. Cervenansky and R. Radi (2005). "Time course and site(s) of cytochrome c tyrosine nitration by peroxynitrite." Biochemistry **44**(22): 8038-8046.

Biemann, K. (1986). "Mass-Spectrometric methods for protein sequencing." Analytical Chemistry **58**(13): DOI: 10.1021/ac00126a001.

Biemann, K. and I. A. Papayannopoulos (1994). "Amino-acid sequencing of proteins." Accounts of

Chemical Research **27**(11): 370-378.

Brunekreef, B. (2001). "NO_2: the gas, that won't go away." Clinical and Experimental Allergy **31**(8): 1170-1172.

Brunekreef, B. and J. Sunyer (2003). "Asthma, rhinitis and air pollution: is traffic to blame?" European Respiratory Journal **21**(6): 913-915.

Curcuruto, O., L. Rovatti, A. M. Pastorino and M. Hamdan (1999). "Peptide nitration by peroxynitrite: characterisation of the nitration sites by liquid chromatography tandem mass spectrometry." Rapid Communications in Mass Spectrometry **13**(3): 156-163.

Delatour, T., F. Fenaille, V. Parisod, J. Richoz, J. Vuichoud, P. Mottier and T. Buetler (2007). "A comparative study of proteolysis methods for the measurement of 3-nitrotyrosine residues: Enzymatic digestion versus hydrochloric acid-mediated hydrolysis." Journal of Chromatography B-Analytical Technologies in the Biomedical and Life Sciences **851**(1-2): 268-276.

Delatour, T., J. Richoz, J. Vuichoud and R. H. Stadler (2002). "Artifactual nitration controlled measurement of protein-bound 3-nitro-L-tyrosine in biological fluids and tissues by isotope dilution liquid chromatography electrospray ionization tandem mass spectrometry." Chemical Research in Toxicology **15**(10): 1209-1217.

Duncan, M. W. (2003). "A review of approaches to the analysis of 3-nitrotyrosine." Amino Acids **25**(3-4): 351-361.

Fenn, J. B., M. Mann, C. K. Meng, S. F. Wong and C. M. Whitehouse (1989). "Electrospray ionization for mass-spectrometry of large biomolecules." Science **246**(4926): 64-71.

Franze, T., M. G. Weller, R. Niessner and U. Pöschl (2005). "Protein nitration by polluted air." Environ. Sci. Technol. **39**(6): 1673-1678.

Greenacre, S. A. B. and H. Ischiropoulos (2001). "Tyrosine nitration: localisation, quantification, consequences for protein function and signal transduction." Free Radical Research **34**(6): 541-581.

Greis, K. D., S. Zhu and S. Matalon (1996). "Identification of nitration sites on surfactant protein A by tandem electrospray mass spectrometry." Archives of Biochemistry and Biophysics **335**(2): 396-402.

Gruijthuijsen, Y. K., I. Grieshuber, A. Stoecklinger, U. Tischler, T. Fehrenbach, M. G. Weller, L. Vogel, S. Vieths, U. Pöschl and A. Duschl (2006). "Nitration enhances the allergenic potential of proteins." International Archives of Allergy and Immunology **141**: 265-275.

Halliwell, B. and M. Whiteman (2004). "Measuring reactive species and oxidative damage *in vivo* and in cell culture: how should you do it and what do the results mean?" British Journal of Pharmacology **142**(2): 231-255.

Herce-Pagliai, C., S. Kotecha and D. E. G. Shuker (1998). "Analytical methods for 3-nitrotyrosine as a marker of exposure to reactive nitrogen species: a review." Nitric Oxide-Biology and Chemistry **2**(5): 324-336.

Ischiropoulos, H. (2003). "Biological selectivity and functional aspects of protein tyrosine nitration." Biochemical and Biophysical Research Communications **305**(3): 776-783.

Jiao, K. S., S. Mandapati, P. L. Skipper, S. R. Tannenbaum and J. S. Wishnok (2001). "Site-selective nitration of tyrosine in human serum albumin by peroxynitrite." Analytical Biochemistry **293**(1): 43-52.

Kaminsky, D. A., J. Mitchell, N. Carroll, A. James, R. Soultanakis and Y. Janssen (1999). "Nitrotyrosine formation in the airways and lung parenchyma of patients with asthma." Journal of Allergy and Clinical Immunology **104**(4): 747-754.

Karas, M. and F. Hillenkamp (1988). "Laser desorption ionization of proteins with molecular masses exceeding 10000 Daltons." Analytical Chemistry **60**(20): 2299-2301.

Lennon, C. W., H. D. Cox, S. P. Hennelly, S. J. Chelmo and M. A. McGuirl (2007). "Probing structural differences in prion protein isoforms by tyrosine nitration." Biochemistry **46**(16): 4850-4860.

Ling, V., A. W. Guzzetta, E. Canovadavis, J. T. Stults, W. S. Hancock, T. R. Covey and B. I. Shushan (1991). "Characterization of the tryptic map of recombinant-DNA derived tissue plasminogen-activator by high-performance liquid-chromatography electrospray ionization mass-spectrometry." Analytical Chemistry **63**(24): 2909-2915.

Martin, S. E., J. Shabanowitz, D. F. Hunt and J. A. Marto (2000). "Subfemtomole MS and MS/MS peptide sequence analysis using nano-HPLC micro-ESI Fourier transform ion cyclotron resonance mass spectrometry." Analytical Chemistry **72**(18): 4266-4274.

Pacher, P., J. S. Beckman and L. Liaudet (2007). "Nitric oxide and peroxynitrite in health and disease." Physiological Reviews **87**(1): 315-424.

Ryberg, H. and K. Caidahl (2007). "Chromatographic and mass spectrometric methods for quantitative determination of 3-nitrotyrosine in biological samples and their application to human samples." Journal of Chromatography B-Analytical Technologies in the Biomedical and Life Sciences **851**(1-2): 160-171.

Saleh, D., P. Ernst, S. Lim, P. J. Barnes and A. Giaid (1998). "Increased formation of the potent oxidant peroxynitrite in the airways of asthmatic patients is associated with induction of nitric oxide synthase: effect of inhaled glucocorticoid." Faseb Journal **12**(11): 929-937.

Sharov, V. S., N. A. Galeva, T. V. Knyushko, D. J. Bigelow, T. D. Williams and C. Schoneich (2002). "Two-dimensional separation of the membrane protein sarcoplasmic reticulum Ca-ATPase for high-performance liquid chromatography-tandem mass spectrometry analysis of posttranslational protein modifications." Analytical Biochemistry **308**(2): 328-335.

Souza, J. M., E. Daikhin, M. Yudkoff, C. S. Raman and H. Ischiropoulos (1999). "Factors determining the selectivity of protein tyrosine nitration." Archives of Biochemistry and Biophysics **371**(2): 169-178.

Tsikas, D. and K. Caidahl (2005). "Recent methodological advances in the mass spectrometric analysis of free and protein-associated 3-nitrotyrosine in human plasma." Journal of Chromatography B-Analytical Technologies in the Biomedical and Life Sciences **814**(1): 1-9.

Walcher, W., T. Franze, M. G. Weller, U. Pöschl and C. G. Huber (2003). "Liquid- and gas-phase nitration of bovine serum albumin studied by LC-MS and LC-MS/MS using monolithic columns." Journal of Proteome Research **2**(5): 534-542.

Whitehouse, C. M., R. N. Dreyer, M. Yamashita and J. B. Fenn (1985). "Electrospray interface for liquid chromatographs and mass spectrometers." Analytical Chemistry **57**(3): 675-679.

Yang, H., Zhang, Y. and Pöschl, U. (2010): Quantification of nitrotyrosine in nitrated proteins, Analytical and Bioanalytical Chemistry, doi:10.1007/s00216-010-3557-3.

Appendix

A1 Chromatograms of reference standard and aerosol particle sample (Chapter 2).

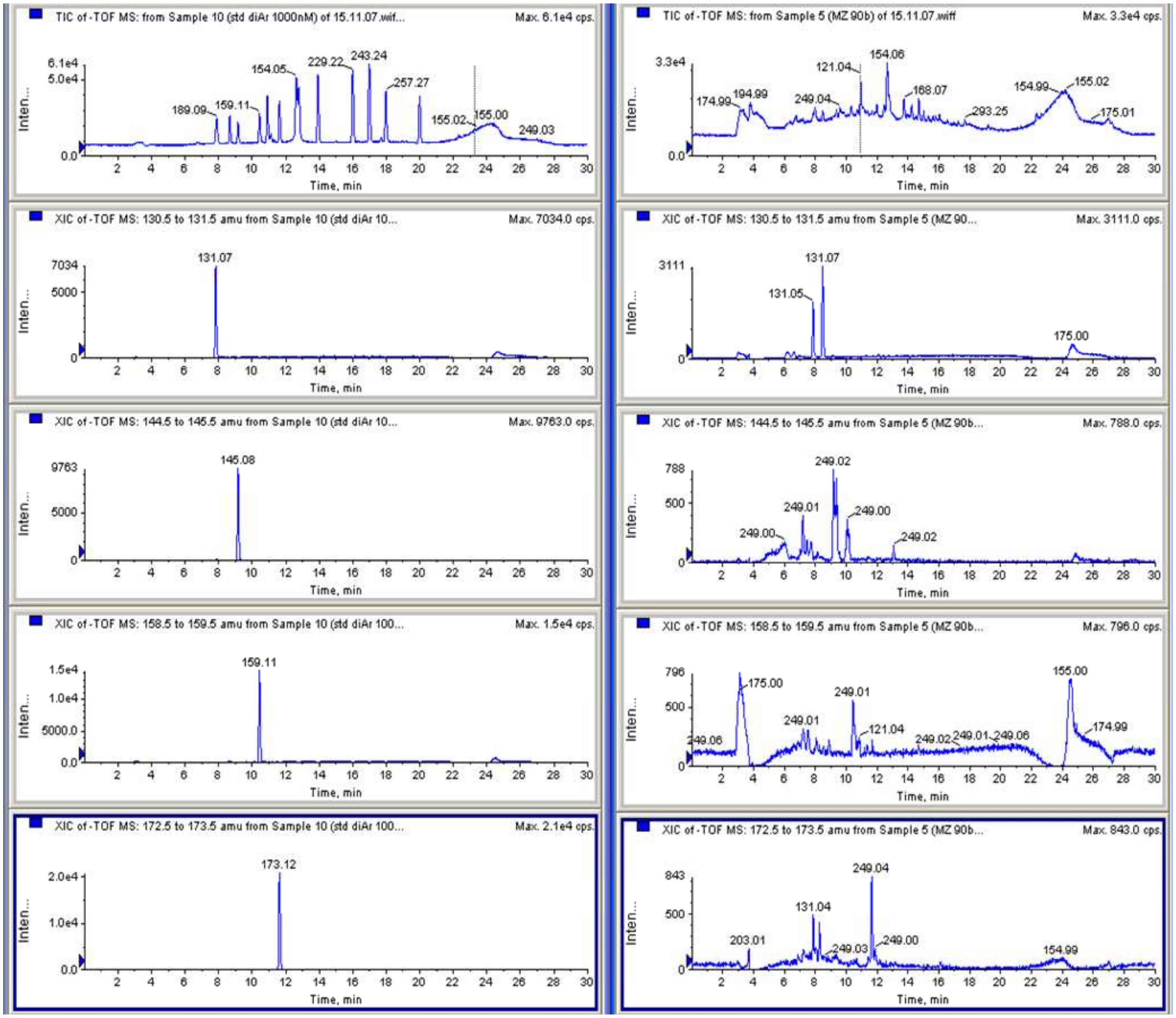

Figure A1 Typical chromatograms of standard (left side) and aerosol particle sample (right side). From top to bottom: total ion chromatogram of standard and aerosol particle sample; extract ion chromatogram of C_5; extract ion chromatogram of C_6; extract ion chromatogram of C_7; extract ion chromatogram of C_8.

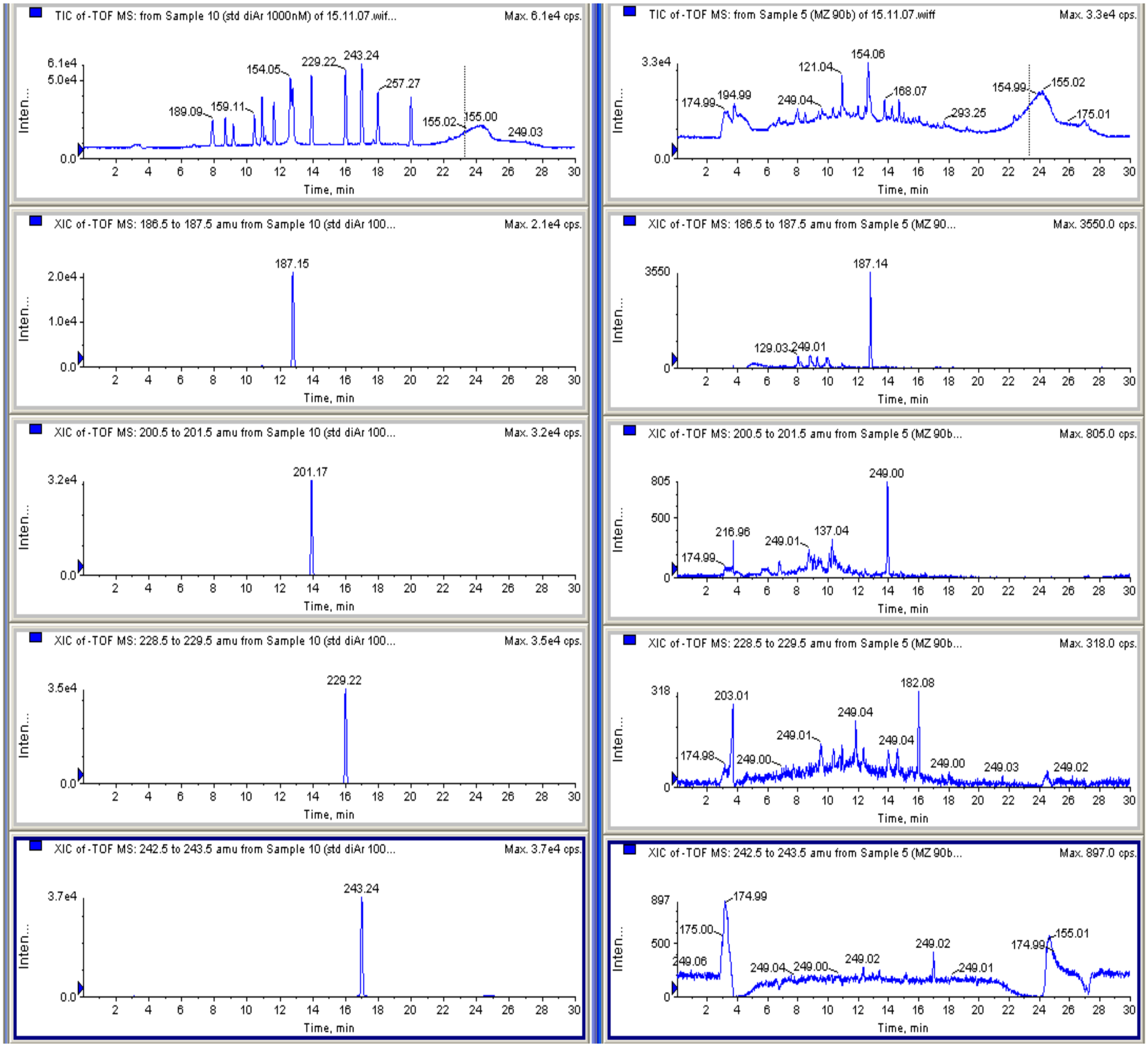

Figure A2 Typical chromatograms of standard (left side) and aerosol particle sample (right side). From top to bottom: total ion chromatogram of standard and aerosol particle sample; extract ion chromatogram of C_9; extract ion chromatogram of C_{10}; extract ion chromatogram of C_{12}; extract ion chromatogram of C_{13}.

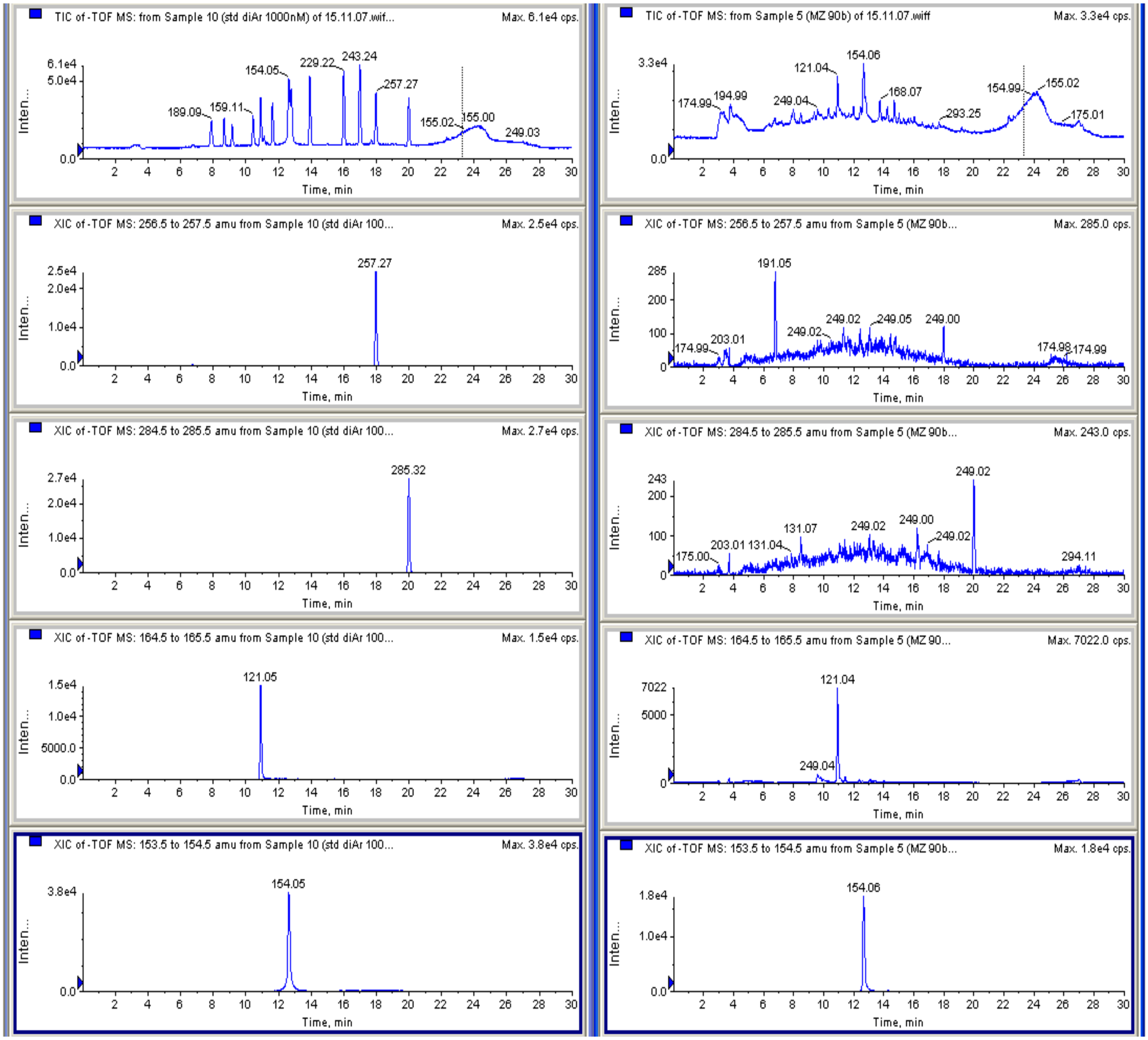

Figure A3 Typical chromatograms of standard (left side) and aerosol particle sample (right side). From top to bottom: total ion chromatogram of standard and aerosol particle sample; extract ion chromatogram of C_{14}; extract ion chromatogram of C_{16}; extract ion chromatogram of phthalic acid; extract ion chromatogram of 4-nitrocatechol.

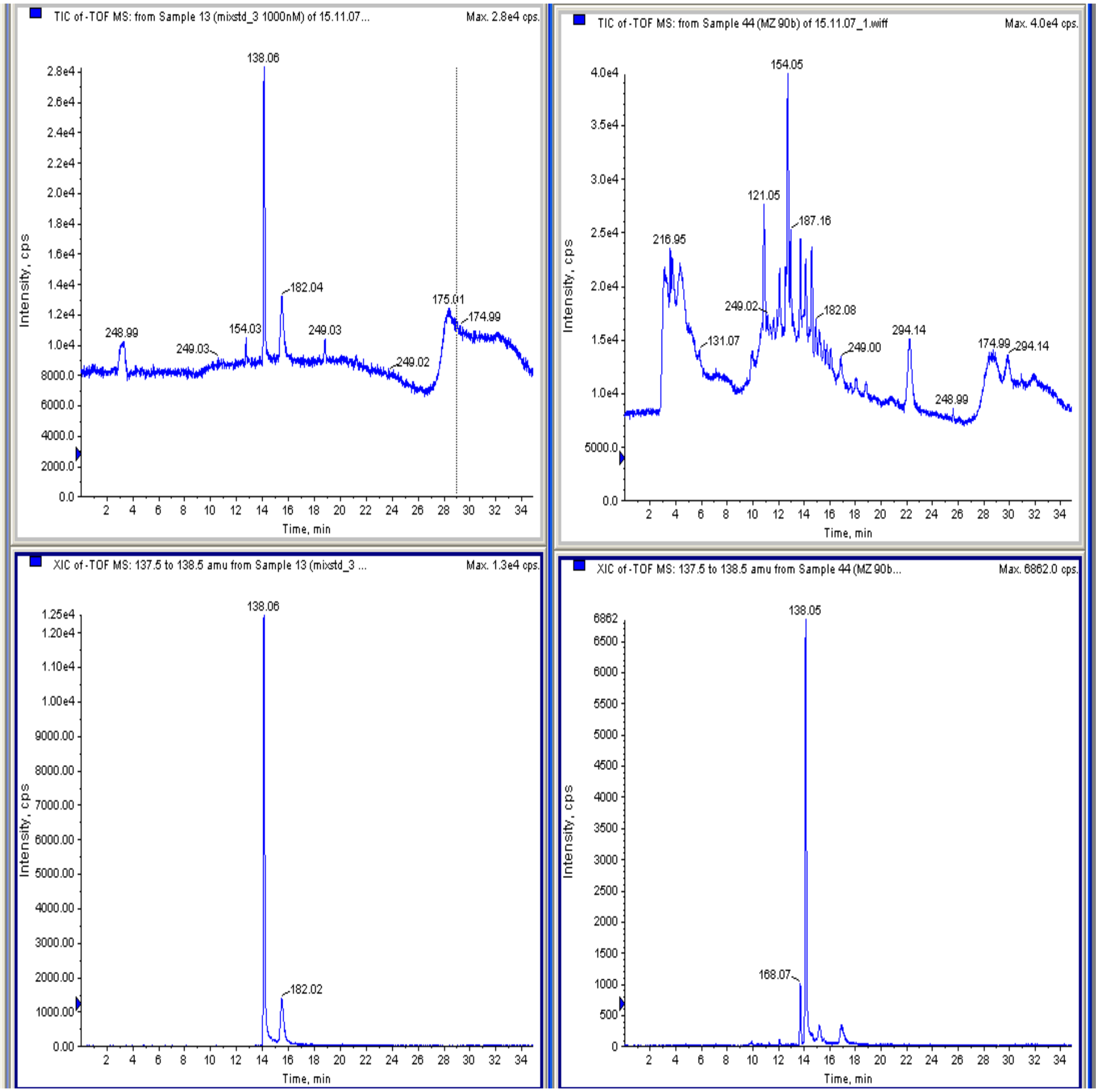

Figure A4 Typical chromatograms of standard (left side) and aerosol particle sample (right side). From top to bottom: total ion chromatogram of standard and aerosol particle sample; extract ion chromatogram of 2-nitrophenol and 4-nitrophenol.

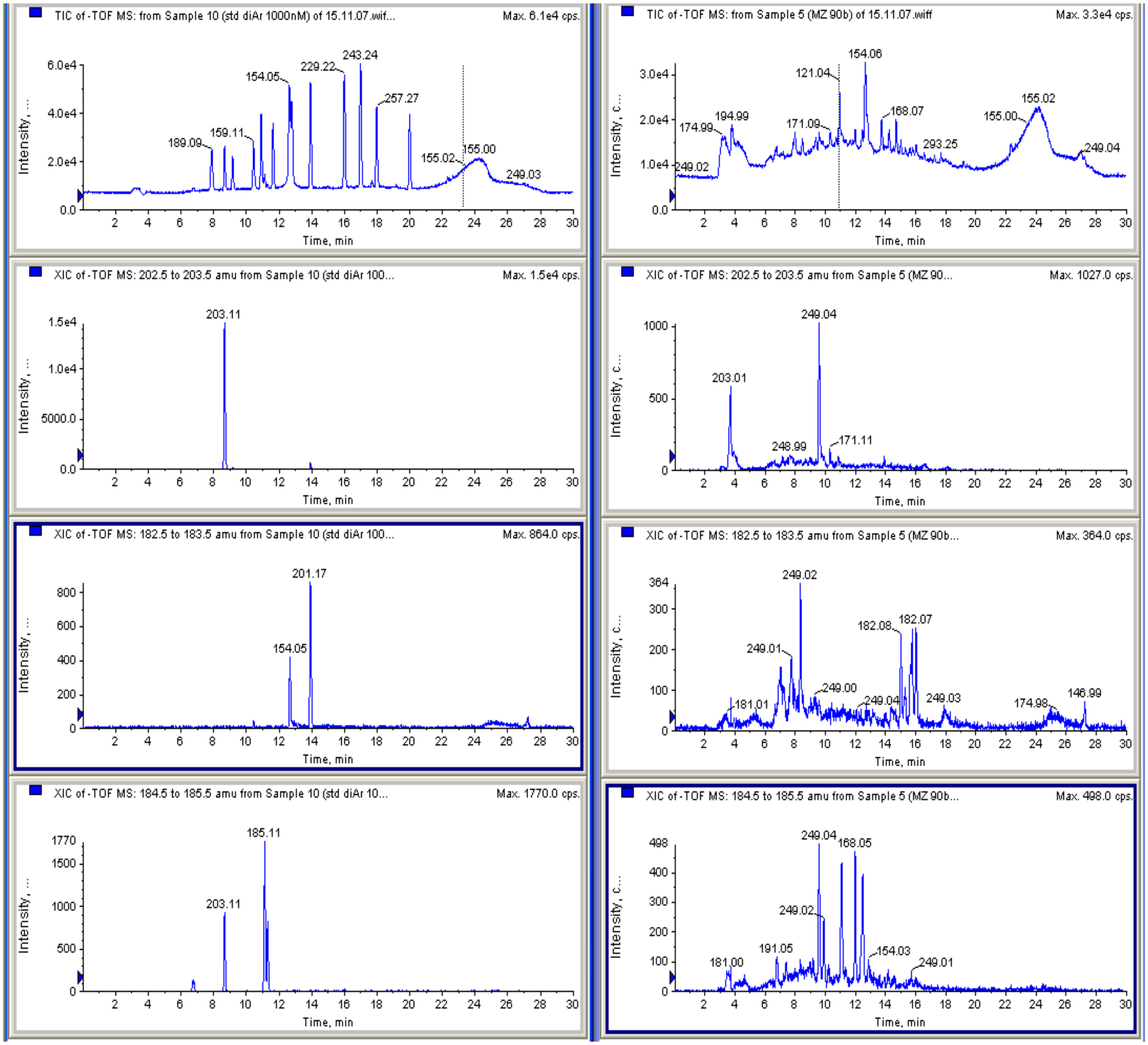

Figure A5 Typical chromatograms of standard (left side) and aerosol particle sample (right side). From top to bottom: total ion chromatogram of standard and aerosol particle sample; extract ion chromatogram of 3-MBTCA; extract ion chromatogram of pinonic acid; extract ion chromatogram of pinic acid.

A2 Overviews of air samples (Chapter 2)

Table A1. Overview of air samples in coarse particulate matter. Sample ID (running number); sampling period and time; sampled air volume; concentrations of dicarboxylic acids (a), nitrophenols and pinene oxidation products (b). Abbreviations are the same as Table 2-1.

a Dicarboxylic acid concentrations in coarse particulate matter

Sample ID	Sampling Period	Sampling time	Sampled air volume	Ph	C_5	C_6	C_7	C_8	C_9	C_{10}	C_{12}	C_{13}	C_{14}	C_{16}
		d	m^3	ng m^{-3}	ng m^3	ng m^3	ng m^3	ng m^3	ng m^3	ng m^3	ng m^3	ng m^3	ng m^3	ng m^3
MZ31a	01.06.06-06.06.06	5	1961.18	1.64	1.66	0.78	0.14	0.40	1.55	0.11	0.06	0.06	0.05	BDL[a]
MZ32a	06.06.06-08.06.06	2	776.32	2.53	1.98	1.05	BDL	0.47	1.65	0.20	0.10	0.05	0.08	0.01
MZ33a	08.06.06-13.06.06	5	1921.01	2.73	1.77	0.60	0.29	0.34	1.43	0.17	0.06	0.04	0.06	0.03
MZ34a	13.06.06-14.06.06	1	381.27	5.02	3.61	2.81	0.70	0.64	1.35	0.25	0.08	0.04	0.08	0.03
MZ35a	14.06.06-21.06.06	7	2645.96	1.35	1.55	0.58	0.23	0.36	1.31	0.14	0.06	0.03	0.06	0.03
MZ36a	21.06.06-22.06.06	1	381.61	1.57	1.36	1.14	0.30	0.42	0.69	0.09	0.04	BDL	BDL	0.03
MZ39a	22.06.06-27.06.06	5	1931.65	1.78	1.69	0.59	0.24	0.35	1.40	0.12	0.05	0.04	0.03	0.02
MZ40a	27.06.06-04.07.06	7	2697.55	1.31	1.48	0.39	0.15	0.35	0.88	0.22	0.19	0.18	0.22	0.24
MZ41a	04.07.06-11.07.06	7	1325.18	3.82	0.53	0.49	0.17	0.26	0.96	0.14	0.05	0.02	BDL	BDL
MZ42a	11.07.06-14.07.06	3	1152.02	2.99	2.15	0.84	0.36	0.46	1.29	0.15	0.07	0.04	0.07	0.03
MZ43a	14.07.06-17.07.06	3	1158.88	2.17	1.89	0.60	0.28	0.45	0.78	0.15	0.10	0.08	0.17	0.13
MZ44a	17.07.06-19.07.06	2	766.81	4.95	3.56	1.86	0.66	1.03	2.20	0.39	0.25	0.35	0.37	0.24
MZ45a	19.07.06-21.07.06	2	772.81	4.19	3.25	1.26	0.54	0.60	2.07	0.29	0.12	0.06	0.14	0.05
MZ46a	21.07.06-26.07.06	5	1880.60	3.26	3.11	1.61	0.83	0.78	1.84	0.25	0.12	0.25	0.22	0.10
MZ47a	26.07.06-02.08.06	7	2664.70	1.81	1.81	0.68	0.31	0.40	1.98	0.17	0.06	0.04	0.09	0.04
MZ51a	09.08.06-16.08.06	7	2699.24	0.91	0.86	0.38	0.17	0.28	1.14	0.07	0.03	BDL	0.03	0.01
MZ52a	16.08.06-23.08.06	7	2741.76	2.31	1.76	1.33	0.56	0.35	1.80	0.15	0.07	0.03	BDL	0.09
MZ53a	23.08.06-30.08.06	7	2773.07	1.48	0.59	0.46	0.10	0.18	0.92	0.09	0.04	0.02	0.05	BDL
MZ54a	30.08.06-06.09.06	7	1386.06	2.27	1.55	0.42	0.14	0.48	1.42	0.23	0.13	0.12	0.06	0.15
MZ55a	06.09.06-11.09.06	5	2700.44	1.44	0.90	0.47	0.16	0.22	0.79	0.07	0.03	0.02	0.03	0.02
MZ59a	11.09.06-18.09.06	7	2713.60	1.94	1.75	0.52	0.24	0.31	1.08	0.19	0.12	0.12	0.15	0.15
MZ60a	18.09.06-25.09.06	7	2668.37	1.28	1.25	0.45	0.17	0.33	1.19	0.15	0.08	0.06	0.10	0.08
MZ61a	25.09.06-02.10.06	7	2689.52	0.69	0.78	0.77	0.12	0.19	0.73	0.09	0.05	0.07	0.06	0.06

MZ62a	02.10.06-09.10.06	7	2710.88	0.56	0.58	0.23	BDL	0.17	0.49	0.09	0.08	0.08	0.09	0.11
MZ63a	09.10.06-16.10.06	7	2686.32	3.37	1.55	0.52	0.40	0.29	1.20	0.14	0.05	BDL	BDL	0.05
MZ66a	16.10.06-23.10.06	7	2590.56	2.23	1.05	0.80	0.35	0.39	1.83	0.15	0.08	BDL	BDL	0.08
MZ67a	23.10.06-30.10.06	7	2656.42	1.17	0.78	0.75	0.15	0.33	0.89	0.12	0.09	0.16	0.14	0.15
MZ68a	30.10.06-02.11.06	3	1160.89	0.94	0.68	1.14	0.20	0.33	0.80	0.17	0.12	0.11	0.12	0.13
MZ69a	02.11.06-06.11.06	7	2630.88	1.71	1.06	0.44	0.26	0.17	0.71	0.11	0.04	BDL	BDL	0.07
MZ70a	06.11.06-16.11.06	7	2660.38	1.22	0.73	0.31	0.09	0.24	0.64	0.09	0.03	BDL	0.05	0.06
MZ71a	16.11.06-23.11.06	7	2701.44	1.53	0.87	0.60	0.24	0.26	0.99	0.14	0.05	BDL	0.01	BDL
MZ74a	23.11.06-30.11.06	7	2395.36	1.09	0.75	0.42	0.09	0.25	1.42	0.14	0.07	0.06	0.08	0.09
MZ75a	30.11.06-07.12.06	7	2719.58	0.73	0.64	0.61	0.21	0.52	1.93	0.19	0.08	BDL	BDL	0.12
MZ76a	07.12.06-14.12.06	7	2686.52	0.86	0.79	0.77	0.24	0.32	0.56	0.09	0.04	BDL	BDL	0.05
MZ77a	14.12.06-21.12.06	7	2610.72	0.87	0.58	0.44	0.14	0.29	1.03	0.15	0.06	BDL	0.02	0.12
MZ80a	21.12.06-28.12.06	7	2666.67	0.90	0.82	0.37	0.10	0.23	1.42	0.13	0.05	0.03	0.05	BDL
MZ81a	28.12.06-04.01.07	7	2590.56	0.79	0.87	0.53	0.10	0.33	1.30	0.17	0.07	0.05	BDL	0.19
MZ82a	04.01.07-11.01.07	7	2655.53	0.55	0.34	0.23	BDL	0.17	0.40	0.08	0.06	0.06	0.06	0.07
MZ83a	11.01.07-18.01.07	7	2575.42	0.79	0.62	0.38	0.08	0.21	1.08	0.12	0.04	0.03	0.06	0.08
MZ84a	18.01.07-25.01.07	7	2664.46	0.59	0.27	0.32	0.09	0.10	0.42	0.04	0.02	BDL	0.02	0.04
MZ87a	25.01.07-01.02.07	7	2705.00	0.79	0.54	0.53	0.21	0.18	1.14	0.11	BDL	0.04	0.03	0.06
MZ88a	01.02.07-08.02.07	7	2640.71	0.76	0.57	0.57	0.11	0.16	0.83	0.09	BDL	0.02	0.02	0.06
MZ89a	08.02.07-15.02.07	7	2641.13	1.41	0.62	0.63	0.25	0.23	1.60	0.11	0.04	0.04	0.06	0.06
MZ93a	22.02.07-01.03.07	7	2650.72	1.27	0.95	0.74	0.23	0.33	1.63	0.13	0.05	0.04	0.05	0.06
MZ94a	01.03.07-08.03.07	7	2734.60	1.62	0.82	0.71	0.17	0.21	1.11	0.10	0.05	BDL	0.05	0.05
MZ95a	08.03.07-15.03.07	7	2600.49	1.75	0.94	1.03	0.25	0.25	1.24	0.16	0.06	0.04	0.06	0.11
MZ96a	15.03.07-22.03.07	7	2710.10	1.03	0.78	0.47	0.17	0.19	1.05	0.13	BDL	0.03	0.05	0.09
MZ97a	22.03.07-29.03.07	7	2628.44	3.97	1.32	0.75	0.36	0.34	2.23	0.20	0.07	0.05	0.06	0.06
MZ100a	29.03.07-05.04.07	7	2655.48	4.01	1.44	0.81	0.38	0.38	2.28	0.15	0.05	0.03	0.04	0.05
MZ101a	05.04.07-12.04.07	7	2658.98	1.99	1.09	0.70	0.32	0.31	1.35	0.17	0.07	0.05	0.07	0.07
MZ102a	12.04.07-19.04.07	7	2715.17	3.89	1.97	1.10	0.54	0.47	1.67	0.17	0.07	0.04	0.08	0.03
MZ103a	19.04.07-26.04.07	7	2671.53	3.19	1.64	1.06	0.51	0.39	1.63	0.15	0.07	0.04	0.05	0.03
MZ104a	26.04.07-03.05.07	7	2687.44	3.74	2.17	1.15	0.65	0.56	2.73	0.26	0.12	0.08	0.11	0.08
MZ107a	03.05.07-10.05.07	7	2704.59	2.99	1.51	0.81	0.41	0.41	1.77	0.14	0.04	0.04	0.06	0.03
MZ108a	10.05.07-17.05.07	7	2732.36	1.68	1.24	0.79	0.35	0.38	2.09	0.11	0.05	0.04	0.06	0.03
MZ109a	17.05.07-24.05.07	7	2684.00	2.60	1.93	0.99	0.49	0.52	2.27	0.16	0.07	0.06	0.06	0.05
MZ112a	24.05.07-31.05.07	7	2661.35	2.75	1.39	0.67	0.40	0.41	1.75	0.13	BDL	BDL	0.04	0.02

1 b Pinene oxidation products and nitrophenols concentrations in coarse particulate matter.

Sample ID	Sampling Period	Sampling time	Sampled air volume	3-MBTCA	Pinic acid	Pinonic acid	4-Nitrocatechol	2-Nitrophenol	4-Nitrophenol
		d	m^{3}	ng m^{-3}	ng m^{3}	ng m^{3}	ng m^{3}	ng m^{3}	ng m^{3}
MZ31a	01.06.06-06.06.06	5	1961.18	0.50	1.10	0.27	0.20	0.44	0.67
MZ32a	06.06.06-08.06.06	2	776.32	0.95	0.17	BDL	0.56	2.32	2.38
MZ33a	08.06.06-13.06.06	5	1921.01	2.00	1.33	1.90	0.84	0.24	1.44
MZ34a	13.06.06-14.06.06	1	381.27	2.34	2.05	1.29	2.42	BDL	3.83
MZ35a	14.06.06-21.06.06	7	2645.96	1.25	1.13	0.20	0.23	BDL	0.35
MZ36a	21.06.06-22.06.06	1	381.61	0.76	0.45	0.28	1.43	BDL	0.81
MZ39a	22.06.06-27.06.06	5	1931.65	1.11	0.97	0.55	0.25	BDL	0.64
MZ40a	27.06.06-04.07.06	7	2697.55	1.76	2.14	BDL	0.06	BDL	0.27
MZ41a	04.07.06-11.07.06	7	1325.18	11.16	1.65	0.43	12.74	BDL	1.14
MZ42a	11.07.06-14.07.06	3	1152.02	2.60	1.63	0.89	0.78	BDL	1.24
MZ43a	14.07.06-17.07.06	3	1158.88	1.61	1.46	1.56	BDL	BDL	0.07
MZ44a	17.07.06-19.07.06	2	766.81	3.72	3.56	4.51	BDL	BDL	0.15
MZ45a	19.07.06-21.07.06	2	772.81	2.29	1.74	2.86	0.96	BDL	2.92
MZ46a	21.07.06-26.07.06	5	1880.60	2.51	2.62	1.40	BDL	BDL	BDL
MZ47a	26.07.06-02.08.06	7	2664.70	1.59	1.43	BDL	0.01	BDL	0.94
MZ51a	09.08.06-16.08.06	7	2699.24	0.45	0.45	0.27	0.13	BDL	0.60
MZ52a	16.08.06-23.08.06	7	2741.76	1.89	0.92	0.20	0.06	BDL	0.56
MZ53a	23.08.06-30.08.06	7	2773.07	1.88	0.64	0.91	0.78	0.82	0.27
MZ54a	30.08.06-06.09.06	7	1386.06	0.99	0.35	0.73	BDL	BDL	0.25
MZ55a	06.09.06-11.09.06	5	2700.44	1.16	0.84	0.35	0.20	BDL	1.78
MZ59a	11.09.06-18.09.06	7	2713.60	2.67	2.77	BDL	0.10	0.49	0.53
MZ60a	18.09.06-25.09.06	7	2668.37	2.04	2.32	BDL	BDL	0.43	0.56
MZ61a	25.09.06-02.10.06	7	2689.52	0.77	1.37	BDL	BDL	0.23	0.35
MZ62a	02.10.06-09.10.06	7	2710.88	0.22	0.55	BDL	BDL	BDL	0.54
MZ63a	09.10.06-16.10.06	7	2686.32	2.70	0.90	0.30	0.10	1.47	1.50
MZ66a	16.10.06-23.10.06	7	2590.56	1.07	0.75	0.26	BDL	0.52	1.54
MZ67a	23.10.06-30.10.06	7	2656.42	0.39	0.76	0.22	BDL	BDL	0.58
MZ68a	30.10.06-02.11.06	3	1160.89	0.15	0.44	BDL	BDL	BDL	0.72
MZ69a	02.11.06-09.11.06	7	2630.88	0.31	0.29	BDL	BDL	0.89	1.10

MZ70a	09.11.06-16.11.06	7	2660.38	0.15	0.34	0.80	BDL	BDL	BDL
MZ71a	16.11.06-23.11.06	7	2701.44	0.21	0.15	BDL	BDL	1.13	2.67
MZ74a	23.11.06-30.11.06	7	2395.36	0.17	0.28	0.54	BDL	0.41	1.20
MZ75a	30.11.06-07.12.06	7	2719.58	0.18	0.15	BDL	BDL	0.63	1.74
MZ76a	07.12.06-14.12.06	7	2686.52	BDL	0.30	0.78	BDL	BDL	0.05
MZ77a	14.12.06-21.12.06	7	2610.72	0.07	0.18	BDL	0.09	0.79	2.94
MZ80a	21.12.06-28.12.06	7	2666.67	0.06	0.49	BDL	0.55	1.50	6.97
MZ81a	28.12.06-04.01.07	7	2590.56	0.16	0.06	BDL	0.09	0.77	2.30
MZ82a	04.01.07-11.01.07	7	2655.53	BDL	0.03	BDL	BDL	BDL	0.50
MZ83a	11.01.07-18.01.07	7	2575.42	0.14	0.10	BDL	BDL	BDL	0.82
MZ84a	18.01.07-25.01.07	7	2664.46	BDL	0.02	BDL	BDL	BDL	1.12
MZ87a	25.01.07-01.02.07	7	2705.00	BDL	0.10	BDL	BDL	BDL	1.39
MZ88a	01.02.07-08.02.07	7	2640.71	0.04	0.15	BDL	BDL	BDL	1.18
MZ89a	08.02.07-15.02.07	7	2641.13	BDL	0.17	BDL	BDL	BDL	1.28
MZ93a	22.02.07-01.03.07	7	2650.72	0.23	0.31	0.30	BDL	BDL	1.31
MZ94a	01.03.07-08.03.07	7	2734.60	0.16	0.28	0.54	BDL	BDL	1.74
MZ95a	08.03.07-15.03.07	7	2600.49	0.51	0.29	BDL	BDL	BDL	2.35
MZ96a	15.03.07-22.03.07	7	2710.10	0.22	0.10	BDL	BDL	BDL	1.55
MZ97a	22.03.07-29.03.07	7	2628.44	0.69	0.38	1.24	BDL	BDL	2.43
MZ100a	29.03.07-05.04.07	7	2655.48	0.87	0.31	1.24	BDL	BDL	1.81
MZ101a	05.04.07-12.04.07	7	2658.98	0.45	0.25	0.53	BDL	BDL	1.89
MZ102a	12.04.07-19.04.07	7	2715.17	2.54	0.92	3.97	BDL	BDL	3.20
MZ103a	19.04.07-26.04.07	7	2671.53	1.79	1.03	1.75	BDL	0.20	1.60
MZ104a	26.04.07-03.05.07	7	2687.44	2.87	1.01	2.28	BDL	BDL	3.07
MZ107a	03.05.07-10.05.07	7	2704.59	1.04	0.92	1.73	BDL	BDL	0.78
MZ108a	10.05.07-17.05.07	7	2732.36	0.68	0.54	0.16	BDL	BDL	0.49
MZ109a	17.05.07-24.05.07	7	2684.00	2.45	0.59	0.22	BDL	0.15	0.58
MZ112a	24.05.07-31.05.07	7	2661.35	6.05	0.58	0.44	BDL	0.21	0.91

[a] below detection limit (limit of quantification listed in table 2-1).

Table A2. Overview of air samples in fine particulate matter. Sample ID (running number); sampling period and time; sampled air volume; concentrations of dicarboxylic acids (a), nitrophenols and pinene oxidation products (b). Abbreviations are the same as Table 2-1.

a Dicarboxylic acid concentrations in fine particulate matter.

Sample ID	Sampling Period	Sampling time d	Sampled air volume m^3	Ph ng m^{-3}	C_5 ng m^3	C_6 ng m^3	C_7 ng m^3	C_8 ng m^3	C_9 ng m^3	C_{10} ng m^3	C_{12} ng m^3	C_{13} ng m^3	C_{14} ng m^3	C_{16} ng m^3
MZ31b	01.06.06-06.06.06	5	1780.18	1.45	0.93	0.71	0.16	0.36	1.76	0.17	0.08	0.05	0.06	0.01
MZ32b	06.06.06-08.06.06	2	703.43	6.95	2.30	2.19	0.53	0.92	4.64	0.52	0.20	0.12	0.39	0.02
MZ33b	08.06.06-13.06.06	5	1739.10	3.53	0.47	0.34	0.24	0.26	1.15	0.16	0.03	0.02	0.04	BDL[a]
MZ34b	13.06.06-14.06.06	1	345.45	13.38	1.94	1.88	0.73	1.65	3.68	0.61	0.21	0.09	0.20	0.07
MZ35b	14.06.06-21.06.06	7	2393.37	1.83	0.42	0.22	0.12	0.14	0.58	0.06	0.02	BDL	BDL	BDL
MZ36b	21.06.06-22.06.06	1	345.82	9.40	6.15	2.71	0.88	0.85	2.56	0.24	0.17	0.06	0.19	0.04
MZ39b	22.06.06-27.06.06	5	1752.45	2.11	0.54	0.34	0.05	0.25	0.63	0.07	0.03	0.01	0.01	0.01
MZ40b	27.06.06-04.07.06	7	2446.81	2.42	0.16	0.24	0.10	0.38	0.52	0.08	0.02	0.01	0.02	BDL
MZ41b	04.07.06-11.07.06	7	1199.03	3.88	3.34	1.19	0.48	0.87	3.57	0.29	0.14	0.09	0.17	0.07
MZ42b	11.07.06-14.07.06	3	1044.57	4.67	0.65	0.55	0.23	0.52	0.78	0.14	0.04	0.03	0.05	0.02
MZ43b	14.07.06-17.07.06	3	1050.50	6.72	2.02	2.53	1.77	1.87	3.47	1.31	1.24	2.04	2.05	2.05
MZ44b	17.07.06-19.07.06	2	693.33	8.15	2.38	2.53	1.34	1.41	3.82	0.88	0.40	0.50	0.69	0.82
MZ45b	19.07.06-21.07.06	2	701.89	6.35	0.85	0.77	0.41	1.00	2.00	0.52	0.09	0.07	0.03	0.05
MZ46b	21.07.06-26.07.06	5	1700.23	3.54	1.23	0.80	0.26	0.42	0.75	0.22	0.08	BDL	0.09	0.13
MZ47b	26.07.06-02.08.06	7	2414.07	2.90	1.41	0.54	0.47	0.45	0.34	0.26	0.16	0.18	0.16	0.09
MZ51b	09.08.06-16.08.06	7	2431.28	1.36	0.57	0.20	0.09	0.17	0.62	0.06	0.02	0.02	0.02	0.02
MZ52b	16.08.06-23.08.06	7	2449.44	1.61	0.45	0.29	BDL	0.11	0.38	0.06	0.02	BDL	BDL	BDL
MZ53b	23.08.06-30.08.06	7	2487.58	1.32	1.27	0.86	0.12	0.37	1.64	0.10	0.05	0.03	0.05	BDL
MZ54b	30.08.06-06.09.06	7	1246.46	2.89	0.44	0.59	BDL	0.37	1.05	0.21	0.09	0.08	0.12	0.12
MZ55b	06.09.06-11.09.06	5	2433.36	1.62	0.30	0.17	0.12	0.16	0.69	0.08	0.02	0.01	0.01	0.01
MZ59b	11.09.06-18.09.06	7	2439.36	7.46	2.04	1.17	0.26	0.26	0.73	0.09	0.03	0.01	0.03	BDL
MZ60b	18.09.06-25.09.06	7	2390.63	3.22	0.63	0.33	0.32	0.24	1.21	0.19	0.04	0.03	0.04	BDL
MZ61b	25.09.06-02.10.06	7	2402.73	2.13	1.28	0.82	0.17	0.19	0.73	0.10	BDL	0.03	0.03	0.02
MZ62b	02.10.06-09.10.06	7	2441.29	1.19	0.83	0.41	0.15	0.29	0.18	0.12	0.10	0.11	0.10	0.20
MZ63b	09.10.06-16.10.06	7	2419.20	12.46	3.46	0.90	0.58	0.34	1.36	0.17	0.03	BDL	0.06	BDL
MZ66b	16.10.06-23.10.06	7	2318.40	2.92	0.65	0.64	0.22	0.26	1.28	0.16	0.03	BDL	0.02	BDL

MZ67b	23.10.06-30.10.06	7	2380.33	1.78	0.83	0.63	0.26	0.34	0.22	0.23	0.12	0.15	0.09	0.17
MZ68b	30.10.06-02.11.06	3	1045.46	1.42	1.14	0.81	BDL	0.38	1.65	0.27	BDL	0.07	0.14	0.16
MZ69b	02.11.06-09.11.06	7	2358.72	3.80	1.63	0.84	0.29	0.31	1.15	0.21	0.05	0.04	0.02	BDL
MZ70b	09.11.06-16.11.06	7	2384.81	1.67	0.93	0.51	0.17	0.42	1.42	0.27	0.14	0.19	0.20	0.16
MZ71b	16.11.06-23.11.06	7	2419.20	1.65	0.91	1.19	0.25	0.29	1.66	0.30	0.06	0.03	0.03	0.14
MZ74b	23.11.06-30.11.06	7	2084.60	4.07	2.12	0.79	0.58	0.56	3.63	0.39	0.09	0.08	0.10	0.11
MZ75b	30.11.06-07.12.06	7	2449.44	1.94	1.18	0.77	0.23	0.44	2.54	0.37	0.05	0.03	0.04	0.15
MZ76b	07.12.06-14.12.06	7	2414.05	2.08	1.25	0.83	BDL	0.34	1.15	0.20	0.07	0.12	0.10	0.17
MZ77b	14.12.06-21.12.06	7	2338.56	2.88	1.51	1.12	0.39	0.53	2.76	0.33	0.08	0.06	0.06	0.16
MZ80b	21.12.06-28.12.06	7	2392.69	3.86	2.72	0.65	0.31	0.53	3.06	0.28	0.09	0.07	0.10	0.02
MZ81b	28.12.06-04.01.07	7	2308.32	3.06	2.01	1.48	0.42	0.78	3.61	0.43	0.10	0.07	0.04	0.24
MZ82b	04.01.07-11.01.07	7	2381.93	0.69	0.55	0.53	BDL	0.27	0.12	0.13	0.09	0.11	0.09	0.21
MZ83b	11.01.07-18.01.07	7	2297.08	2.45	1.16	0.57	0.25	0.31	1.87	0.23	0.06	0.03	0.07	0.31
MZ84b	18.01.07-25.01.07	7	2392.87	1.40	0.83	0.50	0.16	0.22	1.50	0.17	0.07	0.05	0.05	0.15
MZ87b	25.01.07-01.02.07	7	2437.44	1.99	0.99	0.58	0.13	0.30	1.96	0.23	0.03	0.03	0.05	0.23
MZ88b	01.02.07-08.02.07	7	2369.89	3.60	1.49	0.82	0.38	0.32	2.06	0.30	BDL	0.04	0.06	0.30
MZ89b	08.02.07-15.02.07	7	2372.68	0.82	0.35	0.33	0.15	0.22	1.08	0.13	BDL	0.02	0.04	0.12
MZ90b	15.02.07-22.02.07	7	2297.08	7.65	2.79	1.18	0.45	0.47	0.65	0.31	0.07	0.06	0.06	0.12
MZ93b	22.02.07-01.03.07	7	2384.63	1.71	0.80	0.46	0.24	0.32	2.00	0.25	0.07	0.04	0.08	0.20
MZ94b	01.03.07-08.03.07	7	2462.01	1.64	0.84	0.45	0.26	0.28	1.81	0.18	0.06	0.03	0.05	0.14
MZ95b	08.03.07-15.03.07	7	2315.93	3.97	1.12	0.79	0.31	0.46	1.87	0.21	0.05	0.04	0.04	0.11
MZ96b	15.03.07-22.03.07	7	2443.02	0.98	0.64	0.40	0.20	0.21	1.01	0.14	0.02	0.03	0.03	0.15
MZ97b	22.03.07-29.03.07	7	2352.89	10.57	2.12	0.90	0.87	0.69	1.81	0.28	0.08	0.05	0.06	0.10
MZ100b	29.03.07-05.04.07	7	2379.54	7.21	1.49	0.80	0.48	0.37	1.37	0.20	0.04	0.02	0.05	0.07
MZ101b	05.04.07-12.04.07	7	2390.15	2.86	0.79	0.51	0.30	0.31	1.56	0.21	BDL	0.03	0.04	0.07
MZ102b	12.04.07-19.04.07	7	2442.44	4.40	0.74	0.57	0.30	0.39	1.66	0.23	BDL	0.03	0.06	BDL
MZ103b	19.04.07-26.04.07	7	2403.58	4.18	0.84	0.38	0.21	0.20	1.39	0.17	BDL	BDL	0.03	BDL
MZ104b	26.04.07-03.05.07	7	2414.20	5.62	0.95	0.45	0.33	0.24	2.07	0.21	0.04	0.02	0.03	BDL
MZ107b	03.05.07-10.05.07	7	2436.02	2.08	0.52	0.39	0.20	0.17	0.79	0.09	0.03	0.02	BDL	BDL
MZ108b	10.05.07-17.05.07	7	2462.02	1.21	0.71	0.45	0.20	0.16	0.83	0.09	0.03	BDL	0.03	0.02
MZ109b	17.05.07-24.05.07	7	2415.55	6.74	0.57	0.29	BDL	0.18	0.93	0.13	BDL	BDL	BDL	BDL
MZ112b	24.05.07-31.05.07	7	2392.65	2.83	0.76	0.50	0.28	0.20	1.24	0.14	0.03	BDL	0.04	BDL

1 b Pinene oxidation products and nitrophenols concentrations in fine particulate matter.

Sample ID	Sampling Period	Sampling time d	Sampled air volume m^{3}	3-MBTCA ng m^{-3}	Pinic acid ng m^{3}	Pinonic acid ng m^{3}	4-Nitrocatechol ng m^{3}	2-Nitrophenol ng m^{3}	4-Nitrophenol ng m^{3}
MZ31b	01.06.06-06.06.06	5	1780.18	2.68	0.48	0.82	5.02	1.24	0.93
MZ32b	06.06.06-08.06.06	2	703.43	8.98	7.20	3.98	16.81	5.22	2.76
MZ33b	08.06.06-13.06.06	5	1739.10	11.94	1.81	0.53	10.99	1.47	1.57
MZ34b	13.06.06-14.06.06	1	345.45	22.27	7.28	1.62	26.30	8.51	5.23
MZ35b	14.06.06-21.06.06	7	2393.37	4.97	0.83	0.21	3.49	1.00	0.68
MZ36b	21.06.06-22.06.06	1	345.82	6.07	2.62	3.65	2.14	2.26	2.35
MZ39b	22.06.06-27.06.06	5	1752.45	7.01	0.59	0.59	4.35	0.81	0.85
MZ40b	27.06.06-04.07.06	7	2446.81	10.17	1.02	0.72	4.64	BDL	0.44
MZ41b	04.07.06-11.07.06	7	1199.03	3.38	2.45	0.52	1.17	1.54	2.49
MZ42b	11.07.06-14.07.06	3	1044.57	14.05	1.07	1.03	8.82	1.34	1.74
MZ43b	14.07.06-17.07.06	3	1050.50	16.85	8.25	1.65	BDL	BDL	BDL
MZ44b	17.07.06-19.07.06	2	693.33	26.00	8.61	0.88	BDL	BDL	BDL
MZ45b	19.07.06-21.07.06	2	701.89	15.36	1.47	0.36	17.81	3.21	2.82
MZ46b	21.07.06-26.07.06	5	1700.23	15.16	5.11	BDL	1.03	BDL	BDL
MZ47b	26.07.06-02.08.06	7	2414.07	9.17	9.05	1.33	1.73	0.76	1.08
MZ51b	09.08.06-16.08.06	7	2431.28	2.31	0.61	BDL	5.36	0.57	0.95
MZ52b	16.08.06-23.08.06	7	2449.44	4.59	0.04	BDL	0.21	1.06	0.76
MZ53b	23.08.06-30.08.06	7	2487.58	0.55	1.33	0.83	0.17	0.77	0.71
MZ54b	30.08.06-06.09.06	7	1246.46	7.57	1.49	BDL	0.45	1.37	0.65
MZ55b	06.09.06-11.09.06	5	2433.36	5.17	1.21	BDL	11.33	1.03	2.28
MZ59b	11.09.06-18.09.06	7	2439.36	14.38	0.27	0.22	1.66	2.08	1.34
MZ60b	18.09.06-25.09.06	7	2390.63	12.00	3.01	1.25	2.04	1.78	1.97
MZ61b	25.09.06-02.10.06	7	2402.73	4.75	2.31	BDL	1.14	0.85	0.93
MZ62b	02.10.06-09.10.06	7	2441.29	1.32	1.79	BDL	1.30	1.29	1.64
MZ63b	09.10.06-16.10.06	7	2419.20	12.42	0.07	1.23	3.36	4.36	4.50
MZ66b	16.10.06-23.10.06	7	2318.40	5.31	0.00	0.38	1.84	2.83	2.59
MZ67b	23.10.06-30.10.06	7	2380.33	1.70	1.82	0.58	1.17	1.26	1.63
MZ68b	30.10.06-02.11.06	3	1045.46	0.66	1.40	BDL	2.08	1.30	2.54
MZ69b	02.11.06-09.11.06	7	2358.72	1.67	0.46	0.38	2.59	2.38	2.34

MZ70b	09.11.06-16.11.06	7	2384.81	0.98	1.13	0.16	1.98	BDL	0.04
MZ71b	16.11.06-23.11.06	7	2419.20	0.62	0.35	BDL	3.07	3.10	7.94
MZ74b	23.11.06-30.11.06	7	2084.60	1.12	2.60	0.89	2.71	1.34	2.31
MZ75b	30.11.06-07.12.06	7	2449.44	1.16	0.40	0.49	2.15	2.20	4.82
MZ76b	07.12.06-14.12.06	7	2414.05	0.24	0.56	0.76	3.17	0.75	0.47
MZ77b	14.12.06-21.12.06	7	2338.56	0.46	0.05	0.17	8.09	2.73	6.76
MZ80b	21.12.06-28.12.06	7	2392.69	0.31	0.20	-	-	0.72	2.15
MZ81b	28.12.06-04.01.07	7	2308.32	0.87	0.00	BDL	8.08	4.56	10.22
MZ82b	04.01.07-11.01.07	7	2381.93	0.21	0.69	0.58	0.61	0.43	1.12
MZ83b	11.01.07-18.01.07	7	2297.08	0.78	0.37	0.21	2.79	0.80	1.58
MZ84b	18.01.07-25.01.07	7	2392.87	0.34	0.23	0.27	2.53	0.79	3.43
MZ87b	25.01.07-01.02.07	7	2437.44	0.15	0.15	BDL	3.62	0.63	3.10
MZ88b	01.02.07-08.02.07	7	2369.89	0.25	0.36	0.26	9.47	1.19	5.73
MZ89b	08.02.07-15.02.07	7	2372.68	0.13	0.16	0.21	1.36	0.48	1.78
MZ90b	15.02.07-22.02.07	7	2297.08	1.30	0.43	0.16	4.15	2.08	6.33
MZ93b	22.02.07-01.03.07	7	2384.63	0.77	0.41	BDL	1.82	0.66	2.46
MZ94b	01.03.07-08.03.07	7	2462.01	1.01	0.37	BDL	2.85	0.86	2.61
MZ95b	08.03.07-15.03.07	7	2315.93	3.30	1.44	0.19	12.29	2.17	5.26
MZ96b	15.03.07-22.03.07	7	2443.02	0.60	0.17	BDL	0.88	0.39	3.02
MZ97b	22.03.07-29.03.07	7	2352.89	5.02	0.54	0.21	6.31	2.91	6.70
MZ100b	29.03.07-05.04.07	7	2379.54	5.39	0.60	0.29	4.76	2.30	4.57
MZ101b	05.04.07-12.04.07	7	2390.15	3.17	0.80	BDL	5.47	1.44	2.62
MZ102b	12.04.07-19.04.07	7	2442.44	10.57	0.48	BDL	2.29	1.35	3.09
MZ103b	19.04.07-26.04.07	7	2403.58	9.75	0.31	BDL	1.95	1.64	2.03
MZ104b	26.04.07-03.05.07	7	2414.20	14.34	0.49	BDL	4.27	2.13	2.12
MZ107b	03.05.07-10.05.07	7	2436.02	5.12	0.02	BDL	BDL	0.64	0.55
MZ108b	10.05.07-17.05.07	7	2462.02	1.89	0.14	BDL	BDL	0.56	0.85
MZ109b	17.05.07-24.05.07	7	2415.55	16.87	0.41	0.18	2.09	1.39	1.12
MZ112b	24.05.07-31.05.07	7	2392.65	6.48	0.08	BDL	0.22	0.59	1.01

[a] below detection limit (limit of quantification listed in table 2-1).

A3 Temperature dependences of 3-MBTCA formation processes (Chapter 2)

To analyze the observed temperature dependence (275 – 300 K) of the 3-MBTCA concentration, we have compiled a simple conceptual model considering the temperature dependences during the following steps and processes in the production and loss of 3-MBTCA.

A3.1 Temperature dependence of emission and oxidation of pinene

The mechanism of emission from plants is usually explained as emission from terpene pools within the plant needles or leaves (from resins stored in ducts, glands or trichomes) and the emission rate is typically reported to be only temperature dependent. The quantitative dependence has been described by several authors (Juuti et al.,1990, Lamb et al.,1985, Tingey et al.,1980). For the current simulation of pinene emission, we used the empiric temperature dependent emission model for Scots Pine (pinus silvestris) to estimate the temperature dependence(Komenda et al.,2003):

$$C_{Emission} = \Phi_{Emission} \text{ *EF}$$

$$C_{Emission}^{P,S} = \Phi_{VOC}^{P,S} \text{ *EF}$$

$$\Phi_{Emission} = \Phi_{VOC}^{P,S} \text{ *exp}\left[\frac{c_{TP}}{R} * \left(\frac{T - T_S}{T * T_S}\right)\right]$$

$$\ln\left(\frac{C_{Emission}}{C_{Emisssion}^{P,S}}\right) = -\frac{C_{TP}}{R} * \left(\frac{1}{T} - \frac{1}{T_s}\right)$$

$C_{Emission}$ is the concentration of emitted pinene; $\Phi_{Emission}$ is pinene emission rate (ng g(dry weight)$^{-1}$ h^{-1}), and EF is the emission factor, which is to scale the linear fit of pinene emission and assumed as 1.5 g h m^{-3}. $\Phi_{VOC}^{P,S}$ is the pinonic acid emission rate from pool (ng g(dry weight)$^{-1}$ h^{-1}) at standard temperature T_S, c_{TP} is the empirical parameter describing the temperature dependence (J mol^{-1}), and T_S is the standard temperature. At 298 K, $\Phi_{VOC}^{P,S}$ = (23±9.3) ng g(dw)$^{-1}$ h^{-1}, $\frac{c_{TP}}{R}$ = (9.1±0.4)*10^{3} K (Komenda et al., 2003) ; R is the gas constant (8.31J K^{-1} mol^{-1}). T is temperature (K) and T_S is standard temperature (300 K).

We assume as a first approximation this first step to be independent of environmental conditions (e.g. oxidant concentration) and to yield a constant amount of pinonic acid (PA) (linearly scaling with the precursor emission), which essential means that the lifetime of pinene is shorter than the average transport time of the emitted biogenic VOC to the sampling site. This assumption was supported by the fact that pinic acid has a similar temperature dependence value to that of pinene emission (see temperature dependence of pinic acid). As a result:

$C_{\mathrm{Pinene(emission)}} = C_{\mathrm{PA(produced)}}$.

A3.2 Temperature dependence of gas-particle partitioning of pinonic acid

The partitioning of a semi-volatile compound between the gas and particle phase is generally described by the ratio of the particle phase concentration and the concentration in the gas phase (FGP), normalized by the total concentration of organic material in the particle phase (FPP). The resulting partitioning coefficient K_i (m³/μg) (Odum et al., 1996) or its inverse C_i^* (μg/m³) (Donahue et al., 2006) of a compound *i* strongly depends on the vapor pressure of ***i***. Pinonic acid is a semi-volatile species with a C* value between 900-4000 μg/m³ (Jimenez et al., 2009). Applying these values together with a typical ambient organic aerosol mass loading (i.e. 5 μg/m³) (Hock et al., 2008) to the temperature range of interest shows that the relative amount of pinonic acid in the gas phase is always more than 99 %, which means that even at lower ambient temperatures pinonic acid is dominantly present in the gas phase.

$$\mathrm{FGP_{PA}} = 1 - \mathrm{FPP_{PA}} = \frac{1}{1+\frac{C_{PA}^*}{C_{OA}}} = \frac{C_{PA}^*}{C_{PA}^* + C_{OA}}$$

$$\frac{FGP_{PA}}{FGP_{PA}^S} = \frac{C_{PA}^{*,S} + C_{OA}}{C_{PA}^{*,S} + C_{OA} * \frac{C_{PA}^{*,S}}{C_{PA}^*}}$$

$$C_{PA}^* = \frac{1}{K_{PA}}$$

$$\frac{C_{PA}^{*,S}}{C_{PA}^*} = \frac{K_{PA}}{K_{PA}^S}$$

Since the vapor pressure is a function of temperature, following the Clausius Clapeyron equation, also K_i or C_i^* vary with temperature (Chung and Seinfeld,2002, Takekawa et al.,2003).

$$\frac{K_{PA}(T_2)}{K_{PA}(T_1)} = \frac{T_2}{T_1}\exp\left[\frac{\Delta H_{PA}^0}{R}\left(\frac{1}{T_2} - \frac{1}{T_1}\right)\right]$$

$$\frac{K_{PA}}{K_{PA}^{s}} = \frac{T}{T_S}\exp\left[\frac{\Delta H_{PA}^{0}}{R}\left(\frac{1}{T}-\frac{1}{T_S}\right)\right]$$

$$\ln\left(\frac{FGP_{PA}}{FGP_{PA}^{S}}\right) = \ln\left\{\frac{C_{PA}^{*,S}+C_{OA}}{C_{PA}^{*,S}+C_{OA} * \frac{T}{T_S}\exp\left[\frac{\Delta H_{PA}^{0}}{R}\left(\frac{1}{T}-\frac{1}{T_S}\right)\right]}\right\}$$

C_{OA} is organic aerosol concentration (5 µg m^{-3}) (Hock et al.,2008). $C_{PA}^{*,S}$ is the effective saturation concentration at standard temperature (T_S =300K) (4000 µg m^{-3}) (Jimenez et al., 2009); ΔH_{PA}^{0} is the enthalpy of pinonic acid vaporisation (5.90*10^{4}J mol^{-1}) (Saathoff et al., 2009). T is temperature (K). The calculated natural logarithms of ratios FGP_{PA} over FGP_{PA}^{S} were plotted against inverse temperature (Fig. A6), and good linear correlation was found (R^2 = 0.95). E_a/R is opposite number of linear fit slope (26 K), and $\Delta E_a/R$ is the deviation of linear fit slope (1.4 K).

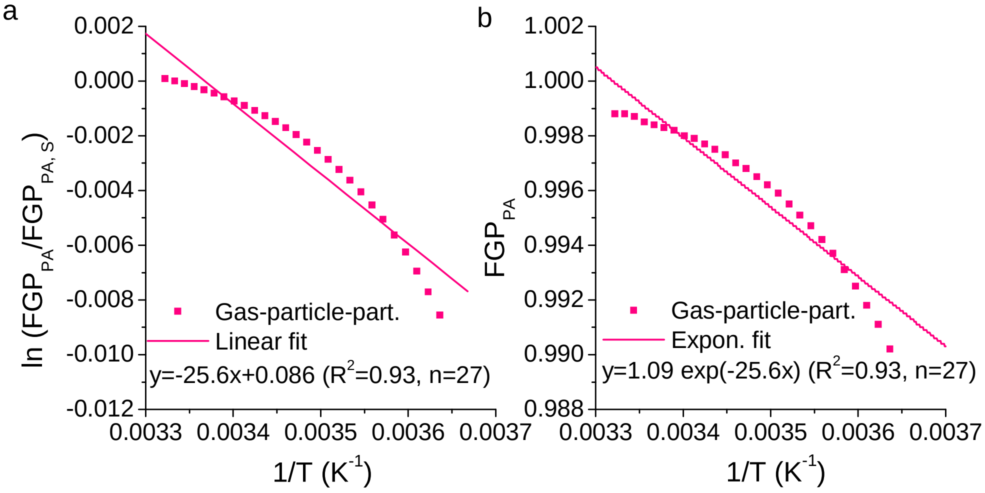

Figure A6 Natural logarithm of ratio FGP_{PA} over FGP_{PA}^{S} plotted against inverse temperature. Line is linear fit.

With an opposite sign the same is true for the temperature dependent partitioning of 3-MBTCA itself, since the very low vapor pressure of this compound always (i.e. independent from temperature within the relevant temperature range) drives 3-MBTCA into the condensed phase. In summary, the gas-particle-partitioning has no contribution to the observed temperature dependence of the observed 3-MBTCA concentration (also indicated by the almost horizontal line in Fig. 2-6).

A3.3 Temperature dependence of OH oxidation of pinonic acid

Pinonic acid is known to be an essential precursor of 3-MBTCA (Szmigielski et al.,2007). During this process, we considered the temperature dependence of reaction rate and OH concentration (C_{OH}).

$$\ln(\frac{k_{OH(PA)}}{k^{S}_{OH(PA)}}) = \ln(\frac{A*\exp(-\frac{E_a}{RT})}{A*\exp(-\frac{E_a}{RT_S})}) = -\frac{E_a}{R}*(\frac{1}{T}-\frac{1}{T_S})$$

E_a is the enthalpy of reaction between pinonic acid and OH, which is not available. Since the reaction between pinonic acid and OH takes place at the aldehyde group, we took the empirical temperature dependence (E_a/R) of propionaldehyde (410±250 K) (Atkinson et al. 2006) to estimate E_a of OH oxidation of pinonic acid. E_a is (-3.4±2.1 kJ mol^{-1}), and thus cause insignificant temperature dependence of overall OH oxidation of pinonic acid.

The natural logarithms of ratios between OH concentration data and OH concentration at highest temperature (300 K) were plotted against inverse temperature (Fig. S3), and linear correlation was found (R^2 = 0.79). The OH data used were taken from simulations with the ECHAM/MESSy Atmospheric Chemistry (EMAC) model (Jöckel et al., 2006). E_a/R is opposite number of linear fit slope (13000 K), and $\Delta E_a/R$ is the deviation of linear fit slope (910 K).

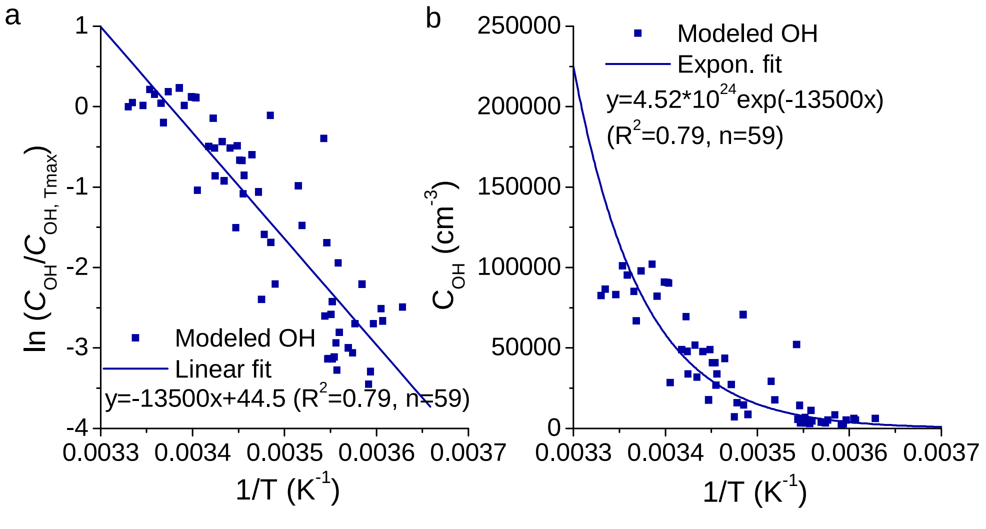

Figure A7 Natural logarithm of ratio OH concentration over OH concentration at 300 K plotted against inverse temperature. Line is linear fit.

A3.4 References

Chung, S. H. and J. H. Seinfeld (2002). "Global distribution and climate forcing of carbonaceous aerosols." Journal of Geophysical Research-Atmospheres **107**(D19): 4407, Doi 10.1029/2001jd001397.

Donahue, N. M., A. L. Robinson, C. O. Stanier and S. N. Pandis (2006). "Coupled partitioning, dilution, and chemical aging of semivolatile organics." Environmental Science & Technology **40**(8): 02635-02643.

Hock, N., J. Schneider, S. Borrmann, A. Rompp, G. Moortgat, T. Franze, C. Schauer, U. Poschl, C. Plass-Dulmer and H. Berresheim (2008). "Rural continental aerosol properties and processes observed during the Hohenpeissenberg Aerosol Characterization Experiment (HAZE2002)." Atmospheric Chemistry and Physics **8**(3): 603-623.

Jimenez, J. L., M. R. Canagaratna, N. M. Donahue, A. S. H. Prevot, Q. Zhang, J. H. Kroll, P. F. DeCarlo, J. D. Allan, H. Coe, N. L. Ng, A. C. Aiken, K. S. Docherty, I. M. Ulbrich, A. P. Grieshop, A. L. Robinson, J. Duplissy, J. D. Smith, K. R. Wilson, V. A. Lanz, C. Hueglin, Y. L. Sun, J. Tian, A. Laaksonen, T. Raatikainen, J. Rautiainen, P. Vaattovaara, M. Ehn, M. Kulmala, J. M. Tomlinson, D. R. Collins, M. J. Cubison, E. J. Dunlea, J. A. Huffman, T. B. Onasch, M. R. Alfarra, P. I. Williams, K. Bower, Y. Kondo, J. Schneider, F. Drewnick, S. Borrmann, S. Weimer, K. Demerjian, D. Salcedo, L. Cottrell, R. Griffin, A. Takami, T. Miyoshi, S. Hatakeyama, A. Shimono, J. Y. Sun, Y. M. Zhang, K. Dzepina, J. R. Kimmel, D. Sueper, J. T. Jayne, S. C. Herndon, A. M. Trimborn, L. R. Williams, E. C. Wood, A. M. Middlebrook, C. E. Kolb, U. Baltensperger and D. R. Worsnop (2009). "Evolution of Organic Aerosols in the Atmosphere." Science **326**(5959): 1525-1529.

Juuti, S., J. Arey and R. Atkinson (1990). "Monoterpene Emission Rate Measurements from a Monterey Pine." Journal of Geophysical Research-Atmospheres **95**(D6): 7515-7519.

Komenda, M., K. Kobel, R. Koppmann and J. Wildt (2003). "Comparability of biogenic VOC emission rate measurements under laboratory and ambient conditions at the example of monoterpene emissions from Scots pine (Pinus sylvestris)." Journal of Atmospheric Chemistry **45**(1): 1-23.

Lamb, B., H. Westberg, G. Allwine and T. Quarles (1985). "Biogenic Hydrocarbon Emissions from Deciduous and Coniferous Trees in the United-States." Journal of Geophysical Research-Atmospheres **90**(ND1): 2380-2390.

Odum, J. R., T. Hoffmann, F. Bowman, D. Collins, R. C. Flagan and J. H. Seinfeld (1996). "Gas/particle partitioning and secondary organic aerosol yields." Environmental Science & Technology **30**(8): 2580-2585.

Saathoff, H., K. H. Naumann, O. Mohler, A. M. Jonsson, M. Hallquist, A. Kiendler-Scharr, T. F. Mentel, R. Tillmann and U. Schurath (2009). "Temperature dependence of yields of secondary organic aerosols from the ozonolysis of alpha-pinene and limonene." Atmospheric Chemistry and Physics **9**(5): 1551-1577.

Szmigielski, R., J. D. Surratt, Y. Gomez-Gonzalez, P. Van der Veken, I. Kourtchev, R. Vermeylen, F. Blockhuys, M. Jaoui, T. E. Kleindienst, M. Lewandowski, J. H. Offenberg, E. O. Edney, J. H. Seinfeld, W. Maenhaut and M. Claeys (2007). "3-methyl-1,2,3-butanetricarboxylic acid: An atmospheric tracer for terpene secondary organic aerosol." Geophysical Research Letters **34**(24): L24811, doi:10.1029/2007GL031338.

Takekawa, H., H. Minoura and S. Yamazaki (2003). "Temperature dependence of secondary organic aerosol formation by photo-oxidation of hydrocarbons." Atmospheric Environment **37**(24): 3413-3424.

Tingey, D. T., M. Manning, L. C. Grothaus and W. F. Burns (1980). "Influence of Light and Temperature on Monoterpene Emission Rates from Slash Pine." Plant Physiology **65**(5): 797-801.

A4 Chromatograms of native and nitrated proteins (Chapter 3)

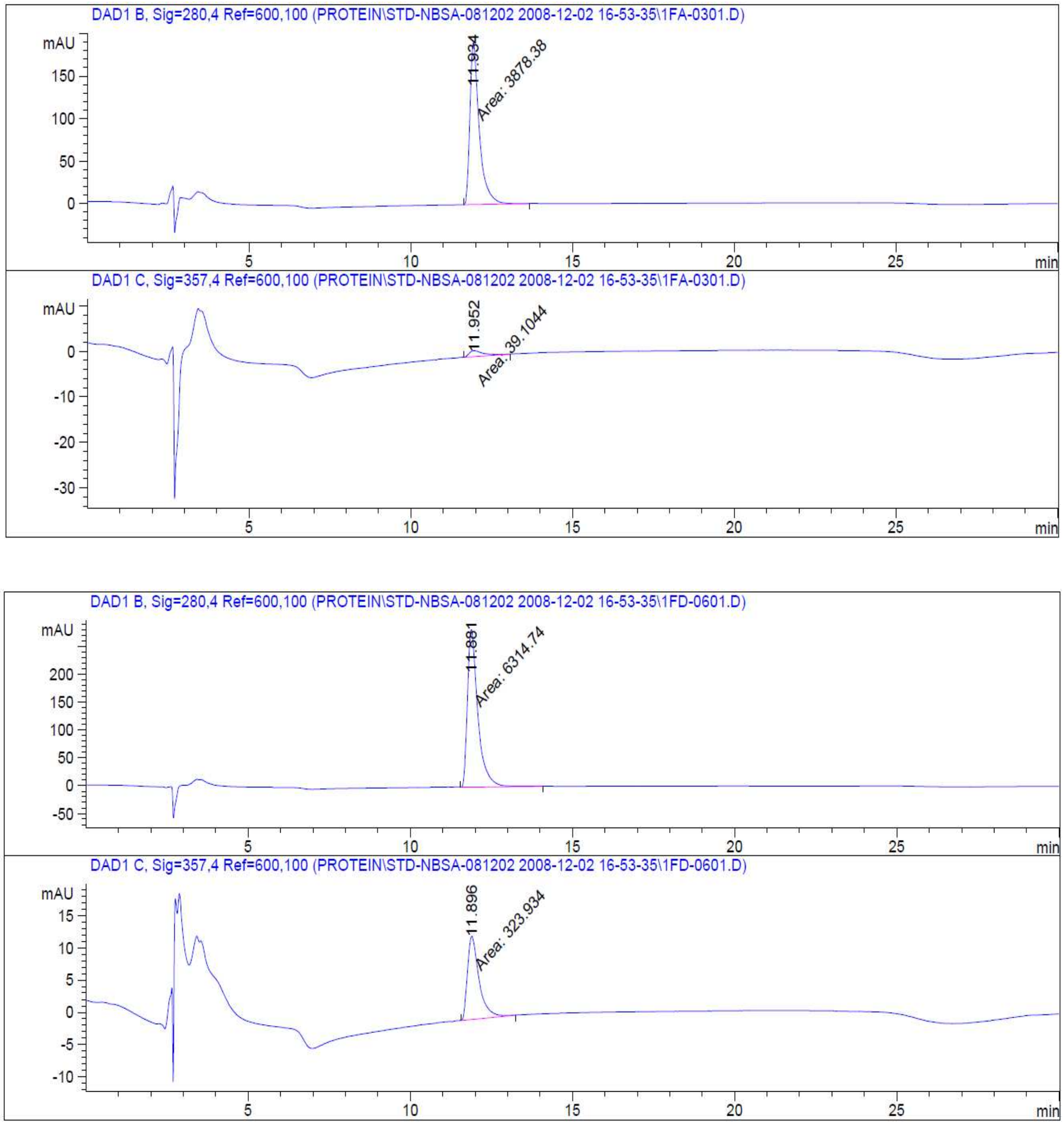

Figure A8 Chromatogram of native (upper) and nitrated BSA (lower) at 280 nm and 357 nm.

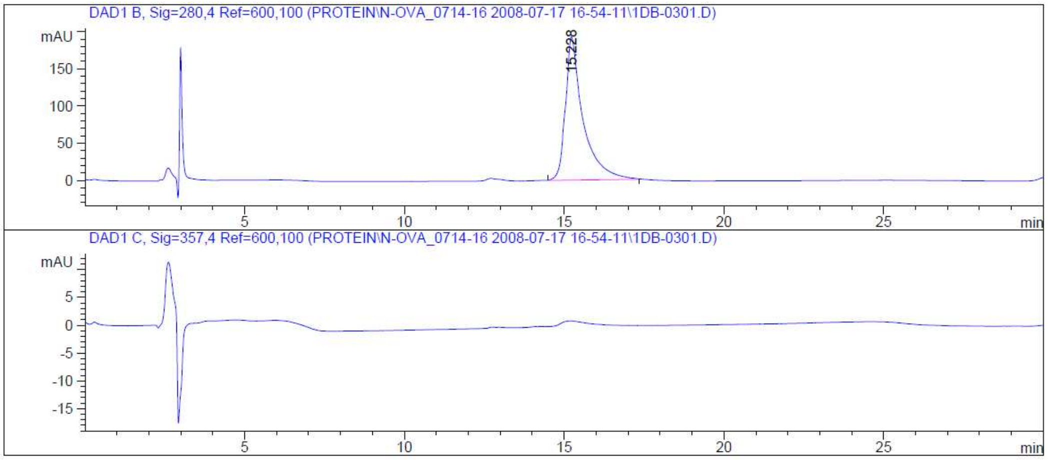

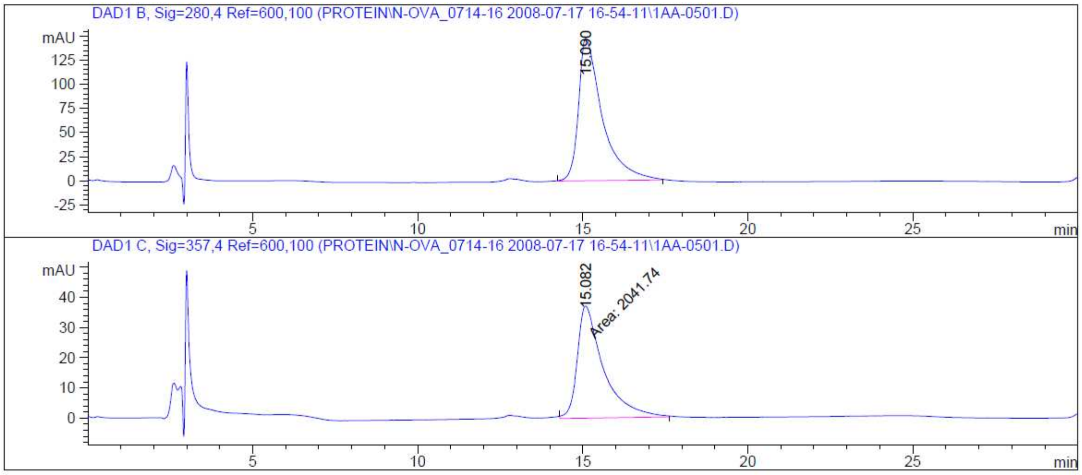

Figure A9 Chromatogram of native (upper) and nitrated OVA (lower) at 280 nm and 357 nm.

A5 Chromatograms of tryptic digested peptides (Chapter 4)

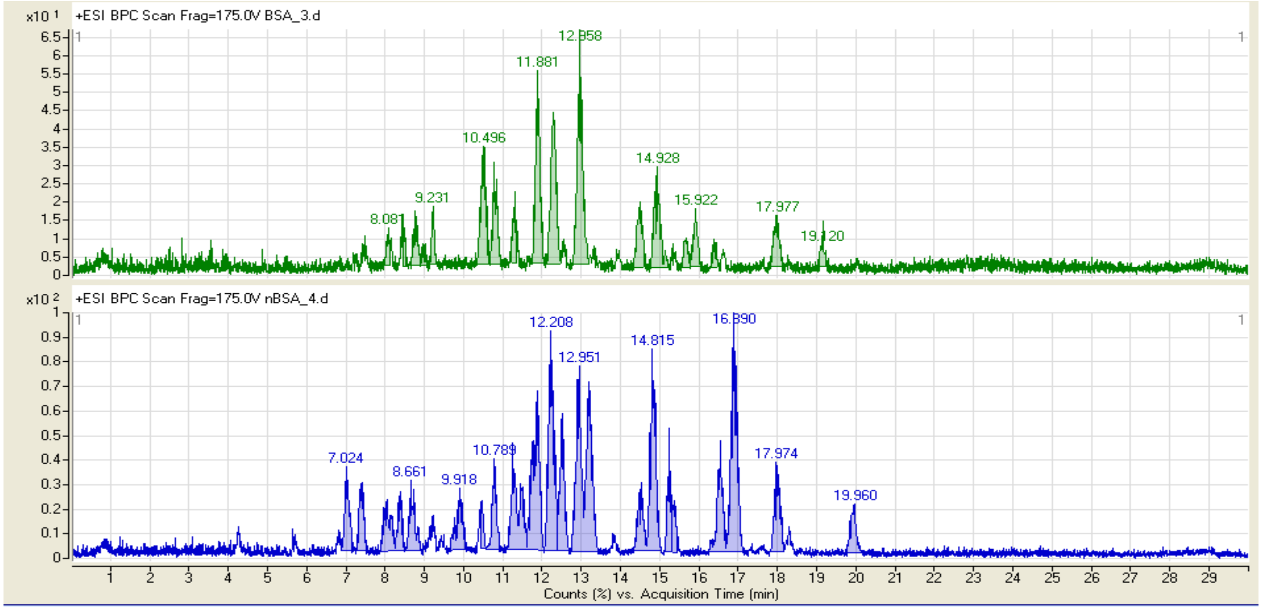

Figure A10 HPLC-chip-MS analysis of tryptic peptides from native BSA (upper) and nitrated BSA (lower).

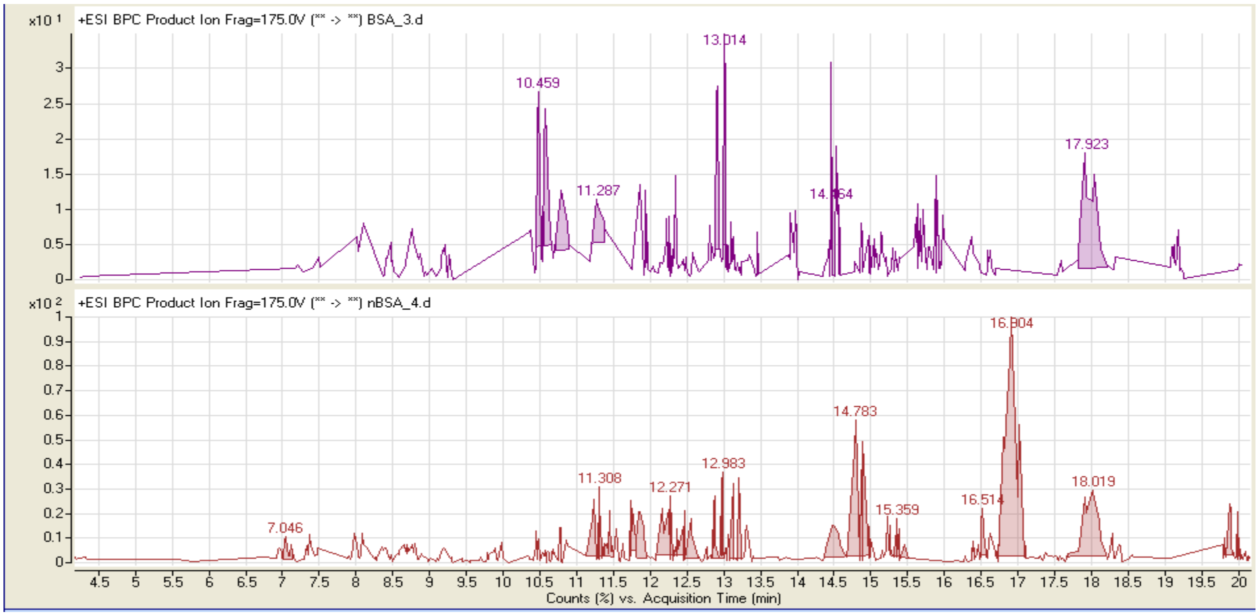

Figure A11 HPLC-chip-MS/MS analysis of tryptic peptides from native BSA (upper) and nitrated BSA (lower).

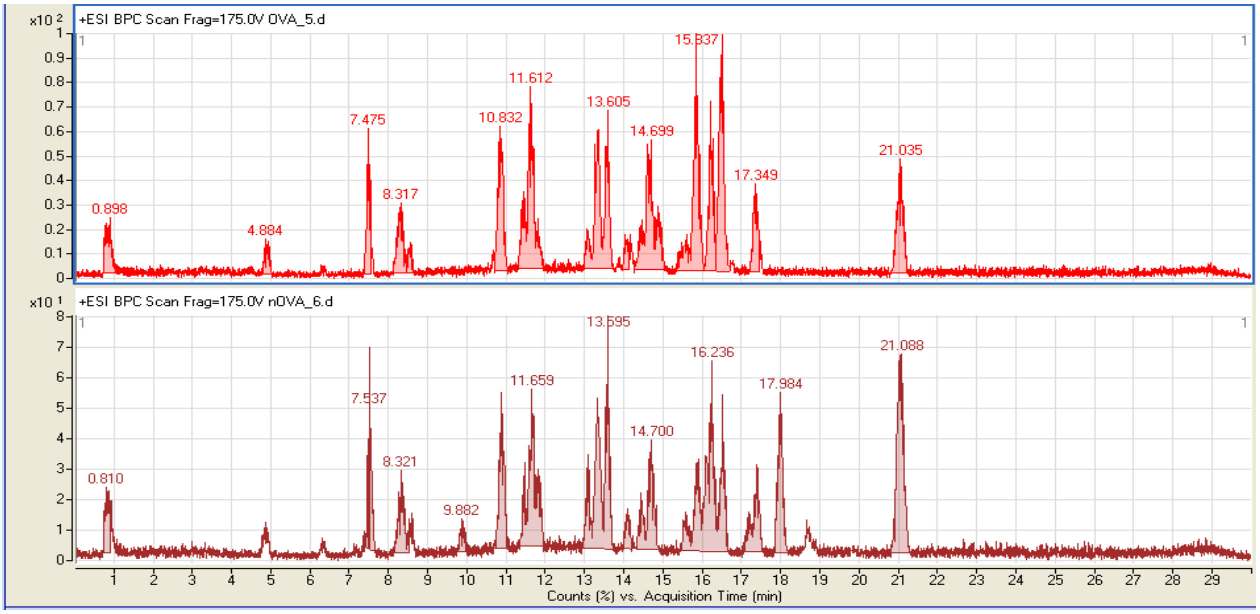

Figure A12 HPLC-chip-MS analysis of tryptic peptides from native OVA (upper) and nitrated OVA (lower).

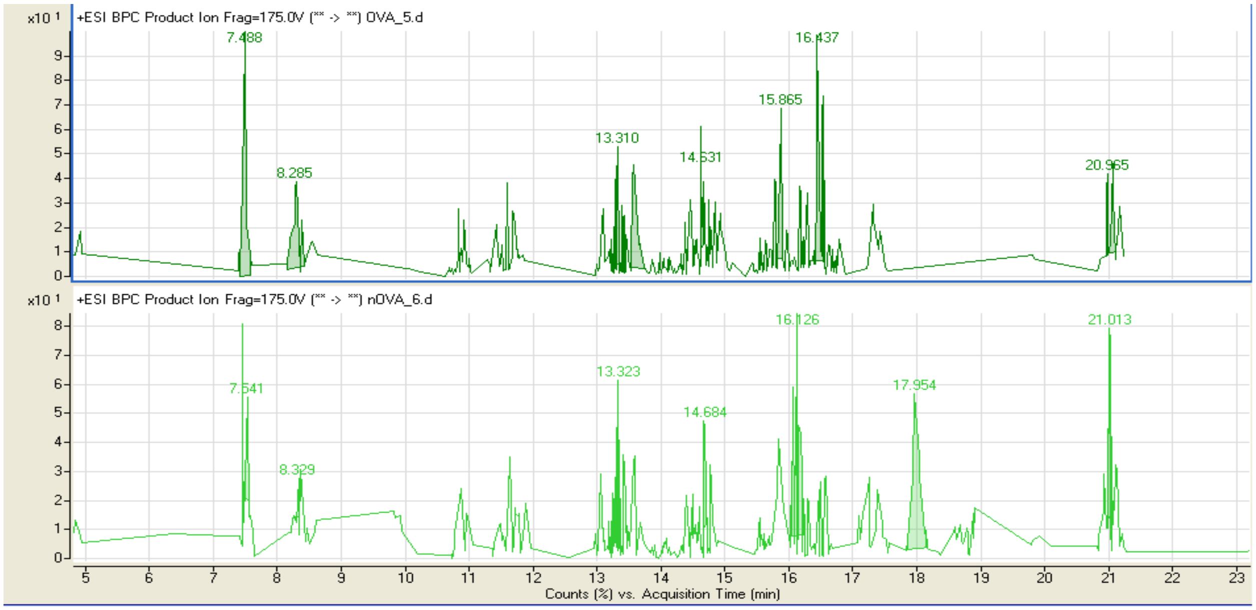

Figure A13 HPLC-chip-MS/MS analysis of tryptic peptides from native OVA (upper) and nitrated OVA (lower).

A6 Mass spectra of peptides containing native and nitrated tyrosine (Chapter 4)

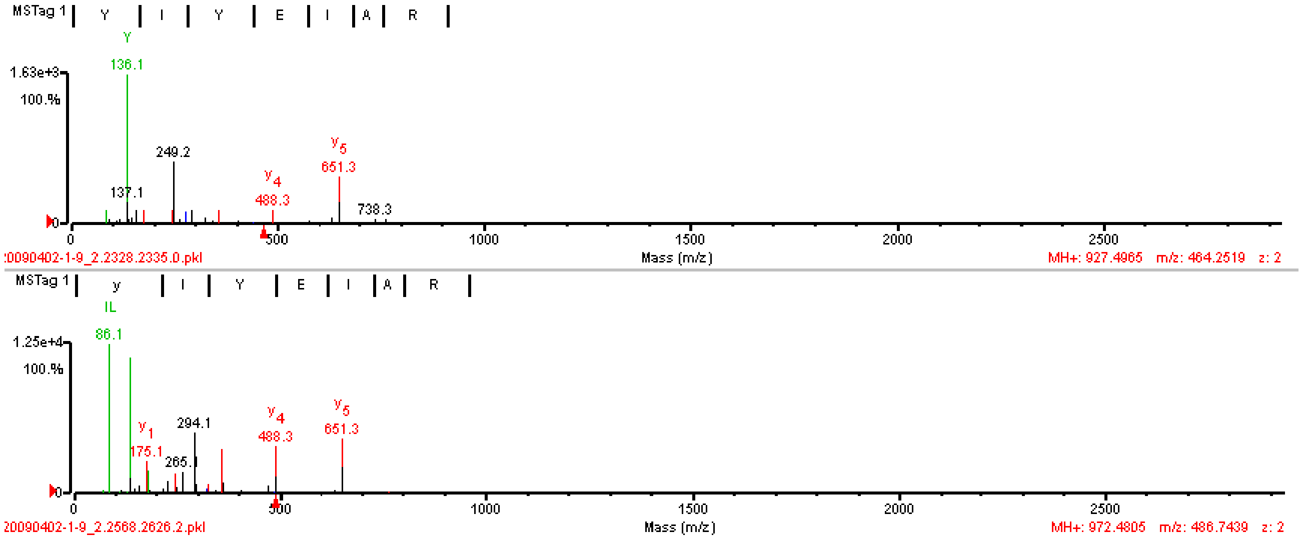

Figure A14 Mass spectra of peptides containing native (upper) and nitrated tyrosine (lower) 161 in nitrated BSA.

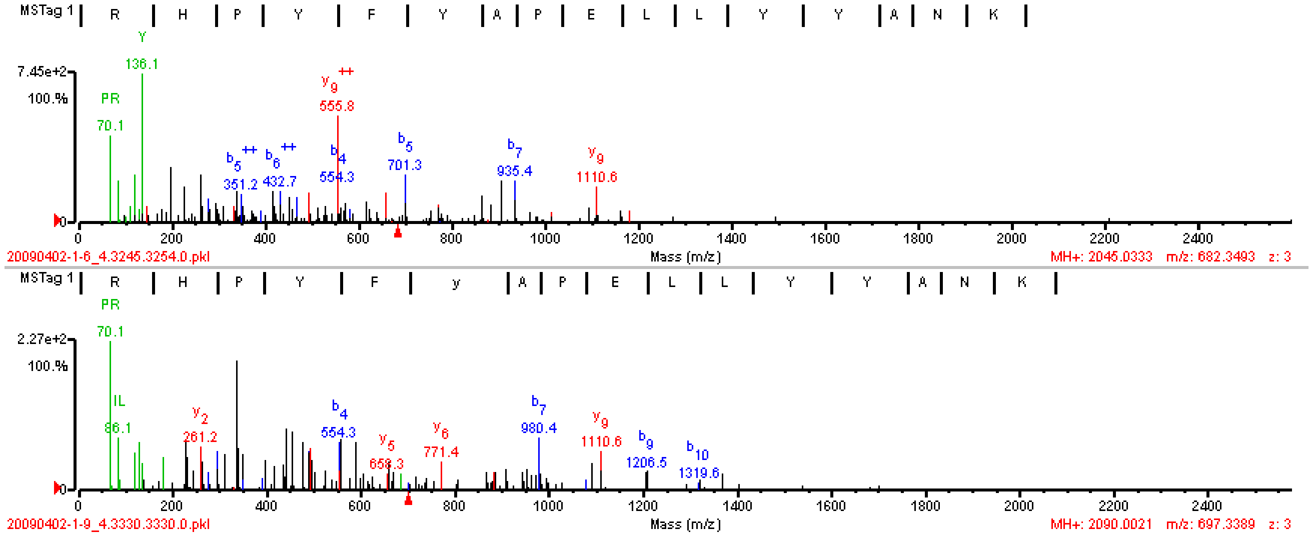

Figure A15 Mass spectra of peptides containing native (upper) and nitrated tyrosine (lower) 173 in nitrated BSA.

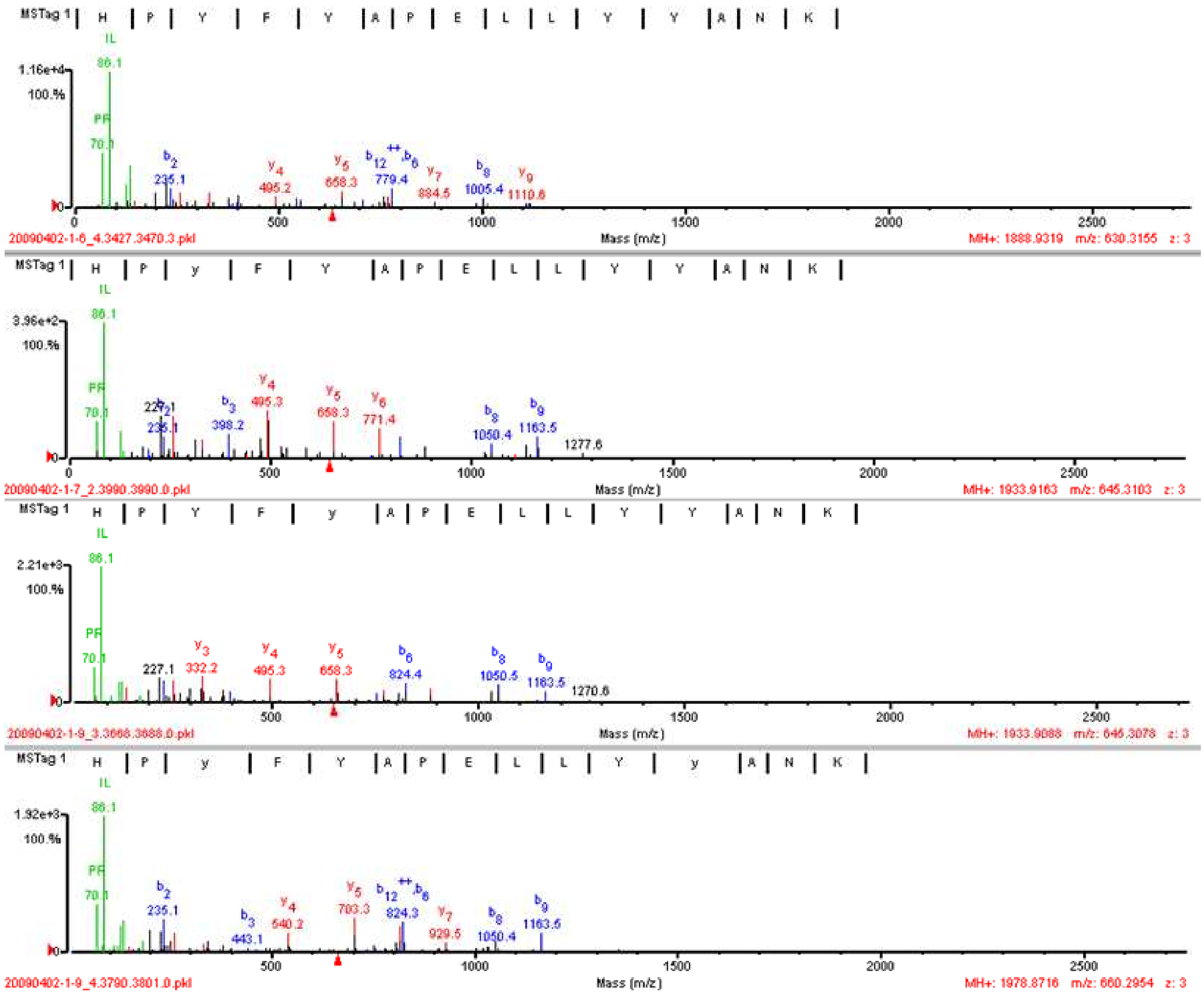

Figure A16 Mass spectra of peptides containing native (upper) and nitrated tyrosine (lower) 171, 173 and 180 in nitrated BSA.

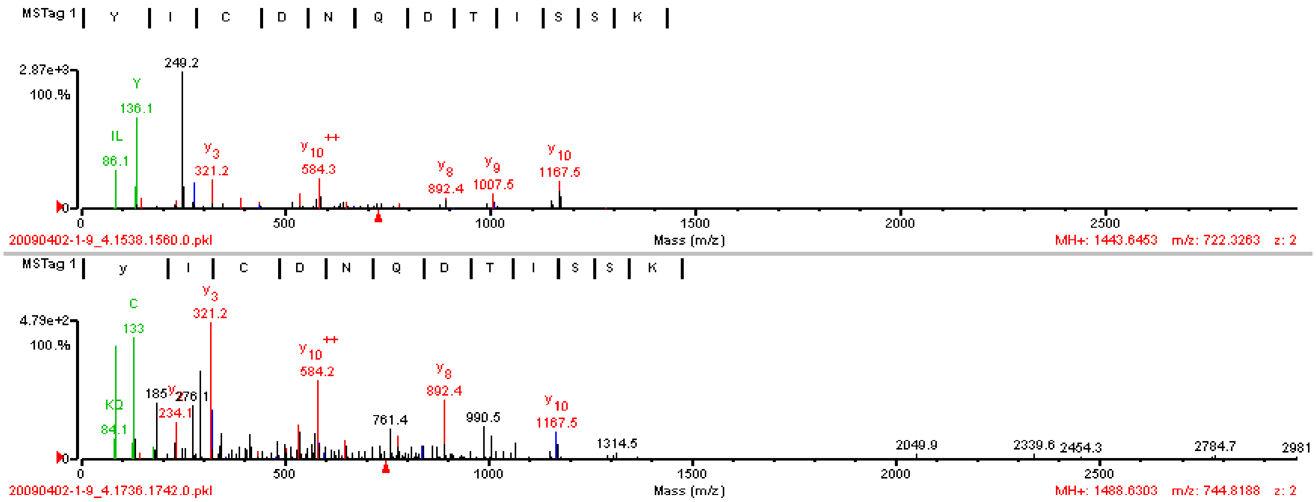

Figure A17 Mass spectra of peptides containing native (upper) and nitrated tyrosine (lower) 286 in nitrated BSA.

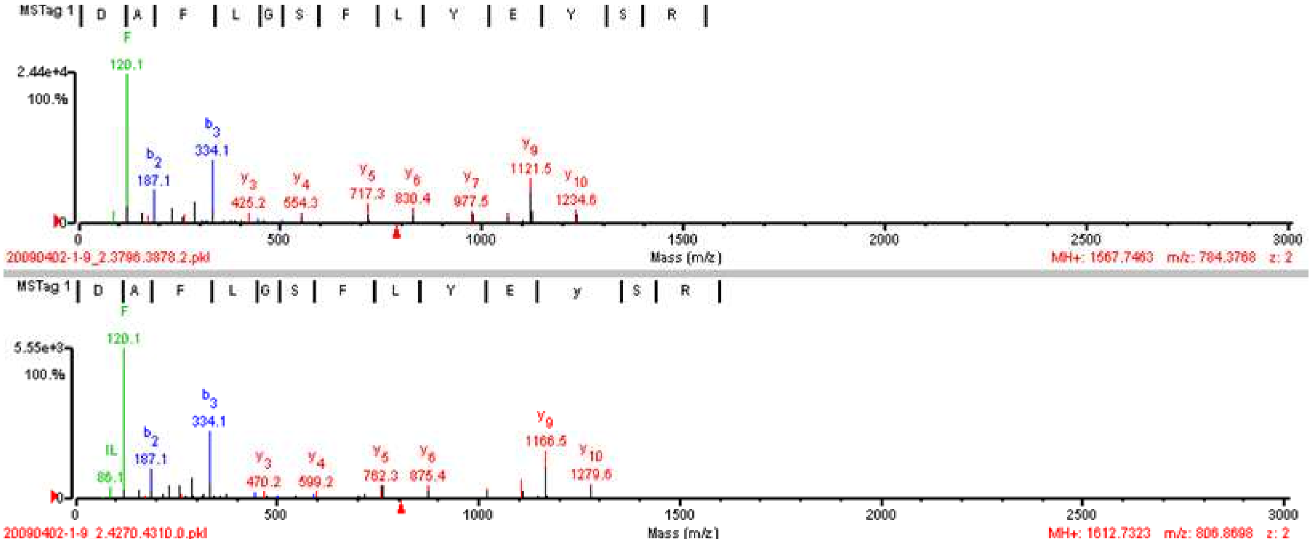

Figure A18 Mass spectra of peptides containing native (upper) and nitrated tyrosine (lower) 357 in nitrated BSA.

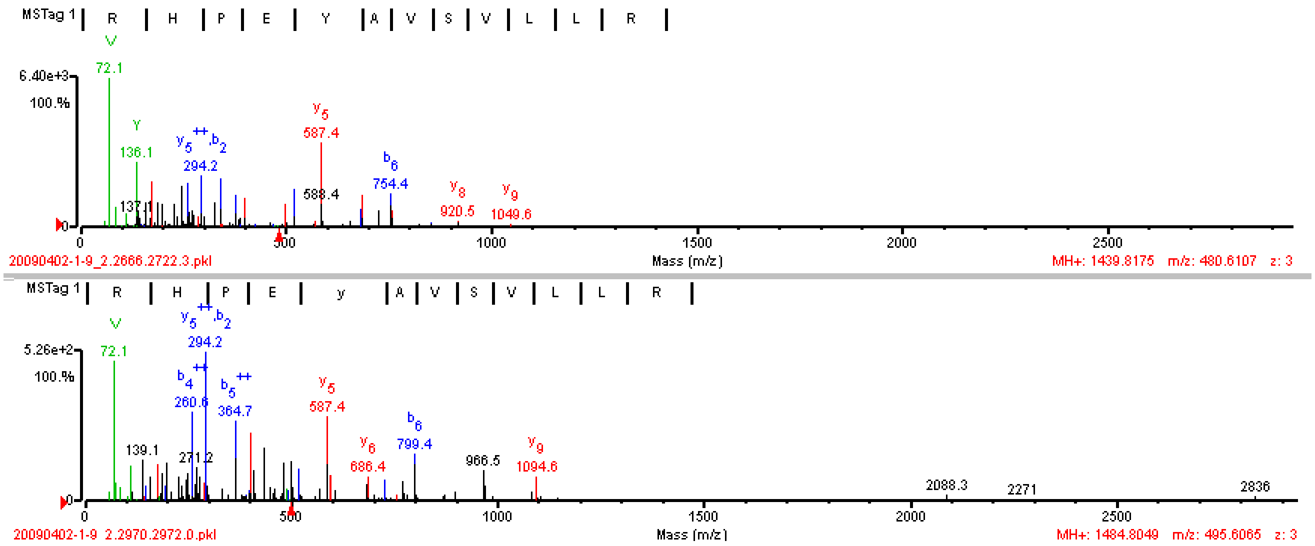

Figure A19 Mass spectra of peptides containing native (upper) and nitrated tyrosine (lower) 364 in nitrated BSA.

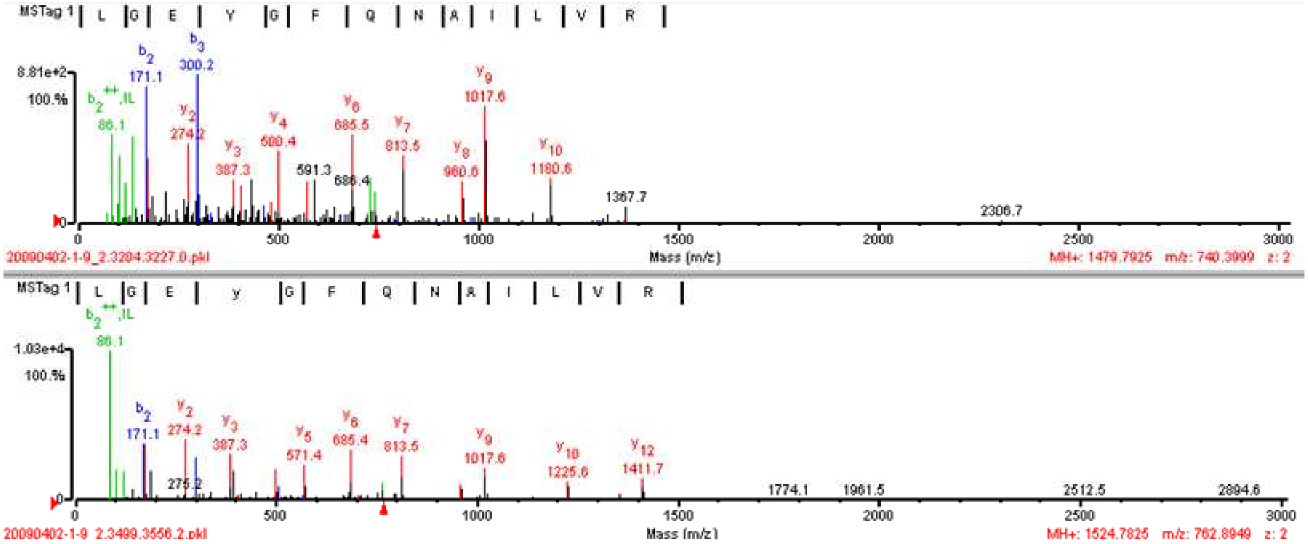

Figure A20 Mass spectra of peptides containing native (upper) and nitrated tyrosine (lower) 424 in nitrated BSA.

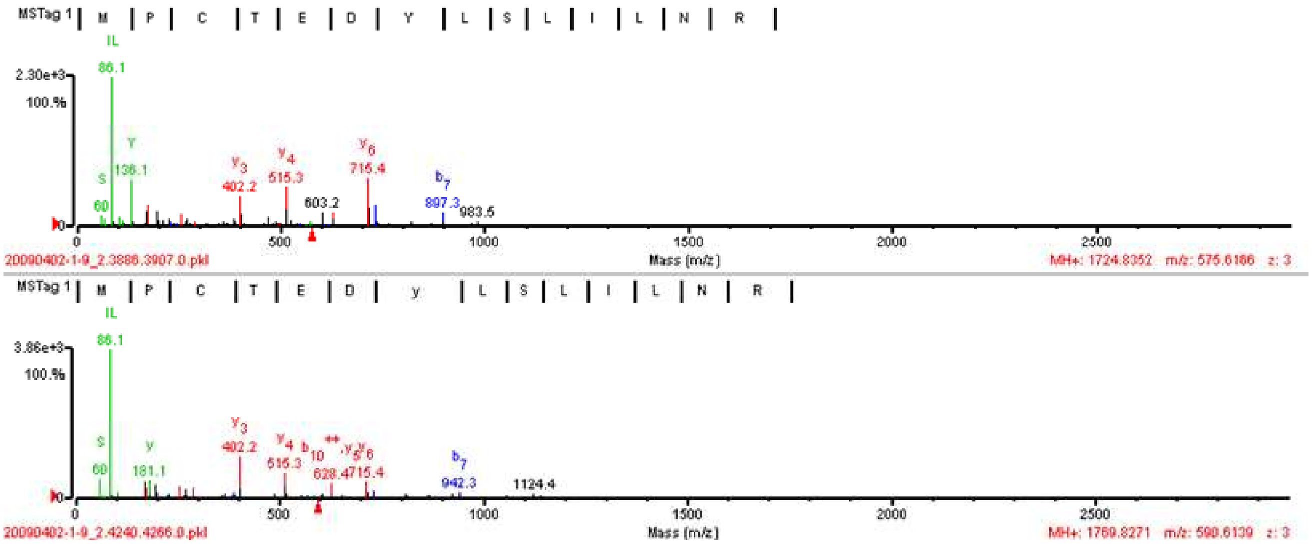

Figure A21 Mass spectra of peptides containing native (upper) and nitrated tyrosine (lower) 475 in nitrated BSA.

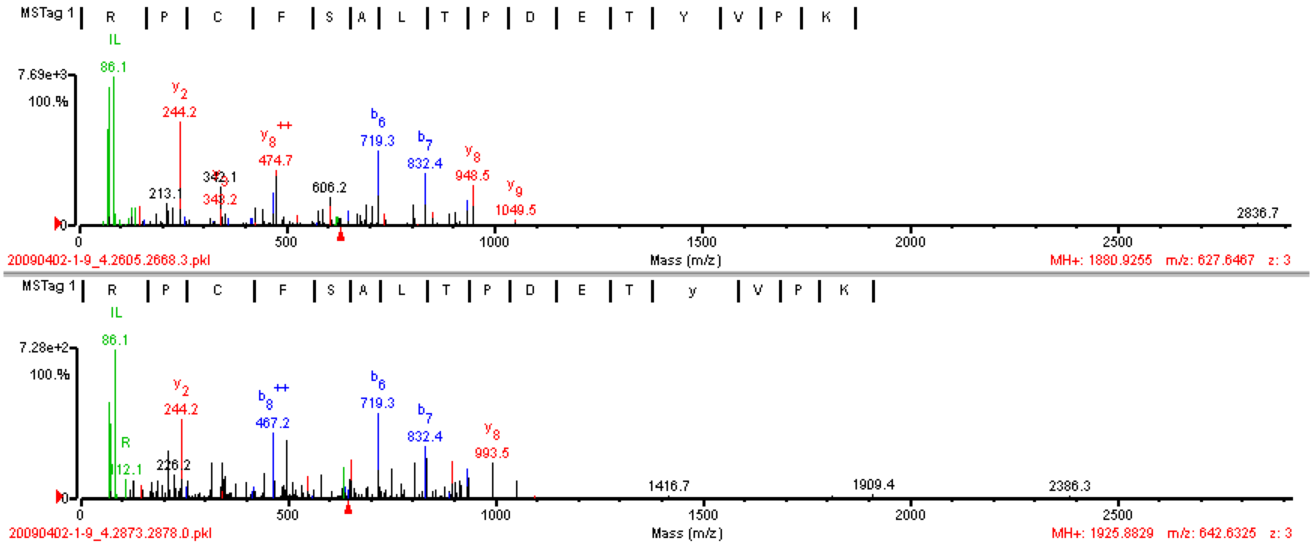

Figure A22 Mass spectra of peptides containing native (upper) and nitrated tyrosine (lower) 520 in nitrated BSA.

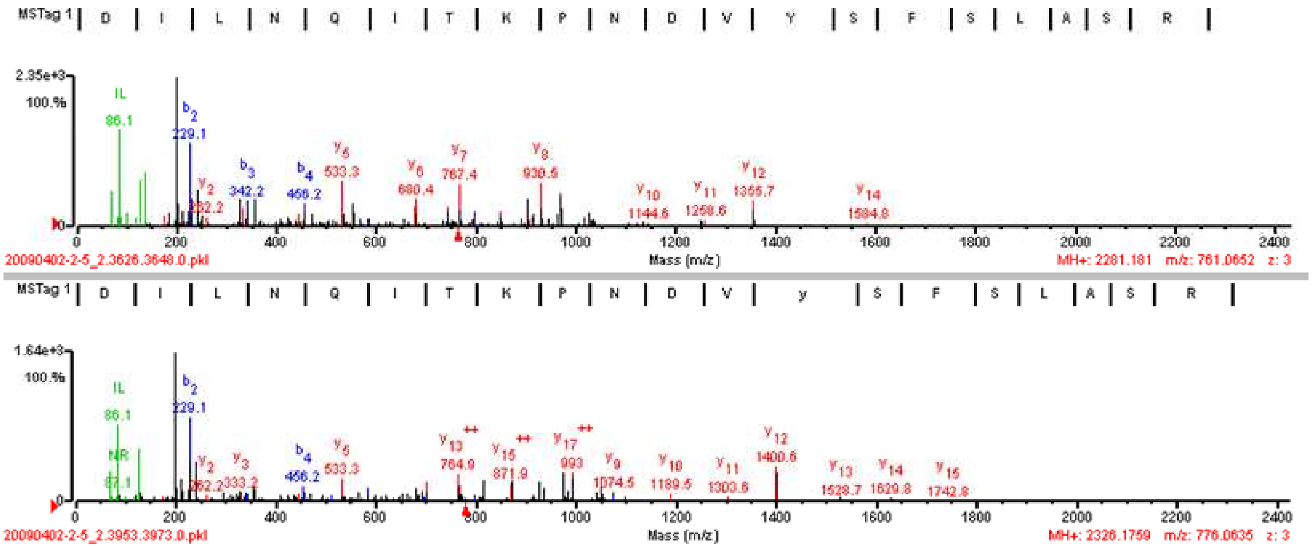

Figure A23 Mass spectra of peptides containing native (upper) and nitrated tyrosine (lower) 98 in nitrated OVA.

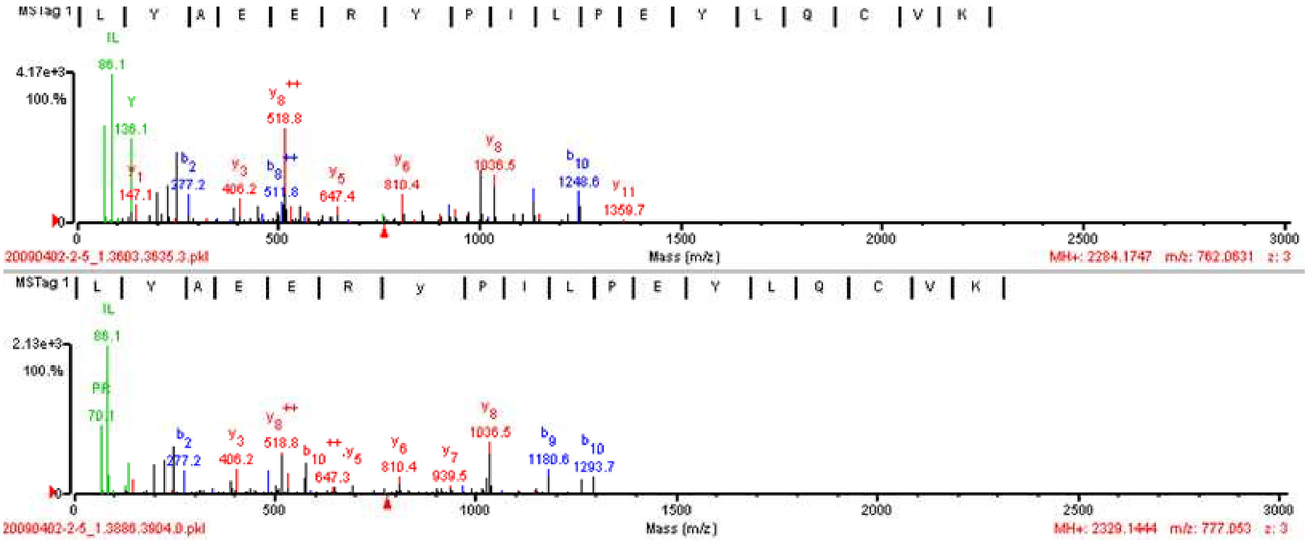

Figure A24 Mass spectra of peptides containing native (upper) and nitrated tyrosine (lower) 112 in nitrated OVA.

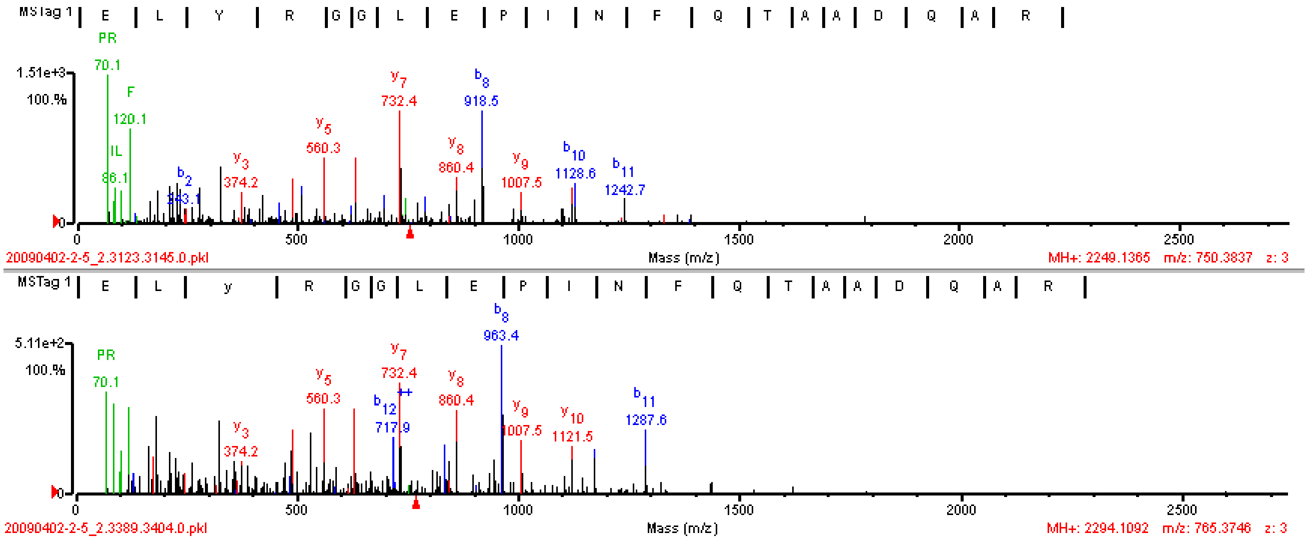

Figure A25 Mass spectra of peptides containing native (upper) and nitrated tyrosine (lower) 126 in nitrated OVA.

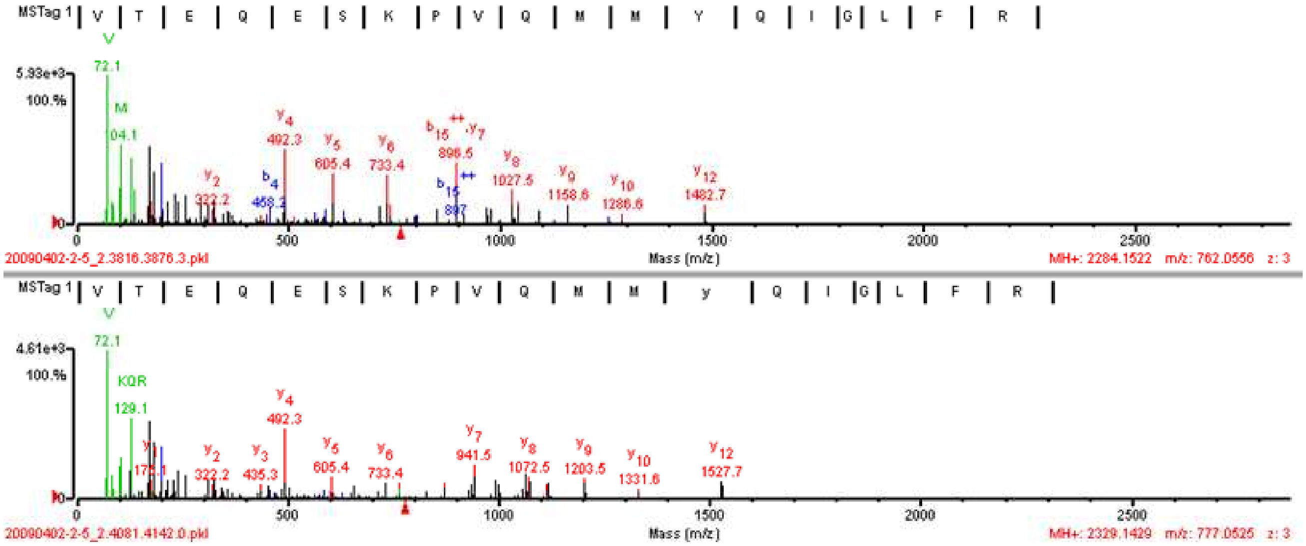

Figure A26 Mass spectra of peptides containing native (upper) and nitrated tyrosine (lower) 213 in nitrated OVA.

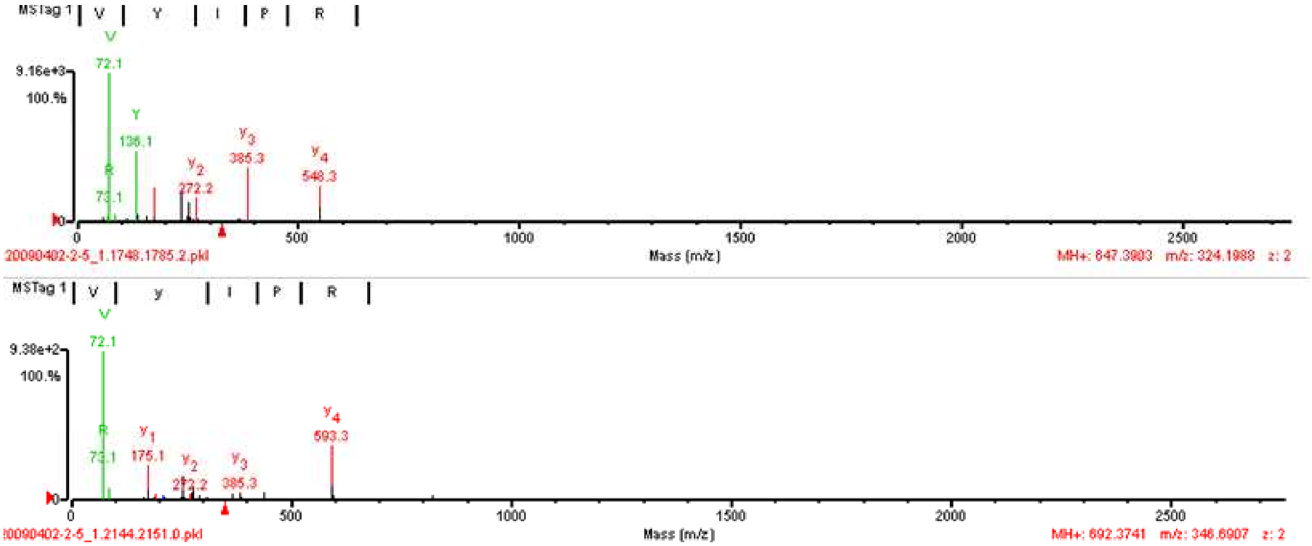

Figure A27 Mass spectra of peptides containing native (upper) and nitrated tyrosine (lower) 282 in nitrated OVA.

Abbreviation Index

2D-GE	Two-dimensional polyacrylamide gel electrophoresis
3-MBTCA	3-Methyl-1,2,3-butanetricarboxylic acid
ACN	Acetonitrile
BCA	Bicinchoninic acid assay
BSA	Bovine serum albumin
BVOC	Biogenic volatile organic compounds
CE	Capillary electrophoresi
CID	Collision-induced dissociation
DTT	Dithiothreitol
ECD	Electric conductivity detector
ELISA	Enzyme-linked immunosorbent assay
EMAC	ECHAM/MESSy Atmospheric Chemistry model
ESI	Electrospray
GC	Gas chromatography
HPLC-DAD	High performance liquid chromatography coupled to diode-array detector
IAM	Iodoacetamide
IC	Ion chromatography

IEF	Solution isoelectric focusing
IP	Immnunoprecipitation
MALDI	Matrix-assisted laser desorption/ionization
nanoESI	Nanoelectrospray
ND	Nitration degree
ND_Y	Nitration degree of nitrotyrosine residue
NPD	Nitrogen phosphorous detection
NTN	Nitrotyrosine residue number per protein molecule
OVA	Ovalbumin
PBS	Phosphate buffered saline
PE	Polyethylene
PTFE	Polytetrafluoroethylene
Qq-TOF	Tandem quadrupole coupled to time of flight mass spectrometer
R^2	Square correlation coefficients
SDS-PAGE	Polyacrylamide gel electrophoresis in the presesence of sodium dodecylsulfate
SOA	Secondary organic aerosol
TFA	Thermal energy analyzer
TFE	Trifluoroethanol

TNM	Tetranitromethane
UV-Vis	Ultraviolet-visible photometry